Geoscience BC Report 2011-3

The application of surface organic materials as sample media over deeply buried mineralization at the Kwanika Central Zone, North-Central British Columbia

by

David R. Heberlein[1] and Colin E. Dunn[2]

[1] Heberlein Geoconsulting, Suite 303-108 West Esplanade, North Vancouver, BC

[2] Colin Dunn Consulting Inc., 8756 Pender Park Drive, North Saanich, BC

EXECUTIVE SUMMARY

As a follow up to the 2009 Geoscience BC study by Heberlein and Samson (2010), the authors carried out an expanded geochemical orientation survey over the Kwanika Central Zone focusing on the geochemical responses in organic materials to the mineralization. Results of the original study showed that the most effective combination of sampling medium and chemical extraction for detection of the deeply buried Cu-Au porphyry mineralization was Ah horizon soil with a modified aqua regia (Ultratrace) digestion with ICP-MS determinations. This project further investigates the use of Ah horizon by comparing sampling results from an offset 100 by 100 metre grid with other organic materials, namely vegetation and charcoal.

Sampling was carried out during September 2010. Five different samples were collected at each site, including: two samples of Ah horizon, lodgepole pine bark, subalpine fir twigs and (where present) charcoal fragments from the LF and Ah horizons. Vegetation samples were oven dried and the dried needles stripped from the fir twigs prior to milling. Both needles and bark scales were milled to a fine powder using a Wiley mill. Ah samples were air dried at 40 °C and milled to -80 mesh. Vegetation samples were decomposed using a conventional aqua regia digestion. Three different extractions were carried out on the Ah samples: distilled water, sodium pyrophosphate and Ultratrace aqua regia. The latter was also carried out on the charcoal samples after manually pulverizing in a pestle and mortar. Analytical determinations were by ICP-MS supplemented by ICP-ES for major elements. Loss on ignition (LOI) was performed on the dry Ah horizon samples to measure the organic carbon content.

Analytical results for the Ah horizon soils were examined to determine whether levelling was necessary to remove the influence of various field parameters. Soil moisture content was found to have an important influence on metal concentrations in the sodium, pyrophosphate and Ultratrace extraction results on the Ah horizon samples. Data were leveled by converting to Log(10) Z-Scores using soil moisture as a classification variable. Sodium pyrophosphate results were also normalized to LOI to correct for variations in organic carbon content. For the vegetation samples, lithology was found to have an influence on metal concentrations in pine bark. These results were also corrected using the Log(10) Z-Score method.

Results were plotted over topography and bedrock lithology using scaled symbol plots and percentile breaks; values above the 80th and 90th percentiles were classified as anomalous and highly anomalous populations, respectively.

The weakest extraction, distilled water, was found to be ineffective at detecting the mineralization. It did produce visually interesting patterns over the zone but hypergeometric probability analysis demonstrated that there is a reasonable chance of similar results being produced by random chance. Sodium pyrophosphate and Ultratrace aqua regia both performed well in defining statistically meaningful apical anomalies for As, Cu and W. Gold and Sb anomalies were also detected by the Ultratrace and sodium pyrophosphate methods respectively. Tungsten has by far the strongest response of all elements tested and appears to be the most effective pathfinder for the blind mineralization.

Charcoal results, while not definitive, do show that this material has promise as a sampling medium. Patterns produced by Ultratrace aqua regia digestion of this medium are comparable to those seen in the Ah soils. Unfortunately the relatively small number of samples over the mineralized zone and the highly variable nature of charcoal distribution across the study area resulted in a relatively poor precision for most elements that translates into noisy patterns. Nevertheless, this study has demonstrated that recognizable anomalies for ore elements can be obtained in this medium over the mineralization and with improved sampling techniques more reliable results could be achieved. More work is needed to refine charcoal as a sample medium.

The vegetation results show different patterns from the Ah soils and charcoal suggesting that the metals in the soil have not been derived exclusively through recycling of plant tissues. Furthermore, the occurrence of halo-like

patterns with lows directly over the mineralization imply that different geochemical dispersion processes are responsible for the formation of soil and vegetation anomalies and this is probably because the roots of an individual large tree integrate the geochemical signature of several cubic metres of the substrate, including all soil horizons. As a sampling medium to detect deeply buried mineralization, fir needles show promise, particularly for pathfinder elements like Tl and As that form compelling halo patterns around the edges of the mineralized zone. Dispersion patterns for these elements significantly enlarge the size of the target making it easier to find. A combination of fir needles and Ultratrace analysis on Ah horizon soils would be an effective exploration approach in forest environments. Pine bark had less clear results but did produce base metal anomalies in close proximity to known faults of which one, the Pinchi Fault, is known to intersect mineralization at depth. This observation could be useful in interpretation of pine bark survey results.

TABLE OF CONTENTS

LIST OF FIGURES

LIST OF TABLES

APPENDICES

INTRODUCTION AND OBJECTIVES

In 2009, as part of Geoscience BC project 2009-019, a soil orientation survey was carried out over the Kwanika Central Zone in north-central British Columbia (Heberlein, 2010; Heberlein and Samson, 2010). The aim of this survey was to investigate the effectiveness of a suite of commonly used chemical digestions, combined with a range of sample media, at detecting deeply buried porphyry Cu-Au mineralization through Quaternary glaciofluvial and post mineralization sedimentary cover. A total of nine digestions were used, including laboratory specific (proprietary and non-proprietary) methods as well as generic methods. Soil material was collected from the upper 50 cm of the profile; specifically from Ah, upper B, lower B and C horizons. In addition, samples for Mobile Metal Ion (MMI®) analysis were collected from a constant depth interval of 10 to 25 cm below the top of the mineral soil following the recommended protocol of SGS Mineral Services (Lakefield, Ontario).

Results showed that soil geochemistry is an effective technique for detecting deeply buried mineralization. Best results were obtained from the Ah horizon using an aqua regia digestion. This combination of sample media and digestion resulted in convincing multi-element anomalies for Cu, Au, W, As, Ag and Mo directly over the surface projection of the mineralized zone. Most convincing responses were obtained over the parts of the mineralized body that are present at more than 300 metres below the surface. Of the generic methods, a sodium pyrophosphate leach on Ah horizon samples was also effective in producing credible anomalies for Cu, Au, Ag, W, U, As, Sb and Mn.

Laboratory specific methods applied to upper B, lower B and C horizons for the most part did not produce credible anomalies. Of the laboratory specific methods only ALS Chemex's (Vancouver, BC) ionic leach technique convincingly identified the deeper parts of the mineralized body but did not produce a response over shallower mineralization. MMI®, bioleach and Enzyme Leach℠ failed to detect the zone. A conclusion of the study therefore was that there was no advantage to using these more expensive proprietary methods in this environment.

The current study builds on the results documented in Geoscience BC Report 2010-3 (Heberlein and Samson, 2010) by investigating the geochemical response to the Kwanika Central Zone in surficial organic materials. It further investigates the effectiveness of the Ah horizon as a sample medium by testing three different chemical digestions (distilled water leach, sodium pyrophosphate leach and Ultratrace aqua regia) on an offset 100 by 100 metre grid over the mineralization. It examines the relationship between the metal contents of vegetation and the Ah horizon and attempts to determine whether metal anomalies detected in Ah horizon material are formed by accumulation from shed plant tissues or by entrapment of mobile metal ions by organic matter in the soil. In addition, charcoal debris in the Ah horizon is investigated as a potential sample medium. Charcoal is a common component of boreal and sub-boreal forest soils. It is formed by the thermo-chemical decomposition of wood by fire (DeLuca and Aplet, 2008). This highly porous material is known to have a strong metal adsorption and absorption capacity (Johns et al., 1993; McMahon, 2006) and therefore should behave as an effective trap for mobile metal ions in the near-surface environment. It is potentially a useful sampling medium in areas of recent forest fires and logged areas where the vegetation and the Ah horizon may have been damaged or completely destroyed.

The project also addresses constructive feedback from the mineral exploration community on the results of the 2009 study, in particular the desire to see how different methods respond on a grid rather than on transects across the mineralization.

OBJECTIVES

This project set out to address the following questions:

- From the analysis of several types of surface organic materials, what are the geochemical characteristics of each?
- Which of these media gives the most definitive surface signature of blind copper-gold porphyry-style mineralization through transported cover?
- Does an aqua regia digestion of organic-rich soils define much the same anomalous areas as that of the less aggressive sodium pyrophosphate leach?
- Is charcoal from forest fires an effective and viable sample medium?
- Does the analysis of pine bark provide different (and more definitive) spatial signatures of this buried mineralization than the needles of the other common species present – subalpine-fir?
- Which of the methods tested provides the most useful geochemical signatures for this style of mineralization in this terrain?
- What are the recommended sampling strategies of the media tested?

BENEFITS TO THE MINING INDUSTRY

This project builds on the results of the 2009 study by exploring geochemical responses at the Kwanika Central Zone on a wide spaced grid. It aims to provide the mineral exploration community with a better understanding of how different organic sampling media can be used as sampling media for geochemical exploration in regions with thick glacial sedimentary cover. It provides comparisons of metal concentrations between vegetation, Ah horizon and charcoal debris and assesses the relative capabilities of each for isolating the secondary geochemical dispersion patterns related to a blind mineral deposit. It also provides guidelines about appropriate sampling media in a number of forest cover situations that are commonly encountered in north-central BC. These include pristine forest, clear-cut logged areas, beetle kill and burned areas.

LOCATION AND ACCESS

The Kwanika project is situated in the Omineca Mining Division of north-central British Columbia, approximately 140 km northwest of Fort St. James (55°30'N, 125°18'W; Fig. 1). It is accessible by well-maintained Forest Service roads from Fort St. James via the community of Takla Landing. Serengeti Resources Inc., the owner, holds the title to 28 contiguous mineral claims covering an area of 8,960 ha (Rennie and Scott, 2009).

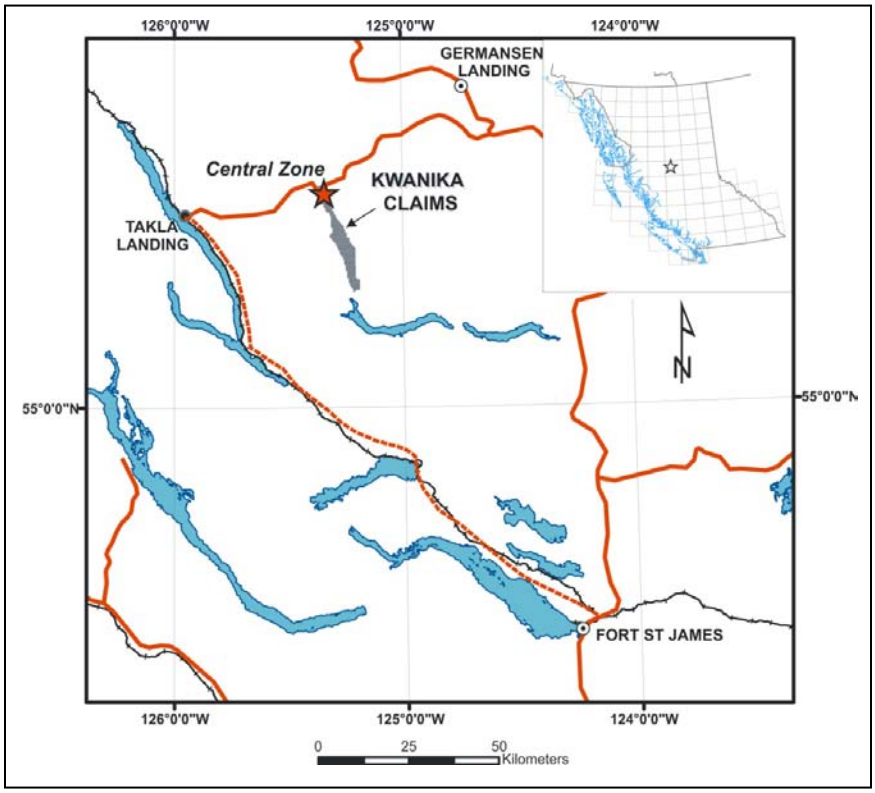

FIGURE 1 LOCATION OF STUDY AREA

SURFICIAL ENVIRONMENT

The Kwanika Central Zone lies in a broad, flat-bottomed valley containing an extensive cover of glacial till and outwash sediments. Locally, elevations range from 900 to 1200 metres, but in the study area itself there is only about 40 metres of relief. Drilling has shown that the cover varies in thickness from a few metres to over 40 metres in thickness in the immediate deposit area (D. Moore, pers. comm., 2009). Outcrops are rare and only seen in the bottom of the Kwanika Creek valley, which is deeply incised into the Quaternary sequence (Rennie and Scott, 2009). Away from the river valley, the surface is well-drained and gently sloping and covered by a relatively open lodgepole pine, white spruce and pacific silver fir woodland (Fig. 2).

Three types of soil profile are present in the Central Zone area. These are for the most part developed on a parent material of cobble-rich sand and gravel. Podzols (Orthic Ferro-Humic; soil nomenclature based on the Canadian System of Soil Classification [Canada Soil Survey Committee, Subcommittee on Soil Classification, 1978]) are the most widespread soil type, occurring on well drained, gentle slopes within the forest. A typical profile (Fig. 3) includes a thin LFH horizon consisting of partially decomposed wood, twigs, needles and mosses and a thin (<1 cm) black to dark brown, organic-rich Ah horizon. The organic-rich layers overlie a distinct white to grey or pinkish, sandy textured Ae or Aej horizon of variable thickness. Below this, the B horizon is made up of an upper Bf horizon (upper B), enriched with iron oxide, and a lower, medium to chocolate brown, BC horizon (lower B), which grades into medium to dark grey sand or gravel of the C horizon.

FIGURE 2 A TYPICAL SAMPLE LOCATION AT THE KWANIKA CENTRAL ZONE

Brunisol, the second soil type, is common at the base of slopes adjacent to boggy areas (Fig. 4a). A typical example has a surficial LFH and Ah horizon up to 4cm thick overlying an undifferentiated olive-brown Bm horizon. The third soil type is represented by Organic soils. These occur in depressions and boggy areas (Fig. 4b). Profiles consist of an upper thick, peaty Om horizon that can be tens of centimetres thick, overlying a lower grey or blue-grey C horizon. A mottled Bg horizon was noted at one locality. In all cases, the lower part of the profile is water saturated.

The forest is sub-boreal and typical of large areas of the gently rolling plateaus of central interior BC. The dominant trees are lodgepole pine (*Pinus contorta*), white spruce (*Picea glauca*) and subalpine fir (*Abies lasiocarpa*). In the boggy swamps, which occur locally in the Kwanika Creek valley, there are thick tangles of willow (*Salix* spp.), and on the drier plains the undergrowth is relatively sparse with mostly soopolallie (*Shepherdia canadensis;* also known as buffaloberry or soapberry), occasional shrub alder (*Alnus* spp.*)* and ferns.

FIGURE 3 A TYPICAL PODZOL PROFILE FROM THE CENTRAL ZONE

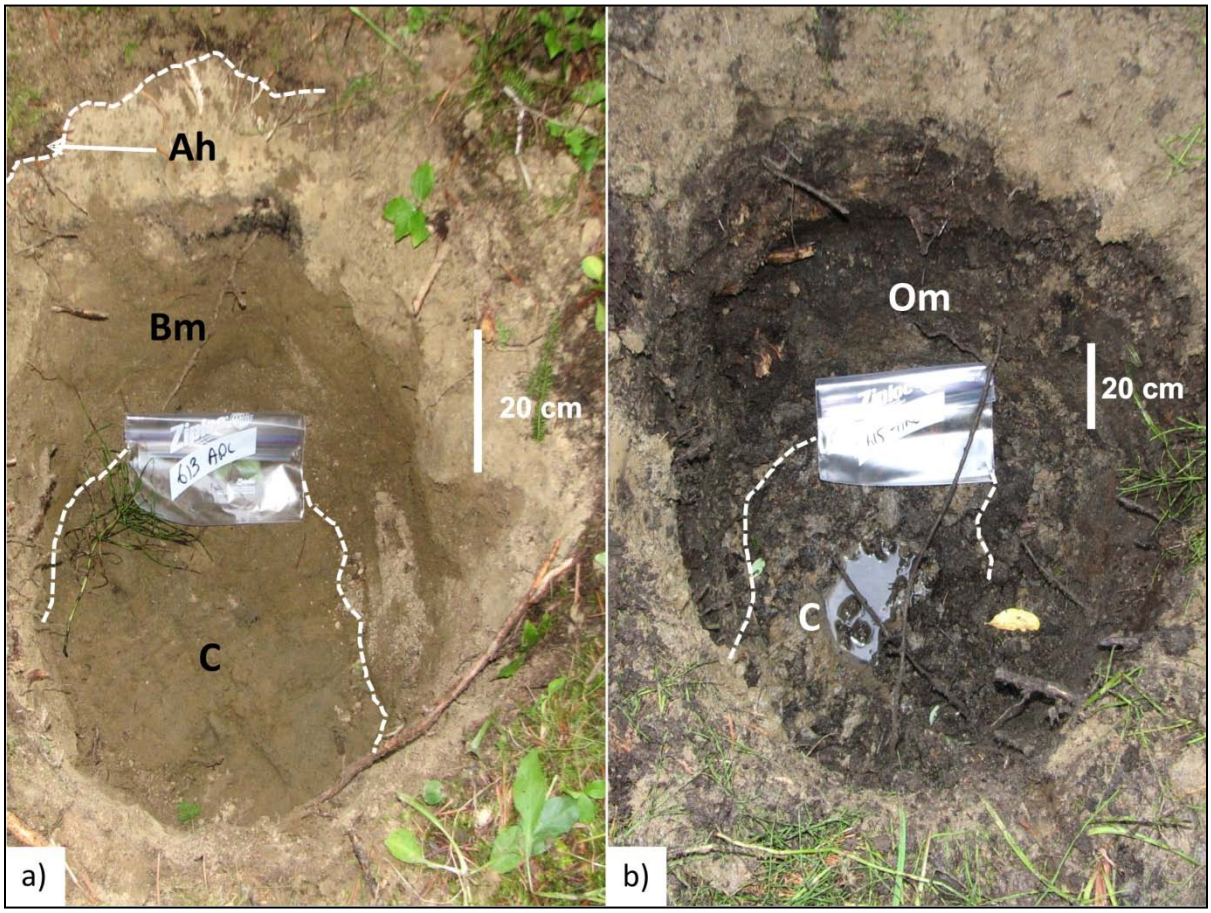

FIGURE 4 BRUNISOL (A) AND ORGANIC SOIL (B) PROFILES FROM THE KWANIKA CENTRAL ZONE

EXPLORATION HISTORY

Copper mineralization was first recognized along Kwanika Creek in 1964. Initial exploration carried out by Hogan Mines Ltd. (later Bow River Resources Ltd.) consisted of geochemistry, trenching, prospecting, mapping and two X-Ray drill holes totalling 26.5 metres. The property was subsequently optioned to several companies, including Canex Aerial Explorations Ltd. (1965), and Great Plains Development Company of Canada Ltd. (1969), Bow River Resources Ltd. (1972) and Pechiney Developments Ltd. (1973). From 1966-1974, these companies carried out several geophysical surveys (magnetic and IP), soil geochemistry, bull dozer trenching as well as percussion and diamond drilling programs totalling 2,707 metres. The historical drilling focused on a small area along Kwanika Creek and was successful in defining a poorly constrained, 36 Mt (non 43-101 compliant) body of mineralized material, grading approximately 0.20% Cu with minor Mo. No significant work was carried out on the property again until 1989 when the area was restaked by W. Halleran, who recognized the copper-gold affinity to the mineralization. Eastfield Resources Ltd. optioned the property that same year and a Joint Venture formed with Northair Mines Ltd. carried out an aggressive exploration program consisting of line cutting, prospecting, mapping, rock and silt sampling on the Swan 1 to 8 claims. Samples from previous drill holes were also reanalyzed. Four diamond drill holes (549 metres) drilled west of the previously defined mineralization in 1991 detected sporadic copper mineralization along the east side of the Pinchi Fault.

Based on the results of the historical exploration, Serengeti Resources Inc. staked the current claims between 2004 and 2006. In 2005, the company conducted a 530 line kilometre airborne magnetic and radiometric survey, and collected 11 rock samples to assist in porphyry target identification (Osatenko, 2005). The airborne survey identified a small magnetic anomaly on the east side of the known deposit, with similar anomalies trending to the north-northwest and south. Over the course of 2006 and 2007, Walcott Geophysics (Walcott) carried out several ground-based induced polarization (IP) surveys to further investigate the trend of magnetic anomalies.

Results from a 2006 IP survey identified a significant chargeability anomaly over the historical mineralization and defined a north-northwest continuation of the anomaly into an area of glaciofluvial cover (Fig. 5). Drill testing of the chargeability anomaly later that summer confirmed the copper grade of the known mineralization, and discovered a new zone with porphyry characteristics approximately 2 km to the north (hole K-06-04, 0.32% Cu and 0.15 g/t Au over 18.3 m). In November and December 2006, five diamond drill holes (totaling 1,215 m) were drilled in the vicinity of hole K-06-04, resulting in the Central Zone discovery hole (K-06-09 - 0.69% Cu and 0.54 g/t Au over 111 m). From 2006-2009, Serengeti drilled 62,280 m of core into the Central and South Zones, defining a measured resource of 182.6 Mt grading 0.29 % Cu and 0.28 g/t Au (Rennie and Scott, 2009) and an additional inferred resource of 28.5 Mt grading 0.19 % Cu and 0.20 g/t Au.

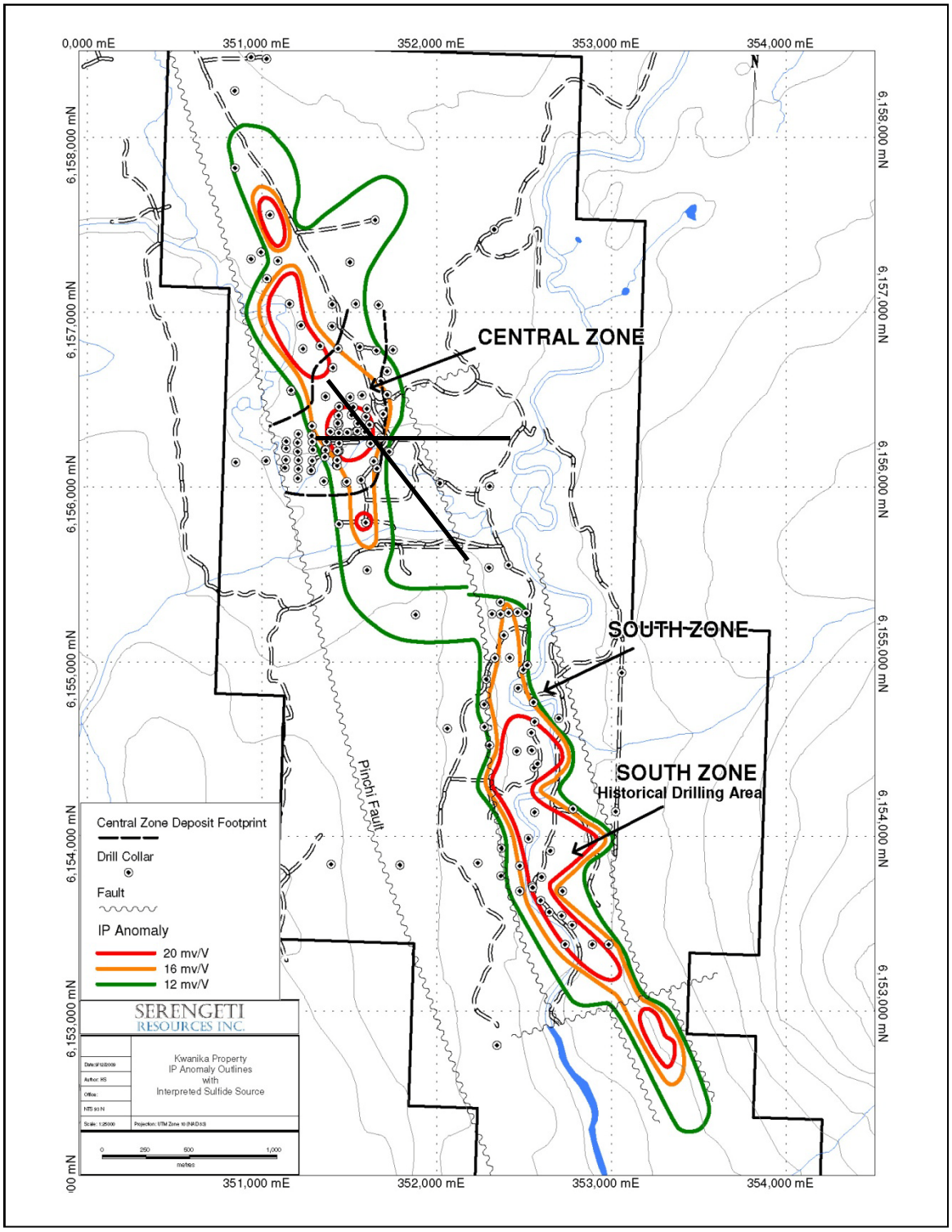

FIGURE 5 KWANIKA PROJECT MAP SHOWING MINERALIZED ZONES AND IP ANOMALIES. (FIGURE COURTESY OF SERENGETI RESOURCES INC.)

GEOLOGY

REGIONAL SETTING

The Kwanika property lies in the northern part of the Quesnel Terrane, which consists of a belt of Early Mesozoic volcanic and intrusive rocks sandwiched between highly deformed Proterozoic and Paleozoic strata of the Slide Mountain Terrane to the east and deformed Upper Paleozoic strata of the Cache Creek Terrane to the west (Garnett, 1978; Fig. 6). The Quesnel Trough hosts numerous alkalic, transitional and calc-alkalic porphyry copper-gold deposits, including Mt. Milligan (590.8 million tonnes at 0.19% Cu and 0.35 g/t Au; Mills, 2008) and Lorraine (31.9 million tonnes at 0.60% Copper; BC Minfile). Porphyry-style mineralization is associated with island arc-related, Upper Triassic to Lower Jurassic volcanism and plutonism (Nelson and Bellefontaine, 1996).

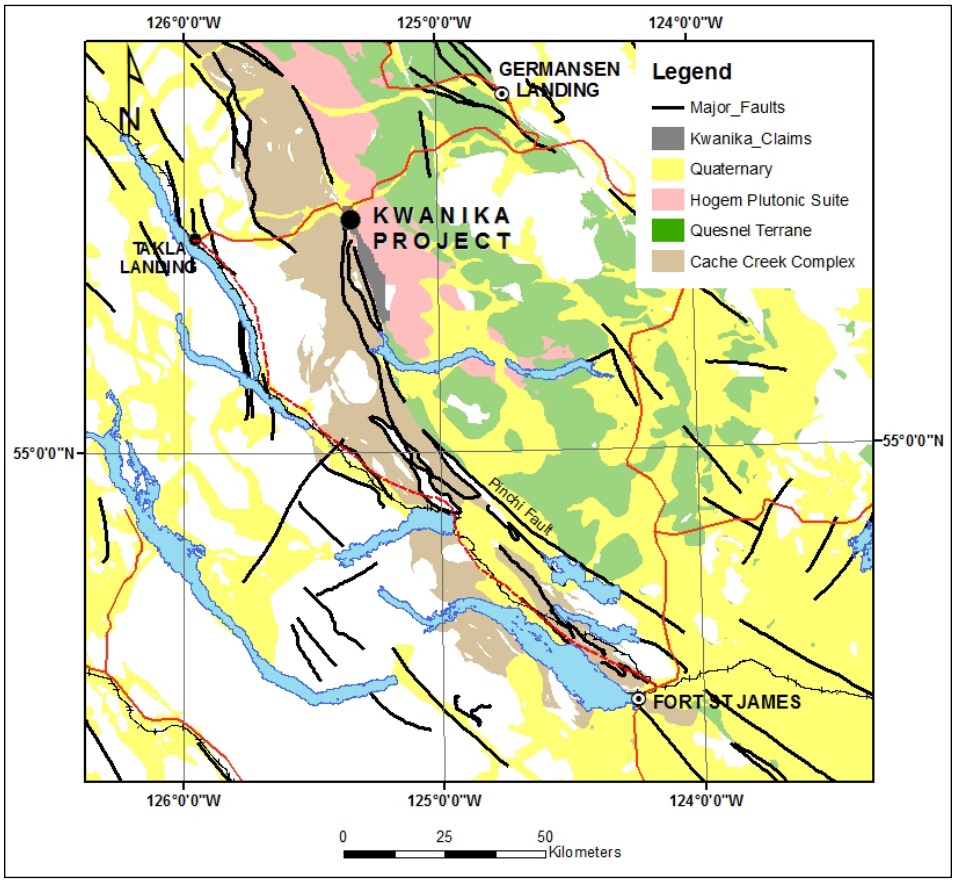

FIGURE 6 REGIONAL GEOLOGICAL SETTING

In the Kwanika area, Quesnellia is bounded by the Pinchi Fault to the west and by the Manson Fault to the east. The Pinchi Fault juxtaposes Permian Cache Creek Terrane rocks to the west against the Upper Triassic Takla Group rocks of the Quesnel Terrane to the east (Fig. 6). Porphyry copper-gold mineralization occurs in the Takla Group rocks and is associated with several irregular-shaped monzonite stocks that intrude along the western margin of the multiphase Hogem batholith (Rennie and Scott, 2009). Host rocks include diorite, quartz monzonite and granite phases of the batholith as well as Takla Group andesitic volcanic rocks.

LOCAL GEOLOGY

Two zones of porphyry-style mineralization occur at Kwanika. These are: the Central Zone (Cu-Au), which is the focus of this study, and the South Zone (Cu-Mo-Au-Ag). Mineralization at the Central Zone is developed in and around a north-northeast trending monzonite stock that dips shallowly to steeply to the west (Fig. 6). The intrusion consists of a medium-grained, equigranular to feldspar porphyritic rock, made up of plagioclase and K-feldspar with lesser amounts of amphibole, biotite, quartz, and tourmaline. Highest grade copper-gold mineralization occurs within, and immediately adjacent the intrusion. The monzonite intrudes into variably copper and gold-mineralized diorites and monzodiorites of the Hogem Batholith Intrusive Suite (Garnett, 1978) as well as Takla Group andesitic volcanic rocks (Fig. 7).

At both zones, mineralization is associated with a core zone of intense, texturally destructive albite alteration associated with a variable strength multiphase quartz veinlets stockwork. Surrounding the albite core is a broad zone of weak to strong, pervasive and fracture-controlled potassic alteration characterized by K-feldspar and secondary biotite (Rennie and Scott, 2009; H. Samson, pers. comm., 2009). This alteration grades laterally into propylitic assemblages. Dominant sulphide minerals include pyrite, which is ubiquitous to the deposit, chalcopyrite and bornite. Molybdenite is also commonly present.

Subsequent to the mineralizing event, the intrusive and volcanic units were locally rotated by listric faulting and overlain to the west by a clastic sediment-filled, half-graben-shaped basin, developed up against the Pinchi Fault (reference?). Post-mineral sedimentary rocks, which consist of conglomerates, sandstones and siltstones, partially cover the Central Zone (Fig. 8). They thicken to the west and attain a maximum observed thickness (from drill holes) of 435 m along the Pinchi Fault. Outcrop on the property is rare as much of the area is covered by 20-40 metres of Quaternary glaciofluvial sediments. For the purpose of this study, these rocks are considered to be part of the cover sequence.

A zone of supergene enrichment consisting of an upper oxide zone containing native copper and a lower sulphide zone with secondary chalcocite and covellite occurs on the upper surface of the hypogene mineralization at the contact with the post mineral sedimentary rocks.

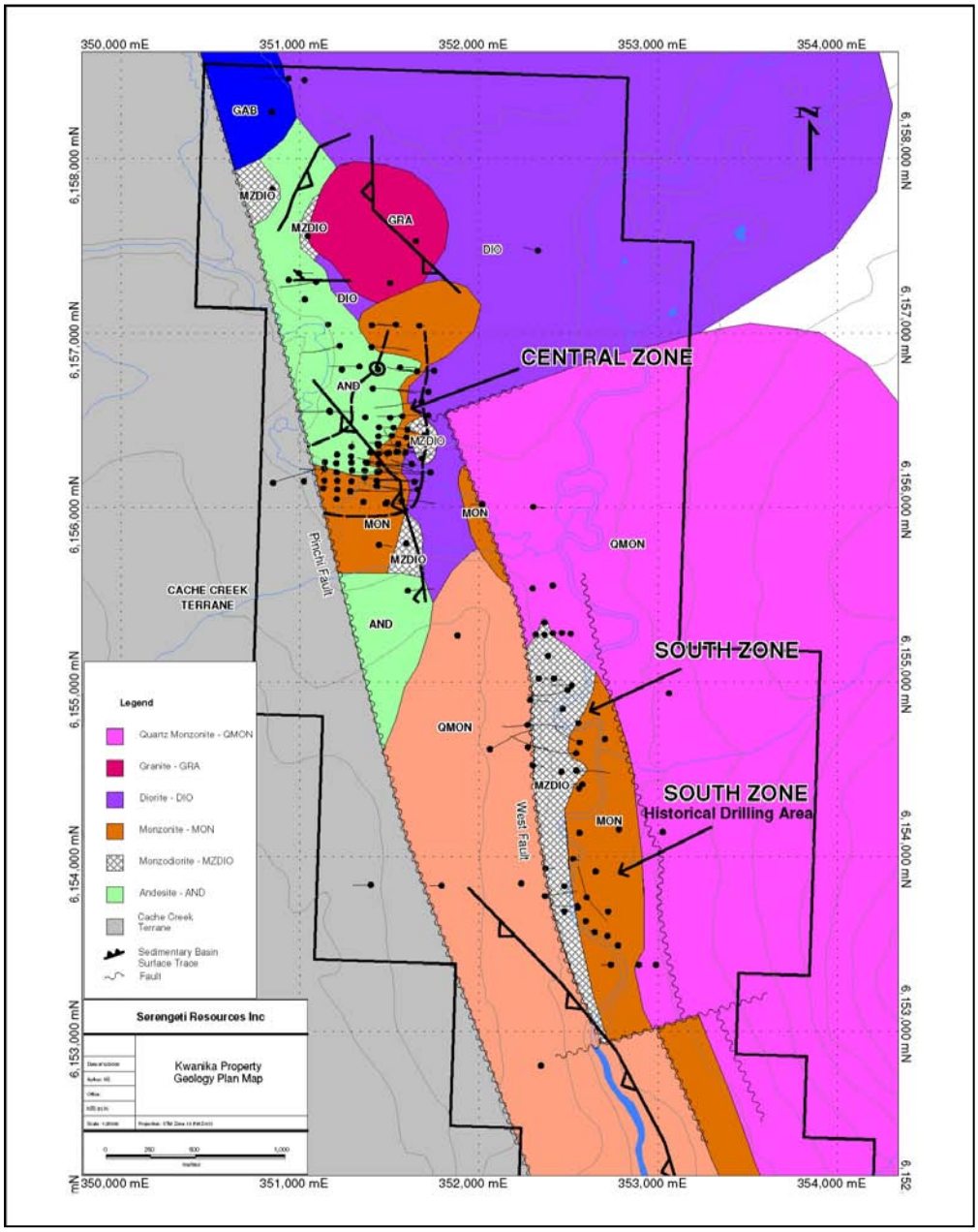

FIGURE 7 LOCAL GEOLOGY OF THE KWANIKA PROPERTY SHOWING THE STUDY AREA AND MAIN GEOLOGICAL UNITS (COURTESY OF SERENGETI RESOURCES INC.)

Bedrock geology (beneath the post-mineral sedimentary cover rocks) of the study area is shown in Figure 8. As there is almost no outcrop in the area, this map has been reconstructed by Serengeti Resources from geophysical and drill hole information. Much of the area is underlain by intrusive rocks belonging to the Hogem Batholith Intrusive Suite. These include a diorite and monzodiorite intrusion that forms an elongated north-south trending body near the eastern boundary of the study area. This unit varies in width from about 300 metres in the southern and central part of the area to over 600 metres in the north. Monzonite occurs on the eastern and western contacts of the diorite-monzodiorite and is spatially associated with Central Zone mineralization on the west side. This monzonite appears to occupy the contact between the diorite-monzodiorite intrusion and Takla Group andesites, which underlie the northwest and southern limits of the study area. An abrupt east-west truncation of the intrusive rocks near the southern limit of the study area suggests that the intrusions are in fault contact with the andesites.

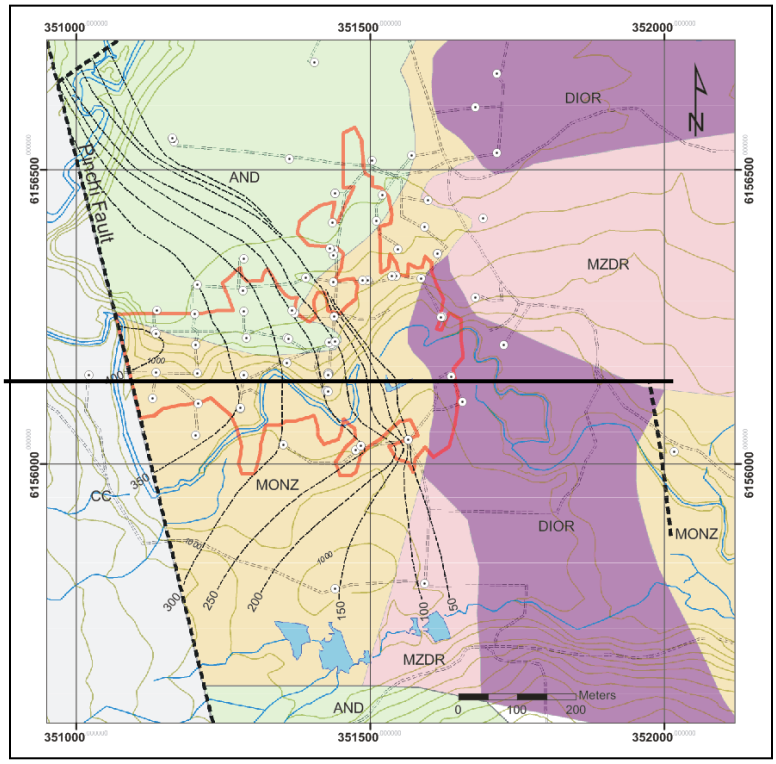

FIGURE 8 GEOLOGY OF THE STUDY AREA SHOWING DRILL COLLARS, SURFACE PROJECTION OF THE LIMITS OF 0.2% COPPER EQUIVALENT MINERALIZATION (RED OUTLINE), TERTIARY BASIN THICKNESS CONTOURS (FINE DASHED LINES), KNOWN FAULTS (DARK DASHED LINES) AND THE LOCATION OF CROSS SECTION A-A'. ABBREVIATIONS: DIOR – DIORITE (PURPLE), MONZ – MONZONITE (ORANGE), MZDR – MONZODIORITE (PINK), AND – ANDESITE (GREEN) AND CC – CACHE CREEK TERRRANE (GREY)

The Pinchi Fault, which crosses the study area from south-southeast to north-northwest, truncates all of these units. The area west of the fault is underlain by shales and cherts of the Cache Creek Terrane.

About a third of the study area is covered by the structurally controlled post-mineral sedimentary basin rocks mentioned earlier. On Figure 8 this is represented by depth contours of the lower contact. The eastern edge of the basin lies close to the eastern margin of the surface projection of the underlying mineralization as defined by the 0.2% Cu equivalent envelope. The sequence thickens rapidly westwards and reaches a maximum thickness of 435 metres against the Pinchi FaultThe geological relationships between the mineralization and the post mineral sedimentary basin cover are illustrated in Cross Section A-A' in Figure 9.

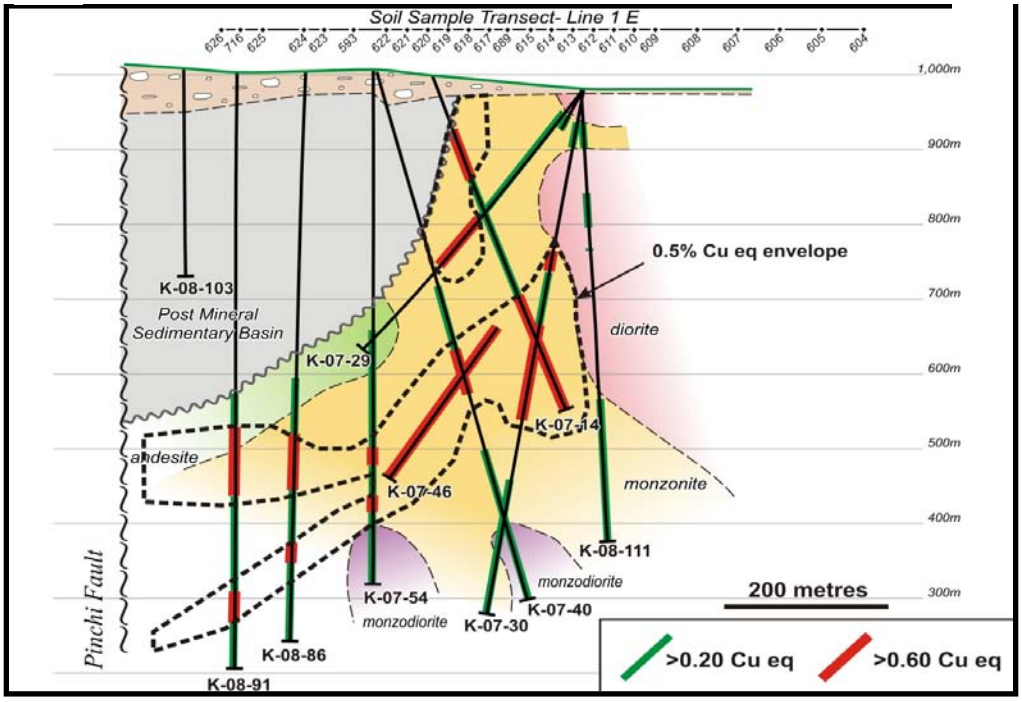

FIGURE 9 AN EAST-WEST CROSS SECTION THROUGH THE CENTRAL ZONE SHOWING THE RELATIONSHIP BETWEEN MINERALIZATION, THE MONZONITE INTRUSION AND THE GEOMETRY OF THE POST-MINERAL SEDIMENTARY BASIN (COURTESY OF SERENGETI RESOURCES INC.)

FIELD METHODS

SAMPLING PROCEDURES

Samples of a variety of media were collected from 84 sites over the Kwanika Central Zone. Locations were arranged on a staggered grid with a nominal spacing of 100 metres and covering an area of approximately one 1km^2 centred on the drill defined mineralization (Fig. 10).

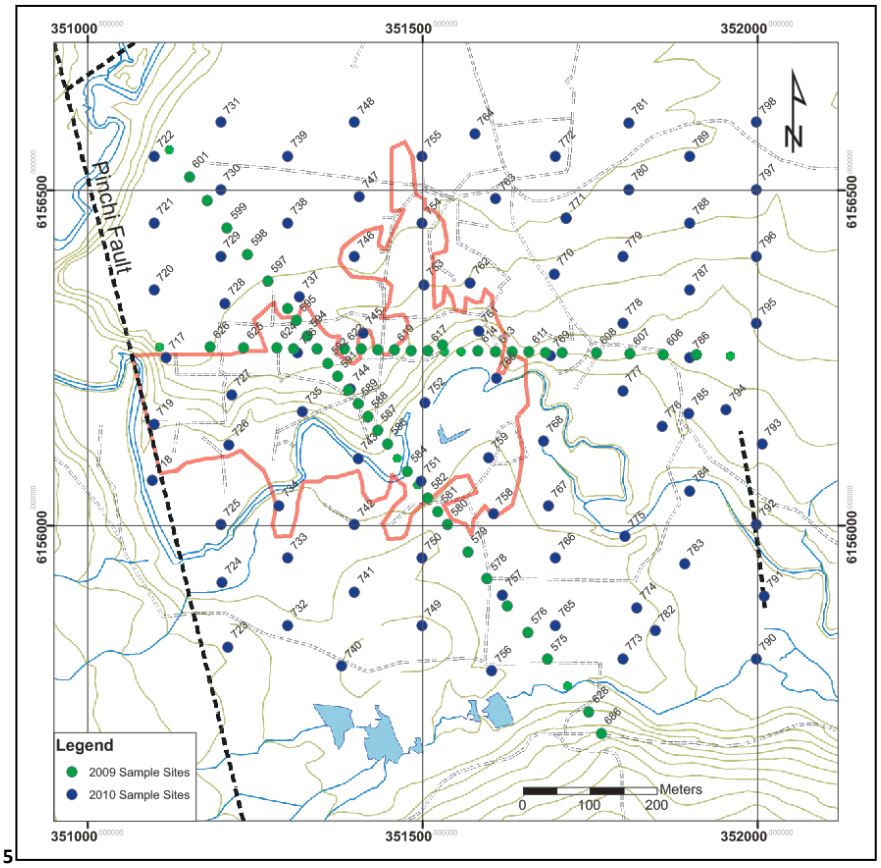

FIGURE 10 SAMPLE LOCATION MAP SHOWING THE 2009 SOIL TRANSECTS (GREEN), 2010 SAMPLE STATIONS (BLUE) AND THE SURFACE PROJECTION OF DRILL-DEFINED MINERALIZATION (RED OUTLINE) AT THE KWANIKA CENTRAL ZONE. KNOWN FAULTS ARE SHOWN AS BLACK DASHED LINES

SOIL AND CHARCOAL

At each sample site, two samples of Ah horizon soil were collected. This was done by peeling back the leaf litter and moss layer (LF horizon) to expose the top of the mineral soil profile. Ah horizon material consisting of black to dark brown decomposed organic matter was picked by hand from the upper surface of the mineral soil and the base of the LF horizon and placed in heavy duty Ziploc® bags. At many sample sites the sparseness of the Ah horizon meant that several locations had to be sampled within a five metre radius in order to obtain sufficient material for analysis. Typical sample weights ranged from 15 to 120 g. Ah sample locations are shown in Figure 11a.

Charcoal was collected from the LF and Ah horizons. The distribution and nature of this material was found to be highly irregular across the grid with 26 sites yielding insufficient material for sampling. Nevertheless enough sites could be sampled to provide a meaningful distribution across the grid. These are illustrated in Figure 11b. Variation in the size and abundance of charcoal fragments at each location was found to be considerable, varying from pieces of carbonized twigs and wood up to several centimeters long to small particles only a few millimeters in diameter. Sample weights varied between 5 and 15g.

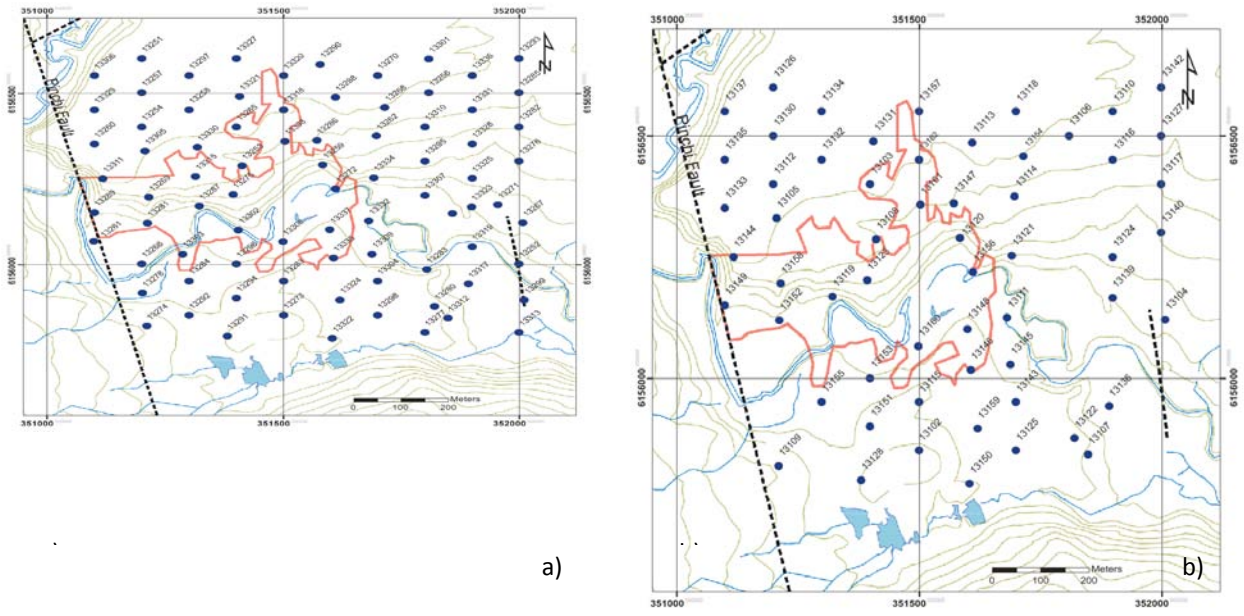

FIGURE 11 SAMPLE LOCATION MAP FOR A) AH HORIZON SOILS AND B) CHARCOAL AT THE KWANIKA CENTRAL ZONE

VEGETATION

The outer bark from lodgepole pine was obtained by scraping the scales from around the circumference of two neighbouring trees using a hardened-steel paint scraper, and pouring the scales into a standard kraft paper soil bag (approximately 50g, a fairly full bag; Figure 12a).

Twigs and foliage of subalpine fir, comprising the most recent 5–7 years of growth, were collected (Fig. 12b). In central BC, this amount of growth is typically about a hand-span in length, at which point, the twig diameter is 4–5 mm. This diameter is quite critical because many trace elements concentrate in the bark part of the twig, while the woody tissue (the cortex) has lower concentrations of most elements. Consequently, unless there is a consistency in the diameters of the twigs that are collected, any analysis of twig tissue can result in variability among samples simply because of the differing ratios of woody tissue to bark. For the current survey, the potential problems that might ensue were not of particular significance because the foliage was used for analysis, not the twigs. However, as a general principle it is wise to follow this practice of consistency in sampling in order to minimize factors, such as plant growth, that might control metal accumulations. The twig with foliage samples (5–7 lengths) were snipped from around the circumference of a single tree and were placed into porous polypropylene bags (Hubco Inc.'s Sentry II). The use of plastic bags is to be avoided because samples soon release their moisture and become very soggy. If there is any delay in processing, they develop moulds and lose their integrity. Pine bark and fir twig sample locations are shown in Figure 13.

FIGURE 12 SAMPLING PROCEDURES FOR: A) OUTER BARK AND B) FIR TWIGS AT THE KWANIKA CENTRAL ZONE

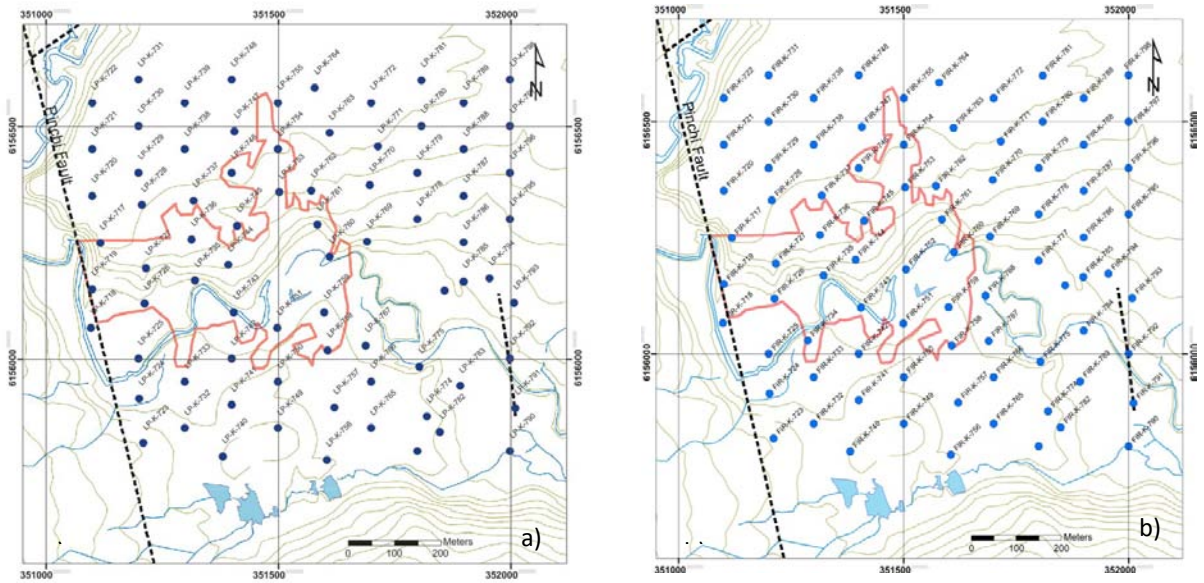

FIGURE 13 SAMPLE LOCATION MAP FOR A) PINE BARK AND B) FIR TWIGS AT THE KWANIKA CENTRAL ZONE

QUALITY CONTROL MEASURES

Quality control (QC) measures used in this study included the collection of field duplicate samples. Seven sites (about 10%) were randomly selected for field duplicate sampling. At each duplicate site, material was collected from within 5 m of the original sample using exactly the same procedures.

For the vegetation, 'blind' control samples (milled vegetation of similar matrix and known composition) were inserted in the sample sequence at a frequency of one in every ten field samples (Table 1). These are used to monitor analytical drift and to determine the precision and accuracy.

No standard reference materials were used in this study. The reason for this is that except for some vegetation control materials (CRM) there are no suitable matrix-matched materials for the range of sample media collected that are certified for the methods being tested. In order to monitor and mitigate analytical drift, the samples were randomized prior to submission to the laboratory. Randomization has the benefit of distributing the effects of instrumental drift randomly throughout the sample population. It also allows for drift monitoring by plotting the samples in analytical order.

In addition to the field QC procedures, a number of steps were taken at the laboratories to ensure the quality of the analytical results. These include the introduction of analytical standards, blanks and lab duplicates into the sample stream.

LABORATORY METHODS

SAMPLE PREPARATION

Soil and charcoal samples were shipped to Acme Analytical Laboratories Ltd. in Vancouver BC for preparation and analysis. Ah samples were air dried at 35° to 40°C and screened to -80 mesh. Charcoal samples were oven dried at 60°C for 24 hours and then manually pulverized using a pestle and mortar.

Vegetation samples were prepared in Victoria BC under the supervision of Colin Dunn. They were oven dried at 80°C for 24 hours to remove moisture. For the fir samples, the foliage was then separated from the twigs. In preparation for chemical analysis, each foliage and bark sample was then milled to a powder using a Wiley mill.

ANALYSES

Analyses of the soil and vegetation samples were carried out at Acme Analytical Laboratories Ltd. (Vancouver, BC). Methods used are summarized in Table 1 and described below.

Distilled water (Code 1SLW): Leaching of Ah soil samples with distilled water was carried out on a 1.0 gram aliquot of -80 mesh (0.177 mm) sample. The sample was mixed with 10ml of distilled water and rolled for two hours at room temperature. Analysis for 63 elements is by ICP-MS. This is a very weak extraction that liberates only the most loosely bound ions from the surface of the sample.

Sodium Pyrophosphate (Code 1SLO): This extraction is selective for elements adsorbed onto organic matter (fulvic and humic compounds). A 1.0 g aliquot of -80 mesh (<0.177 mm) Ah soil was rolled with 0.1M Na_3PO_7 for one hour. Analysis for 58 elements is by ICP-MS.

Ultratrace Aqua Regia (Code 1F): This modified aqua regia digestion utilizes a 2.0/0.02/0.02 HCl:HNO_3:H_2O combination to achieve ultra low detection limits for many elements. Analysis for 53 elements is carried out on a 5 gram aliquot of the <0.18mm fraction using the Perkin Elmer Elan 6000 or 9000 ICP-MS to resolve very low concentrations. This method was used on Ah horizon soil and charcoal media. Aqua regia is an aggressive acid attack that will digest all but the most fibrous portion of the organic matter in the Ah horizon. It will also partially digest clays and oxide minerals present in the inorganic fraction of the sample.

Aqua Regia (Code 1VE2). This method involves dissolution of a 0.5g aliquot of milled vegetation in nitric acid, followed by an aqua regia digestion, heating on a hot plate then diluting to a constant weight with deionized water. The analytical finish is by ICP-MS and data were obtained for 53 elements.

LOI (Code 2A): Loss on ignition. This provides an estimate of the total carbon content of the sample by comparing the weight difference of the sample before and after ignition at 1000°C.

TABLE 1 SUMMARY OF ANALYTICAL METHODS

Medium	Analytical Methods
Pine Bark	Aqua regia
Fir Needles	Aqua regia
Ah Soil	Ultratrace aqua regia Distilled water Sodium Pyrophosphate LOI
Charcoal	Ultratrace aqua regia

DATA PROCESSING

In order to prepare the analytical results for interpretation, a number of steps were taken. First the analytical results were merged with the sample location and field observational data using Geosoft's Target™ Geochemistry software. During this procedure, less than detection limit symbols (< and -) were automatically replaced with a value equal to half the detection limit. Next, results for field and analytical duplicates were extracted from the dataset for QAQC evaluation. The completed datasets were then validated to ensure that sample locations were correct and that no merging errors had occurred.

Merged results were then exported to a csv file and imported into ioGAS™ software where histograms were generated for each element. This was done to assess the type of distribution (i.e. log normal or normal) and to determine which elements require transformation prior to interpretation. Next, box and whisker plots were generated for each element using various field parameters as classification variables. This step assesses whether sample site characteristics such as slope, soil moisture etc. affect element concentrations. An example showing the influence of soil moisture on As and Fe concentrations is shown in Figure 14a. Summary statistics for selected elements for each extraction and sample medium are included in Appendix 2.

Soil moisture was found to have significant influence on the concentrations of many elements in the Ah horizon aqua regia and sodium pyrophosphate extractions with wetter sample locations appearing to have higher element concentrations (Fig. 14a). Total carbon, expressed as LOI also appears to strongly influence element concentrations for the sodium pyrophosphate and distilled water extractions. For the vegetation samples, particularly the pine bark, underlying lithology seems to have the biggest influence on the concentrations of many elements.

These influences need to be removed from the data in order to reveal geochemical patterns of interest. To do this ioGAS software was used to transform the results to Log(10) Z-Scores using soil moisture, LOI and lithology as classification variables. Transformations applied to the data are summarized in Table 2 and an example of transformed results are illustrated in Figure 14b

Results are plotted as proportional dot plots in ArcView over a topographic base.

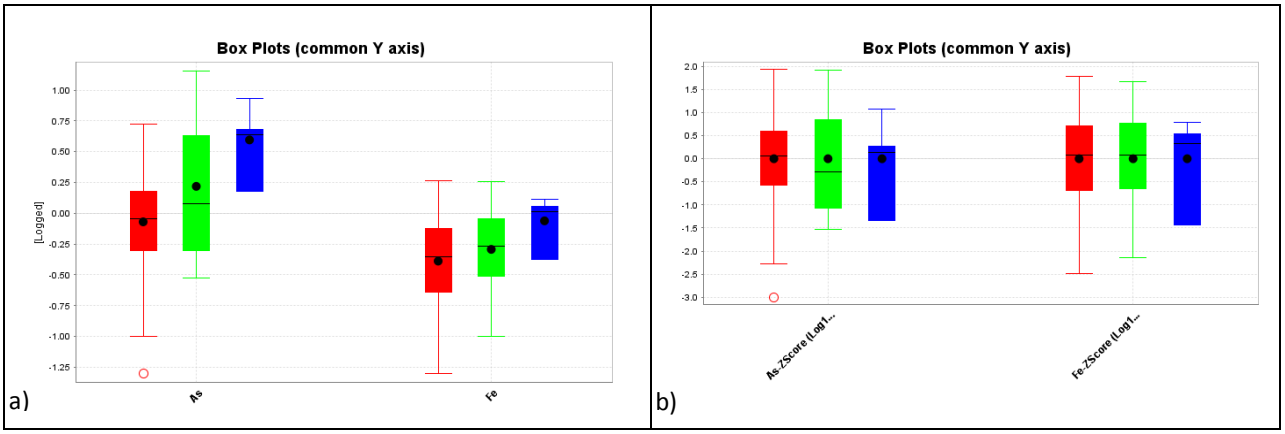

FIGURE 14 A) THE EFFECT OF SOIL MOISTURE ON THE CONCENTRATION OF ARSENIC AND IRON IN AH HORIZON AQUA REGIA ANALYSES. B) THE SAME DATA LEVELLED BY CONVERSION TO LOG(10) Z-SCORES USING SOIL MOISTURE AS THE CLASSIFICATION VARIABLE. COLOURS: DRY SAMPLES (RED), MOIST SAMPLES (GREEN) AND WET SAMPLES (BLUE)

The Log(10) Z-Score transformation has the advantage of levelling the results to remove the effects of the controlling variables and applying a logarithmic transformation to log-normally distributed elements in one step. Z-scores also eliminate differences in concentration range and units that would otherwise complicate interpretation. Transformed variables have a common mean of zero and values normally distributed both positively and negatively around the mean expressed as standard deviation units. The greater the value (positively or negatively) the more anomalous the result is. The following discussion of results is based on the Log(10) Z-Score transformed values.

TABLE 2 SUMMARY OF CORRECTIONS AND TRANSFORMATIONS APPLIED TO THE DATA SETS

Extraction	Controlling variable	Transformation (Levelling Variable)
Ultratrace aqua regia	Soil Moisture	Log(10) Z-Score (Moisture)
Distilled Water	LOI	Log(10) Z-Score (LOI)
Sodium Pyrophosphate	LOI, Soil Moisture	Ratio (LOI) Log(10) Z-Score (Moisture).
Aqua regia (Pine Bark)	Lithology	Log(10) Z-Score (Lithology).
Agua regia (Fir Twigs)	None	Log(10) Z-Score

DATA QUALITY

FIELD DUPLICATES

For the purpose of this report, data quality is assessed using average percent relative standard deviation (also known as the % coefficient of variation), or average RSD% as an estimate of precision or reproducibility of the analytical results. Average RSD% is estimated using the results of the field duplicates and can therefore be considered an estimate of the cumulative uncertainty of the sampling and analytical process. Field duplicate results provide important information about the homogeneity of the sample medium and the representativeness of the sampling method employed.

Average RSD% is determined from the duplicate results by first calculating the mean and standard deviation of each duplicate pair. An RSD% value is then calculated for each duplicate pair using the formula:

RSD% = standard deviation/mean x 100

The average RSD% is then determined by averaging the RSD% values for the duplicate pairs. This has been done for each sample and analytical method. A spreadsheet with the calculations is included in Appendix 1. In the following discussions, average RSD% values below 30% are considered to indicate good data quality (precision); between 30 and 50%, marginal quality and over 50%, poor quality. The higher an average RSD% value is, the less likely it is to be able distinguish real patterns from noise. Noise is considered as the cumulative effect of geological background variation plus sampling error.

Table 3 shows the RSD% values calculated from field duplicate results. The majority of elements show either good or marginal data quality (green and yellow, Table 3) for most sample media. The poorest performing method is the Ultratrace aqua regia extraction on charcoal, which has marginal quality results for As, Cd, Cu, Fe, Hg, Mo, Ni, Pb and Sb; and poor quality for Au, Ba, Bi, Ce and W. The method with the best data quality is the sodium pyrophosphate extraction (1SLO) on Ah horizon soils where most elements have good precisions, as indicated by RSD% values below 30%. Five elements, including: As, Ba, Mo, W and Zn, have values in the marginal range, and only one, Sb, has a poor precision (68.35%)

Results for the distilled water extraction (1SLW) on Ah horizon soils are slightly worse than those for sodium pyrophosphate. The elements Au, Cs and K all have poor precisions while As, Ce, Co, Mn, Mo, Pb and Zn have RSD% values in the marginal range.

Results for the vegetation samples appear to be quite good. For the pine bark duplicates only Au has a poor precision and Ag, Ce, Co, Ni and Sb fall in the marginal range. All other elements have good precision values. Two elements, As and Pb, have poor precisions in the fir twig results. Several others including: Ag, Cd, Ce, Cs, and Tl have precision values in the marginal range.

TABLE 3 SUMMARY OF AVERAGE RSD% VALUES FOR A SELECTION OF ELEMENTS

	Charcoal 1F	Pine Bark 1VE	Fir Twigs 1VE	Ah Soil 1SLO	Ah Soil 1SLW	Ah Soil 1F
Ag	25.09%	45.62%	30.08%	21.54%	25.15%	63.09%
As	47.78%		58.93%	58.50%	35.84%	86.42%
Au	74.77%	56.32%		107.00%	50.39%	90.83%
Bi	61.19%			57.77%		25.95%
Ca	56.56%	19.13%	11.12%	35.95%	18.66%	30.83%
Cd	39.87%	20.03%	31.24%	9.53%	29.87%	49.27%
Ce	60.15%	41.87%	35.03%	76.37%	36.50%	115.10%
Co	21.73%	36.40%	25.57%	35.32%	43.69%	37.67%
Cs	7.08%	25.36%	50.00%	61.87%	52.06%	72.32%
Cu	34.08%	14.22%	9.67%	59.83%	26.92%	31.98%
Fe	37.04%	24.54%	18.07%	55.24%	24.98%	72.13%
Hg	32.53%	19.50%	15.88%	53.98%		24.86%
K	28.43%	21.06%	10.60%	45.92%	59.57%	44.93%
La	62.00%	29.33%	32.79%	75.53%	25.91%	168.42%
Mn	28.74%	28.20%	16.00%	48.18%	45.87%	37.55%
Mo	46.04%	29.55%	16.24%	46.55%	38.82%	82.86%
Pb	40.75%	26.17%	78.36%	30.01%	36.80%	41.97%
S	27.61%	64.65%	11.75%		18.14%	31.57%
Sb	39.26%	35.02%	28.28%	76.58%		175.71%
Tl	23.57%	28.28%	32.47%	37.68%	27.11%	102.14%
W	53.79%			83.29%	4.04%	
Zn	18.59%	20.01%	20.27%	44.58%	32.44%	18.29%

Blanks indicate elements with standard deviations of zero. Colours represent: Good precision – green; marginal precision – yellow; and poor precision - ; Red. RSD values greater than 100% are highlighted in dark red. Blanks represent elements with values at or below detection limit. Abbreviations: 1F – Ultratrace aqua regia; 1VE – aqua regia, 1SLO – sodium Pyrophosphate; 1SLW – Distilled Water.

For individual elements, Au has the poorest overall precision with RSD% values of >50% for three of the five sample media (fir twigs had Au values that were nearly all less than detection limit). Cerium has the next worst overall precision, with charcoal having the poorest result (60.15%) and pine bark, fir twigs and distilled water on Ah horizon soils having marginal values (41.87%, 35.03% and 36.50%). Molybdenum has marginal values for three sample methods: charcoal (46.04%), distilled water (38.82%) and sodium pyrophosphate (41.01%).

In summary, the precision for most elements is acceptable across the range of methods and sample media tested. Caution should be taken when assessing the significance of results for Au, Ce, Mo and W (all elements with low concentrations approaching detection limit in the field duplicates) as these elements have marginal to poor precisions that will almost certainly result in noisy patterns.

CONTROL SAMPLES

In addition to the controls summarized above, control reference material (CRM) V6 (prepared at CANMET 20 years ago) was inserted after every 10th sample. Acme also inserted their own vegetation CRM samples (V14 and v16) after every 20th sample. The average, standard deviations and RSD percentages are shown in Table 4. These data show that the precision for the controls was considerably better than for the duplicates shown in Table 3. Many elements have RSD% values below 20%, and some are <10%. The precision for Au is poor and elements with

inferior precision (>20%) include Cr, Ga, Hf, Li, S, Sc, Se and Sn. The rather poor precision for Mo in the Acme controls is unusual and may be the result of the smaller sample population (n=7) for these controls compared to the blind control (n=21) which shows the usual good precision for Mo. Elements for which no RSD% values are shown were all at or mostly below the detection level.

TABLE 4 CONTROL REFERENCE MATERIALS V6, V14 AND V16 INCLUDED WITH THE VEGETATION SAMPLES. BLANKS DENOTE INSUFFICIENT DATA (ELEMENTS MOSTLY BELOW DETECTION LINMIT)

		Blind control V6			Acme control V14			Acme control V16		
		Average	Std. Dev.	RSD%	Average	Std. Dev.	RSD%	Average	Std. Dev.	RSD%
		n=21			n=7			n=7		
Ag	ppb	18.1	3.13	17	28	7.3	26	37	4	10
Al	%	0.044	0.01	13	0.15	0.008	5	0.05	0.00	8
As	ppm	0.37	0.14	37	11.6	1.0	9	1.57	0.23	15
Au	ppb	0.87	0.52	60	9.8	5.7	58	0.93	0.63	68
B	ppm	28	5.51	19	11.1	0.38	3	5.3	0.76	14
Ba	ppm	9.1	0.55	6	1.4	0.25	18	1.9	0.18	9
Be	ppm									
Bi	ppm				0.09	0.005	6			
Ca	%	0.70	0.03	5	0.65	0.03	4	0.31	0.02	7
Cd	ppm	0.22	0.02	7	0.21	0.010	5	0.09	0.01	13
Ce	ppm	1.77	0.14	8	0.06	0.011	18	0.10	0.02	16
Co	ppm	0.34	0.04	13	0.74	0.05	7	0.99	0.16	17
Cr	ppm	3.3	0.92	28	1.3	0.31	24	282	70	25
Cs	ppm	0.03	0.003	10	0.033	0.002	7	0.04	0.00	9
Cu	ppm	6.9	1.6	23	4.59	0.25	6	6.1	0.69	11
Fe	%	0.076	0.004	6	0.016	0.001	8	0.39	0.09	24
Ga	ppm	0.15	0.05	34				0.11	0.04	33
Ge	ppm							0.06	0.04	73
Hf	ppm	0.010	0.003	33	0.003	0.001	47	0.005	0.00	33
Hg	ppb	33	3.89	12	48	2.7	6	39	4.00	10
In	ppm									
K	%	0.09	0.006	7	0.52	0.04	7	0.23	0.01	6
La	ppm	0.73	0.04	5	0.033	0.008	23	0.05	0.00	8
Li	ppm	0.31	0.06	18	0.10	0.05	52	0.07	0.03	39
Mg	%	0.110	0.007	6	0.08	0.004	4	0.054	0.00	5
Mn	ppm	40	4.03	10	2116	118	6	713	27.08	4
Mo	ppm	0.24	0.03	11	0.06	0.02	29	1.43	0.41	29
Na	%	0.007	0.000	6				0.001	0.00	35
Nb	ppm	0.06	0.01	16				0.11	0.04	37
Ni	ppm	2.8	0.49	17	1.4	0.2	14	6.8	1.31	19
P	%	0.043	0.003	6	0.094	0.007	7	0.053	0.004	7
Pb	ppm	16.0	1.00	6	1.0	0.1	13	2.9	0.18	6
Pd	ppb									
Pt	ppb									
Rb	ppm	1.05	0.09	8	1.86	0.14	8	1.67	0.16	10
Re	ppb									
S	%	0.09	0.04	46	0.1	0.05	49	0.04	0.02	52
Sb	ppm	0.06	0.01	15	0.06	0.008	14	0.07	0.01	20
Sc	ppm	0.33	0.07	22	0.23	0.08	35	0.24	0.10	40
Se	ppm	0.22	0.09	40				0.15	0.05	37
Sn	ppm	0.16	0.03	20	0.05	0.02	31	0.23	0.04	16
Sr	ppm	34	1.4	4	6.8	0.5	8	11.5	0.63	5
Ta	ppm									
Te	ppm									
Th	ppm	0.11	0.01	12						
Ti	ppm	20	1.89	10	6.4	0.53	8	11	0.58	5
Tl	ppm				0.04	0.004	10			
U	ppm	0.05	0.01	12						
V	ppm									
W	ppm									
Y	ppm	0.431	0.04	9	0.021	0.003	15	0.04	0.01	20
Zn	ppm	34	3.28	10	15	3.12	21	37	2.14	6
Zr	ppm	0.29	0.04	12	0.04	0.006	14	0.19	0.06	29

RESULTS

In this section the results for selected elements are discussed for each of the sample media and digestions. For convenience the elements are grouped into three categories:

a) Ore elements: Au, Ag Cu and Mo.
b) Pathfinder elements: As, Bi, Hg, Pb, Sb, Tl, W and Zn.
c) Other elements: Ba, Ca, Cd, Ce, Co and Cs and major elements.

For the Ah horizon soils, the three extractions are discussed in order of increasing strength. References will be made to anomalous and highly anomalous samples, which correspond to the red and magenta dots on the accompanying figures. These are defined as Z-Score values over the 80th and 90th percentiles respectively. The figures also illustrate the surface projection of the mineralized zone (red outline), the thickness contours for the post mineral sedimentary basin (light dashed lines; see Figure 8 for contour intervals), major rock types and topography.

AH HORIZON SOIL - DISTILLED WATER EXTRACTION.

ORE ELEMENTS

Ore element results for the distilled water extraction are illustrated in Figure 15. Silver (Fig. 15a) has a poor correlation with the surface projection of the mineralization with a greater number of highly anomalous samples occurring outside of the zone, particularly on the east side. This area coincides with inferred monzodiorite (MZDR, Fig. 15) and diorite (DIOR) intrusions that are not known to host mineralization. Gold (Fig. 15b) also shows a poor correlation with the mineralized zone with an equal number of highly anomalous samples occurring within and outside the zone, particularly to the north in an area underlain by Takla andesite. The pattern for Cu (Fig. 15c) is even less definitive with only one highly anomalous sample present over the projected mineralization. A cluster of highly anomalous samples occurs to the east of the zone. These correlate well with the above mentioned silver anomalies that overlie the inferred monzodiorite and diorite intrusions. Of the ore elements, Mo has the best correlation with the mineralized zone (Fig. 15d). Four highly anomalous samples lie within the surface projection of the mineralization. Nevertheless, anomalous (red) to highly anomalous values are scattered to the east of the zone in the same area as the anomalous Ag and Cu values.

PATHFINDER ELEMENTS

Of the pathfinder elements, As shows the most compelling pattern (Fig 16a). Highly anomalous values appear to define an apparent halo around the mineralized zone. Anomalous values occur near the west, north and eastern boundaries of the mineralization and define an apparent low over the central part of the mineralized body (this effect may be artificially enhanced by a paucity of samples in this area). Lead (Fig. 16b) does not have a recognizable correlation with the mineralization. In fact, there are as many anomalous and highly anomalous samples outside the zone as there are within of it. The distribution of anomalous samples for this element appears to be quite random. A different but equally random distribution is shown by Sb (Fig. 16c). This element appears to be generally enriched over the monzodiorite and diorite intrusions to the east of the deposit. With the exception of two highly anomalous samples at the eastern margin and one anomalous sample near the northern limit of the zone, all samples over the mineralization have background values. Thallium (Fig 16d) appears to define a halo around the mineralization. Highly anomalous and anomalous values occur outside of the zone on the north, east and south sides and define a central low over the mineralization.

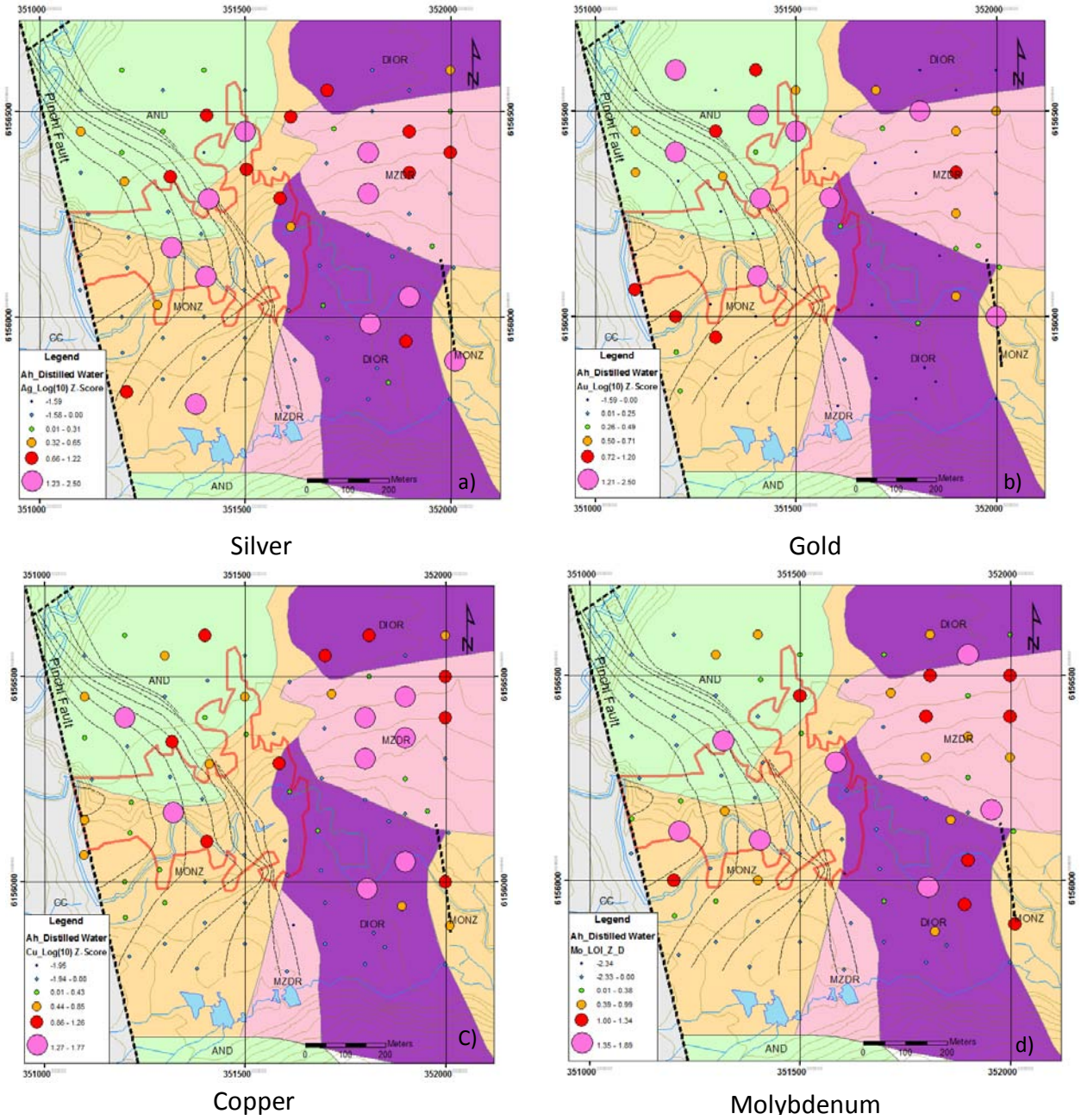

FIGURE 15 RESULTS FOR ORE ELEMENTS FOR THE DISTILLED WATER EXTRACTION OF AH HORIZON SOILS

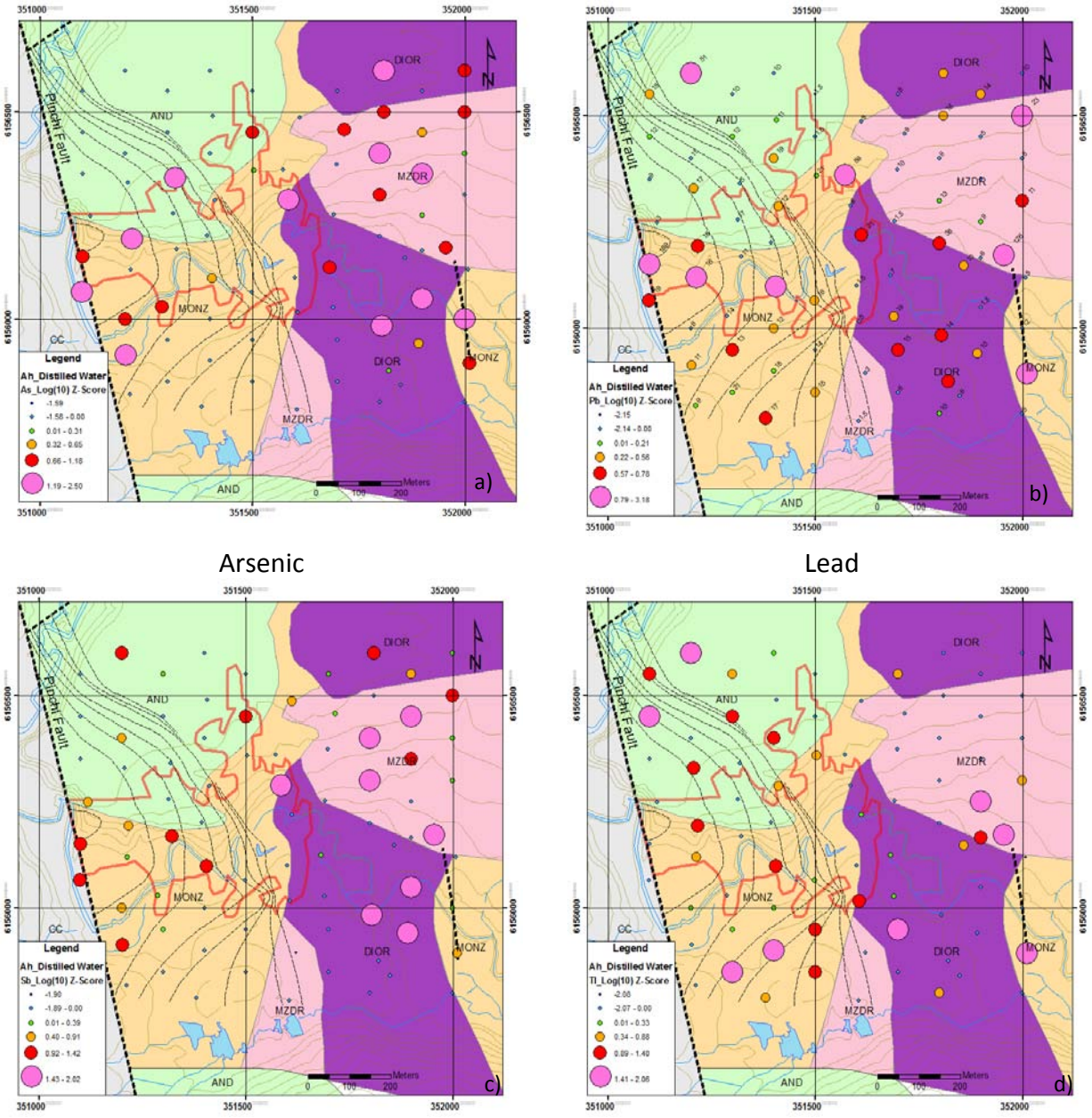

Arsenic

Lead

Antimony

Thallium

FIGURE 16 RESULTS FOR PATHFINDER ELEMENTS FOR THE DISTILLED WATER EXTRACTION OF AH HORIZON SOILS

Tungsten (Fig. 17a) has a reasonable correlation with the mineralization. Four highly anomalous samples occur within the surface projection of the zone and one occurs just outside of it to the south. In addition, four anomalous samples occur close to the Pinchi Fault near the western limit of the mineralization. Anomalous values are also present outside the zone, particularly to the east where a cluster occurs within the monzodiorite and diorite intrusions and close to a north trending fault near the eastern intrusive contact.

Zinc (Fig. 17b) also appears to be associated with these intrusions. The most anomalous samples occur near the western diorite contact at the east margin of the mineralized zone and close to a mapped fault at the eastern diorite contact.

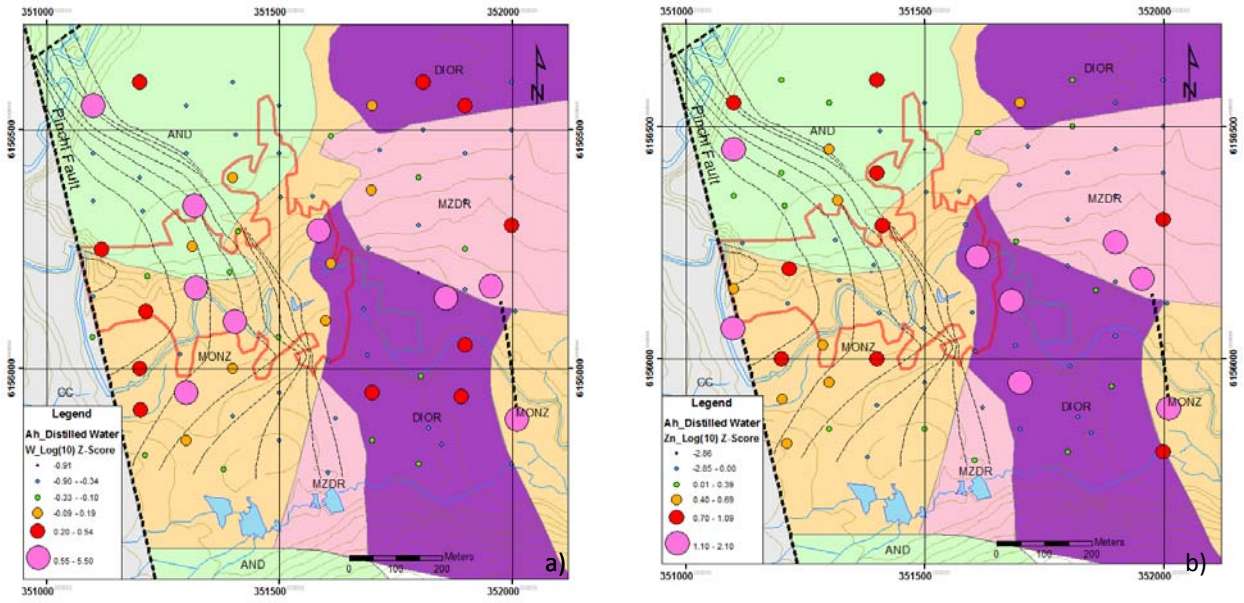

Tungsten Zinc

FIGURE 17 RESULTS FOR PATHFINDER ELEMENTS FOR THE DISTILLED WATER EXTRACTION OF AH HORIZON SOILS: W AND ZN

OTHER ELEMENTS

Of the other elements with recognizable patterns, Ca, Cd, Ce, and Sr (Fig. 18 a-d) all show enrichments over the monzodiorite and diorite intrusions to the east of the mineralization. Values over the mineralization vary from background to slightly anomalous for these elements. These patterns are most likely lithological in nature and reflect compositional differences between the more mafic dioritic intrusions and the mineralization-hosting monzonite (MONZ).

In summary, the distilled water extraction appears to highlight differences in the underlying bedrock but does not convincingly produce anomalies over the known mineralization. Some elements like As and Tl appear to define halo patterns around the mineralization although these are not clear cut responses.

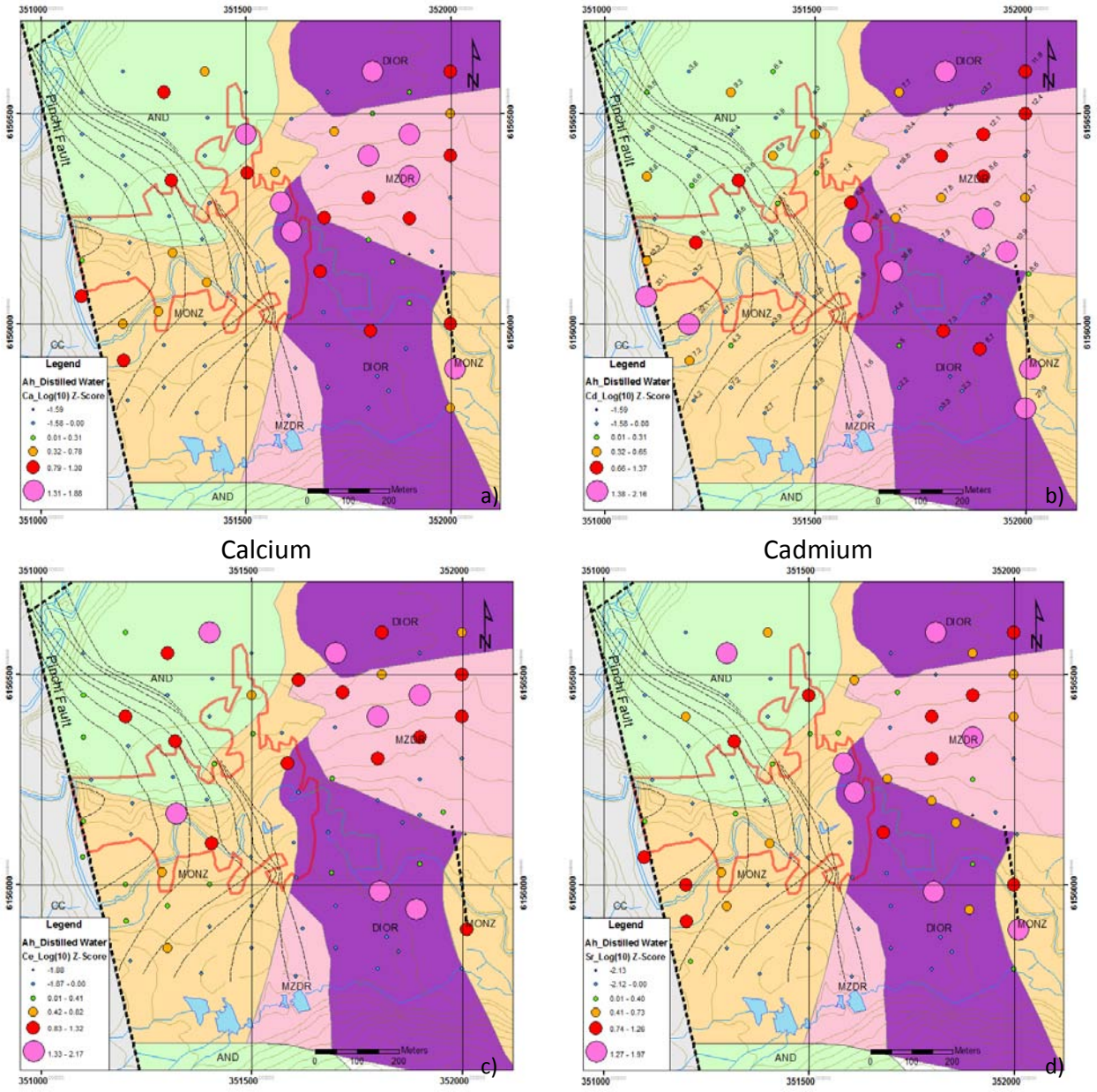

FIGURE 18 RESULTS FOR OTHER ELEMENTS FOR THE DISTILLED WATER EXTRACTION OF AH HORIZON SOILS: CA, CD, CE, SR

AH HORIZON SOIL - SODIUM PYROPHOSPHATE EXTRACTION RESULTS.

The sodium pyrophosphate is a slightly stronger extraction than distilled water. It selectively attacks organic matter in the soil and strips metals chelated from humic and fulvic compounds. Therefore typically extracted metal concentrations are positively correlated with organic carbon content (measured as % LOI in this study). When corrected for LOI, this extraction can be effective at defining signatures from blind mineral deposits.

For the purpose of interpretation, the results of the sodium pyrophosphate analyses from the 2009 transects have been merged with the samples from this project to provide more complete spatial coverage over the mineralized zone.

ORE ELEMENTS

Figure 19 shows the levelled sodium pyrophosphate results for the ore elements. Silver (Fig. 19a) has a cluster of seven highly anomalous samples located within the shape of the projected mineralization. The anomaly appears to continue northwards outside the projected mineralized zone into the Takla andesites where it is defined by two more highly anomalous samples and a group of four anomalous samples. There is little drilling in this area and therefore the presence of undiscovered mineralization explaining the continuation of the anomaly cannot be ruled out. A second cluster of anomalous values is present near to the southern limit of the survey straddling the contact between the mineralized monzonite and monzodiorite. Again it is not known if mineralization is present at depth in this area.

Gold results are presented in Figure 19b. Two clusters of anomalous samples are observed. The most important, consisting of a group of six highly anomalous and four anomalous samples, occurs directly over the central part of the mineralization. A second cluster consisting of four highly anomalous samples occurs over the monzodiorite body east of the mineralized zone. With the exception of a single highly anomalous sample near the southwest limit of the grid, the rest of the samples have low concentrations consistent with background variation.

A similar pattern is shown by Cu (Fig. 19c). Of the nine highly anomalous samples defined by the survey, eight of them occur within the surface projection of the mineralized zone: three of them at the eastern or up dip limit and five in the central part of the zone beneath the post mineral sedimentary basin cover. A single highly anomalous sample is present outside the mineralized area. This occurs in the monzodiorite to the east of the zone in the same area as the cluster of gold anomalies. Values over the rest of the grid show only background variation.

Molybdenum (Fig. 19d) has a very similar distribution to copper. The most highly anomalous samples occur within the projected outline of the mineralization and clearly highlight the position of the mineralization at shallower and intermediate depths. A loose cluster of anomalous and highly anomalous samples is also present in the intrusion to the east of the mineralized zone. These form a north-south trending zone extending from the centre of the monzodiorite south into the diorite intrusion. Coincidence between the anomalous Mo, Cu and Au values in this area may indicate previously unknown mineralization in this area.

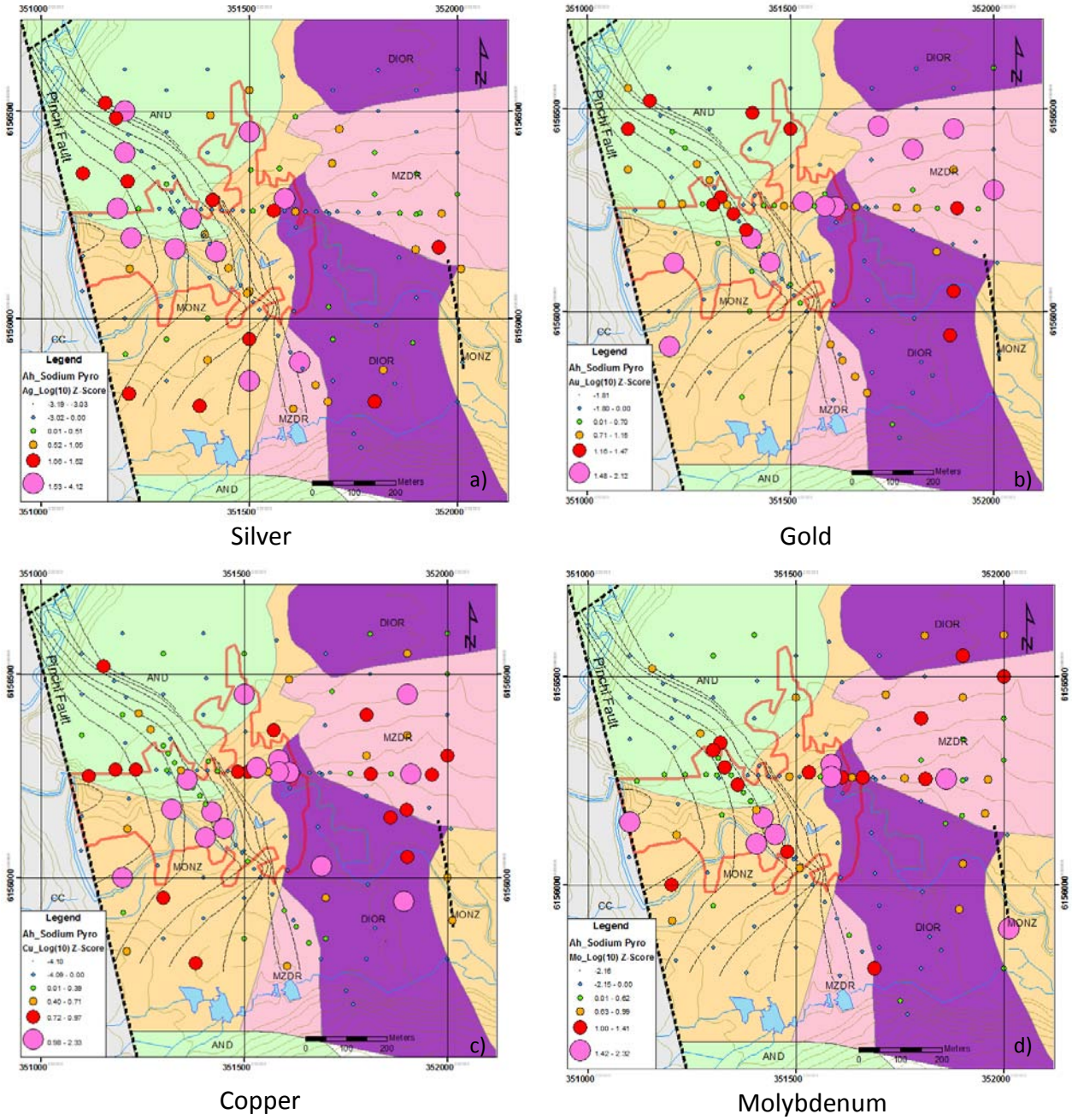

FIGURE 19 ORE ELEMENT RESULTS FOR THE SODIUM PYROPHOSPHATE EXTRACTION OF AH HORIZON SOILS: AG, AU, CU AND MO

PATHFINDER ELEMENTS

Results for selected pathfinder elements are shown in Figures 20 and 21. Arsenic (Fig. 20a) has a very similar pattern to the ore elements discussed above. Anomalous and highly anomalous samples cluster tightly within the area of the mineralization. Scattered anomalous values also occur to the east within the monzodiorite and diorite and close to the Pinchi Fault south of the mineralized zone. Mercury has a similar distribution (Fig. 20b). Maximum concentrations of this element occur within the projected limits of the mineralization. There are also a few scattered anomalous and highly anomalous values in the monzodiorite east of the zone.

Lead (Fig. 20c) has quite a different distribution to As and Hg. A few anomalous values occur over the mineralized zone but the majority of elevated values appear to be scattered in the intrusive rocks to the south and east. They form a crude arcuate pattern suggestive of a halo or partial annular zone around the Cu-Au mineralization. A more convincing halo pattern is shown by Tl (Fig. 20d). Anomalous and highly anomalous values define a circular pattern centred on the mineralized zone. Several elevated values also occur over the mineralization.

Perhaps the most compelling expression of the deep mineralization is shown by W (Fig 21a). This element was identified in the 2010 study (Heberlein and Samson, 2010) as being a potentially useful pathfinder for deep mineralization at Kwanika. Very high contrast anomalous results were identified directly over the mineralization along both sample transects. Results of the present study confirm those preliminary findings. With the exception of one highly anomalous sample located over the Takla andesites to the north of the zone, all of the most elevated values occur within the surface projection of the mineralization. Furthermore, several anomalous samples appear to form a partial halo in the intrusive rocks to the east.

Zinc (Fig. 21b) has a very different distribution from most of the elements described above. It appears to be influenced by drainage more than the underlying geology. All but one of the highly anomalous values occurs on low ground in the Kwanika creek valley suggesting that this element is being hydromorphically concentrated in wet, organic rich soils close to the creek. Despite correcting the results for soil moisture and LOI, this pattern remains very strong. Only one highly anomalous sample occurs within the projected area of mineralization away from the drainage.

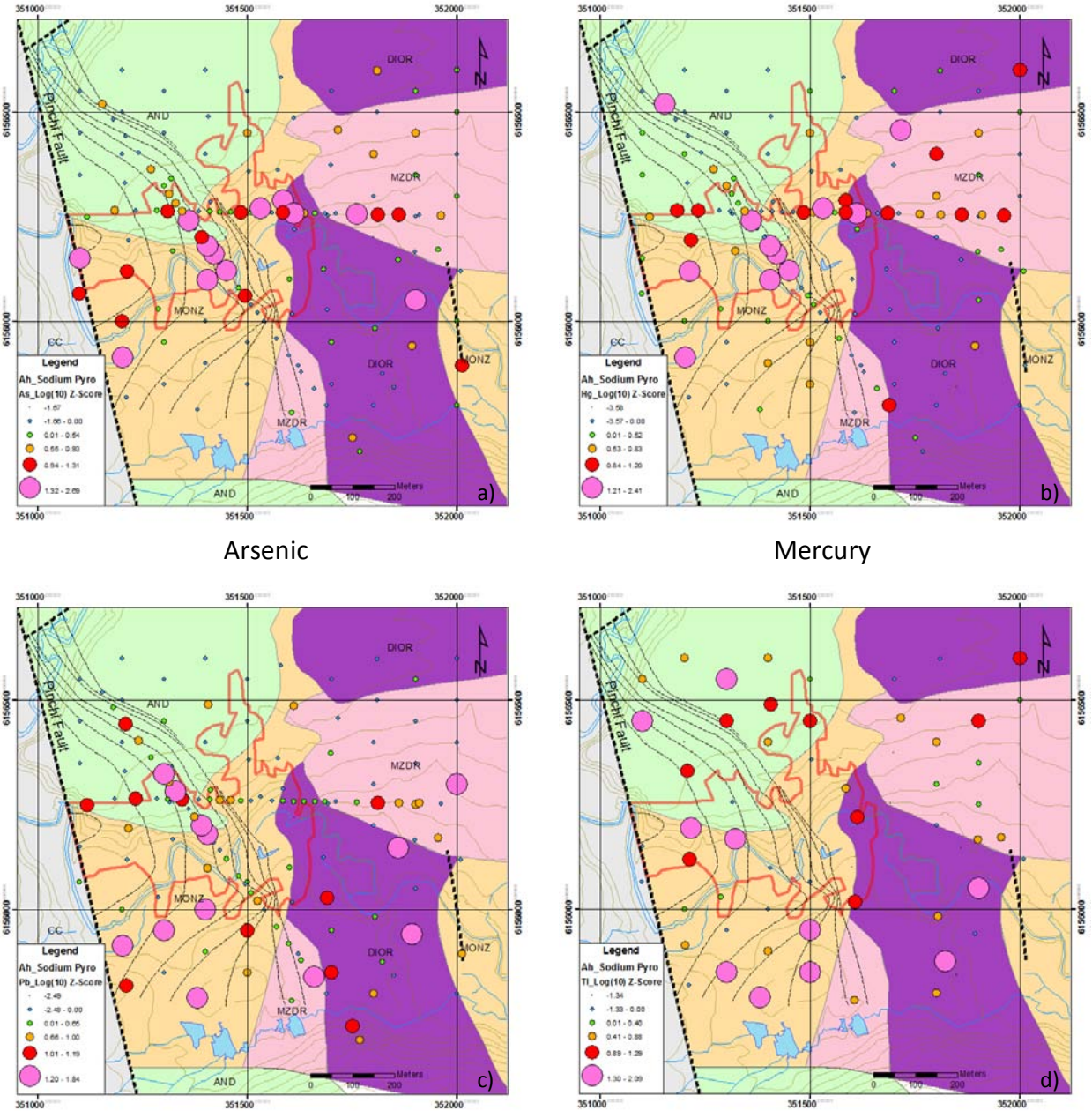

Arsenic Mercury

Lead Thallium

FIGURE 20 PATHFINDER ELEMENT RESULTS FOR THE SODIUM PYROPHOSPHATE EXTRACTION OF AH HORIZON SOILS: AS, HG, PB AND TL

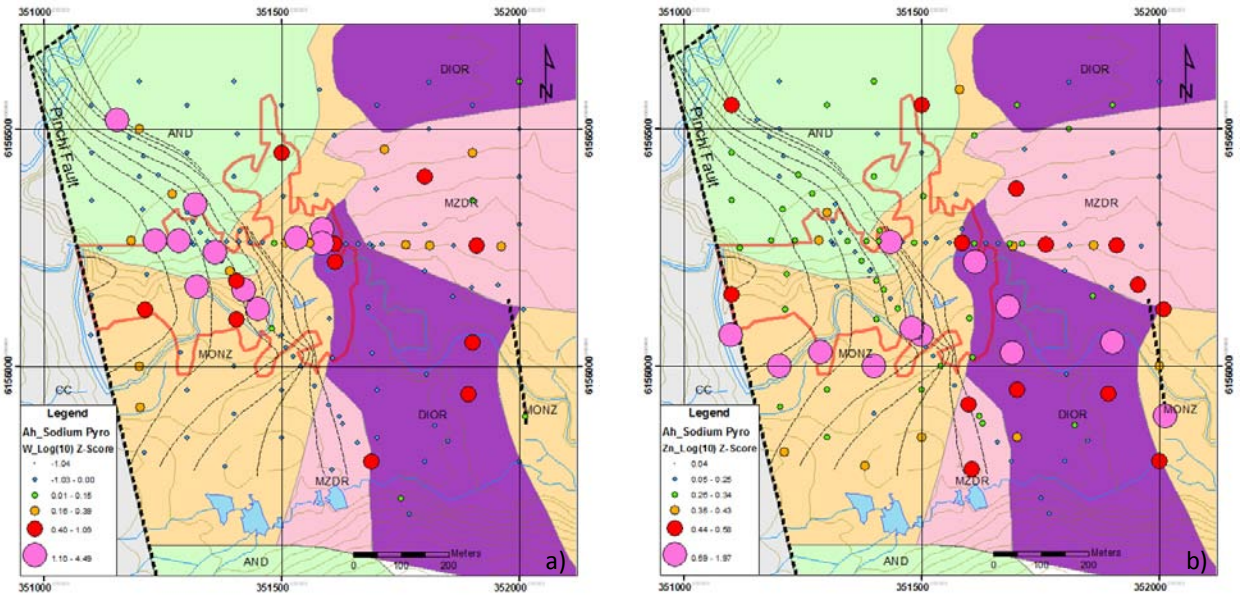

Tungsten Zinc

FIGURE 21 PATHFINDER ELEMENT RESULTS FOR THE SODIUM PYROPHOSPHATE EXTRACTION OF AH HORIZON SOILS: W AND ZN

OTHER ELEMENTS

A number of other elements that are not considered to be ore or pathfinder elements display recognizable patterns over or around the mineralized zone. These are illustrated in Figures 22 and 23.

Barium defines the position of the underlying mineralization quite well (Fig. 22a). It has a cluster of six highly anomalous samples over the northern limit of the mineralized zone and three anomalous values near the eastern margin. Elsewhere on the grid, small clusters of elevated values occur in the monzodiorite east of the mineralized zone and also close the southern boundary adjacent to the Pinchi Fault.

A different pattern is shown by Ca (Fig. 22b). Elevated values for this element define a northeast trend across the study area. About half of the anomalous and highly anomalous samples lie within the projection of the mineralization. The remainder occurs over the monzodiorite and diorite intrusions to the northeast. The significance of this trend is not apparent.

Cadmium (Fig. 22c) quite surprisingly shows a very different distribution from Zn. Typically, this element closely follows Zn but not in this case. Cadmium defines a loose cluster of nine highly anomalous and three anomalous samples over or immediately adjacent to the mineralized zone. The correlation with the projected mineralization is very good. Scattered anomalous samples also occur over the monzodiorite and diorite intrusion to the east of the zone but do not form a coherent cluster.

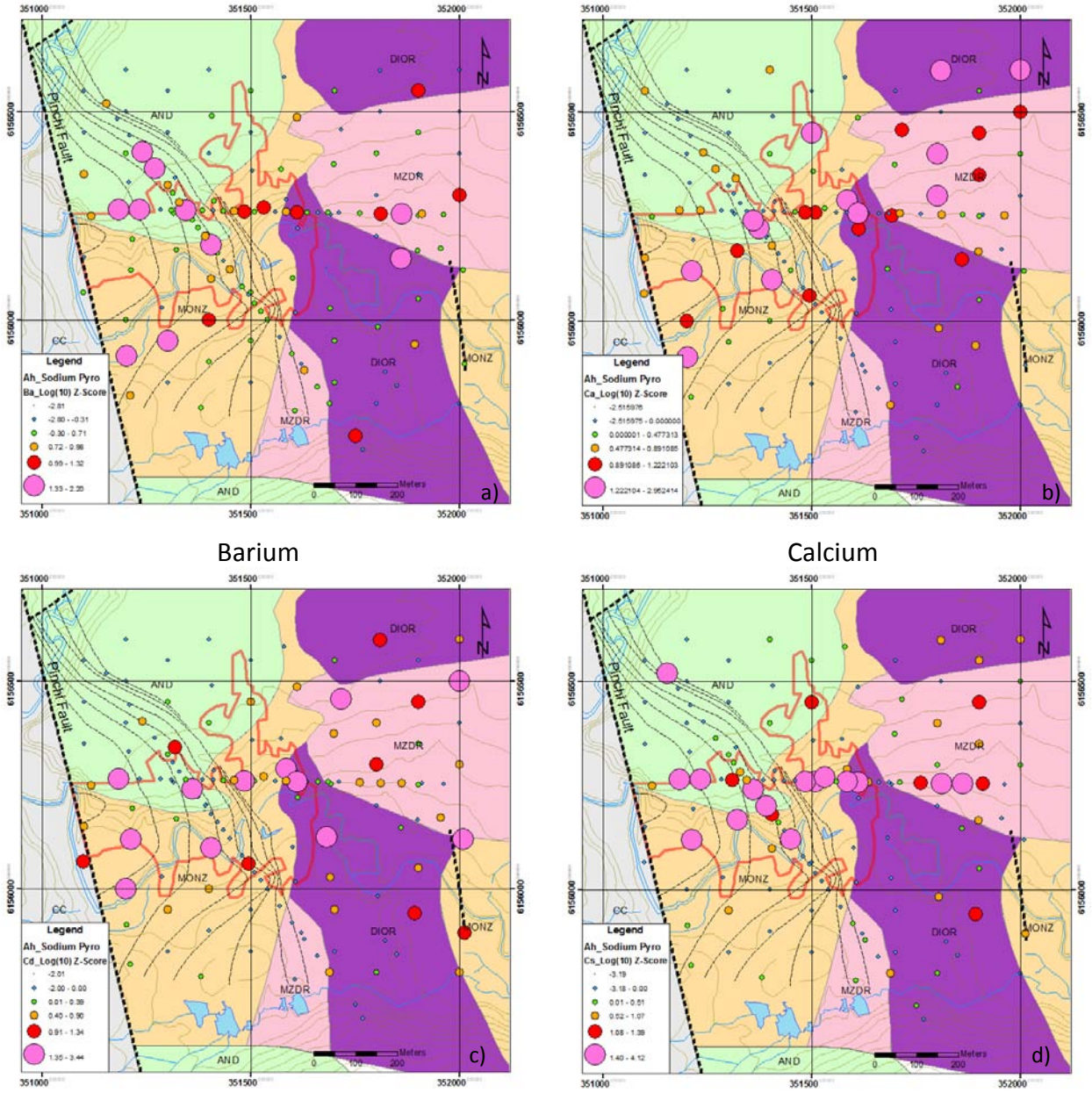

Barium

Calcium

Cadmium

Cesium

FIGURE 22 OTHER ELEMENT RESULTS FOR THE SODIUM PYROPHOSPHATE EXTRACTION OF AH HORIZON SOILS: BA, CA, CD AND CS

Another element that is clearly anomalous over the mineralized zone is Cs (Fig. 22d). This element behaves in much the same way as Rb and K and likely reflects the presence of potassic alteration associated with mineralization at depth. A total of 12 highly anomalous samples and three anomalous samples lie within the projected outline of the mineralized zone. A small group of anomalous samples also occurs in the monzodiorite to the east. Over the remainder of the grid only background values are observed.

Results for the rare earth elements Ce and La are illustrated in Figure 23. As might be expected, these elements show more or less the same patterns. Cerium appears to highlight the underlying mineralization with a group of anomalous and highly anomalous values present within the projected outline of the mineralization. Anomalous values extend to the northwest into the Takla andesite in a pattern similar to that of Ag for this extraction (Fig. 19a). The monzodiorite east of the mineralized zone also appears to be quite anomalous for Ce. Lanthanum (Fig. 23b) highlights these trends even more strongly, showing the monzodiorite unit to be particularly anomalous.

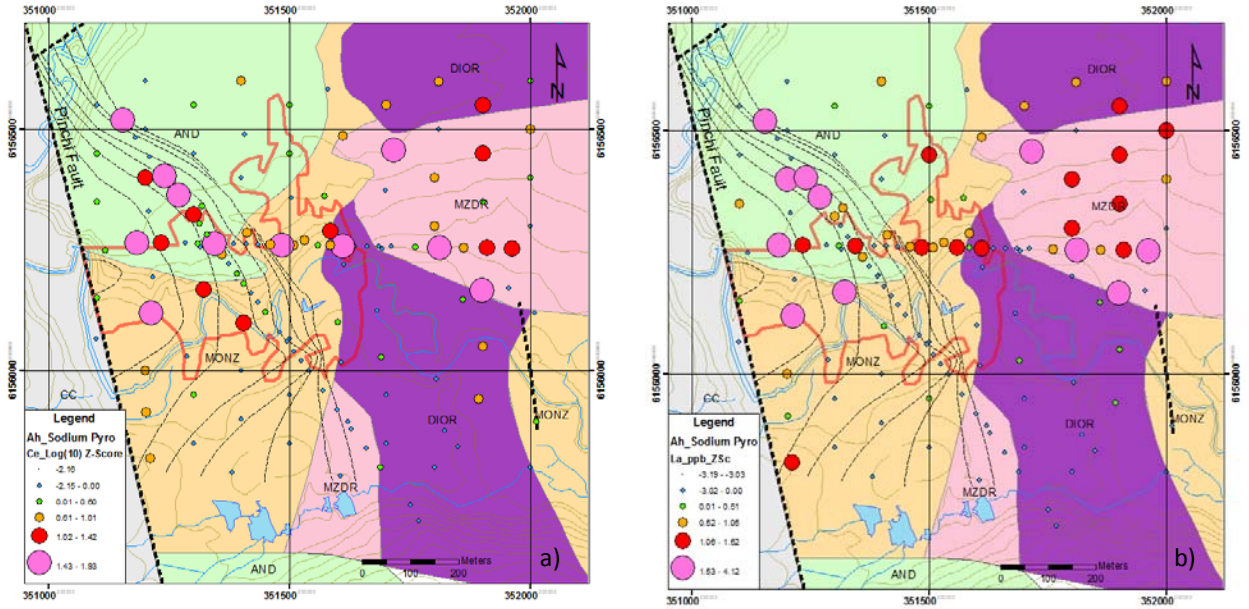

FIGURE 23 OTHER ELEMENT RESULTS FOR THE SODIUM PYROPHOSPHATE EXTRACTION OF AH HORIZON SOILS: CE AND LA

AH HORIZON SOIL - ULTRATRACE AQUA REGIA RESULTS

The Ultratrace aqua regia digestion is the most aggressive of the three extractions performed on the Ah horizon soils. While less aggressive than a conventional aqua regia, the Ultratrace method has the capability to digest precious metals, organic matter, iron and manganese oxides, and to liberate adsorbed metals associated with clays and some silicate minerals.

ORE ELEMENTS

Results for the ore elements Ag, Au, Cu and Mo are presented in Figure 24.

Silver (Fig 24a) shows a reasonable correlation with the projected limits of the mineralization. Four highly anomalous and two anomalous values occur directly over the zone. A second cluster of elevated values is present to the south of the mineralization over a small wedge of monzodiorite. This area has no known mineralization and the reason for these elevated values is unknown.

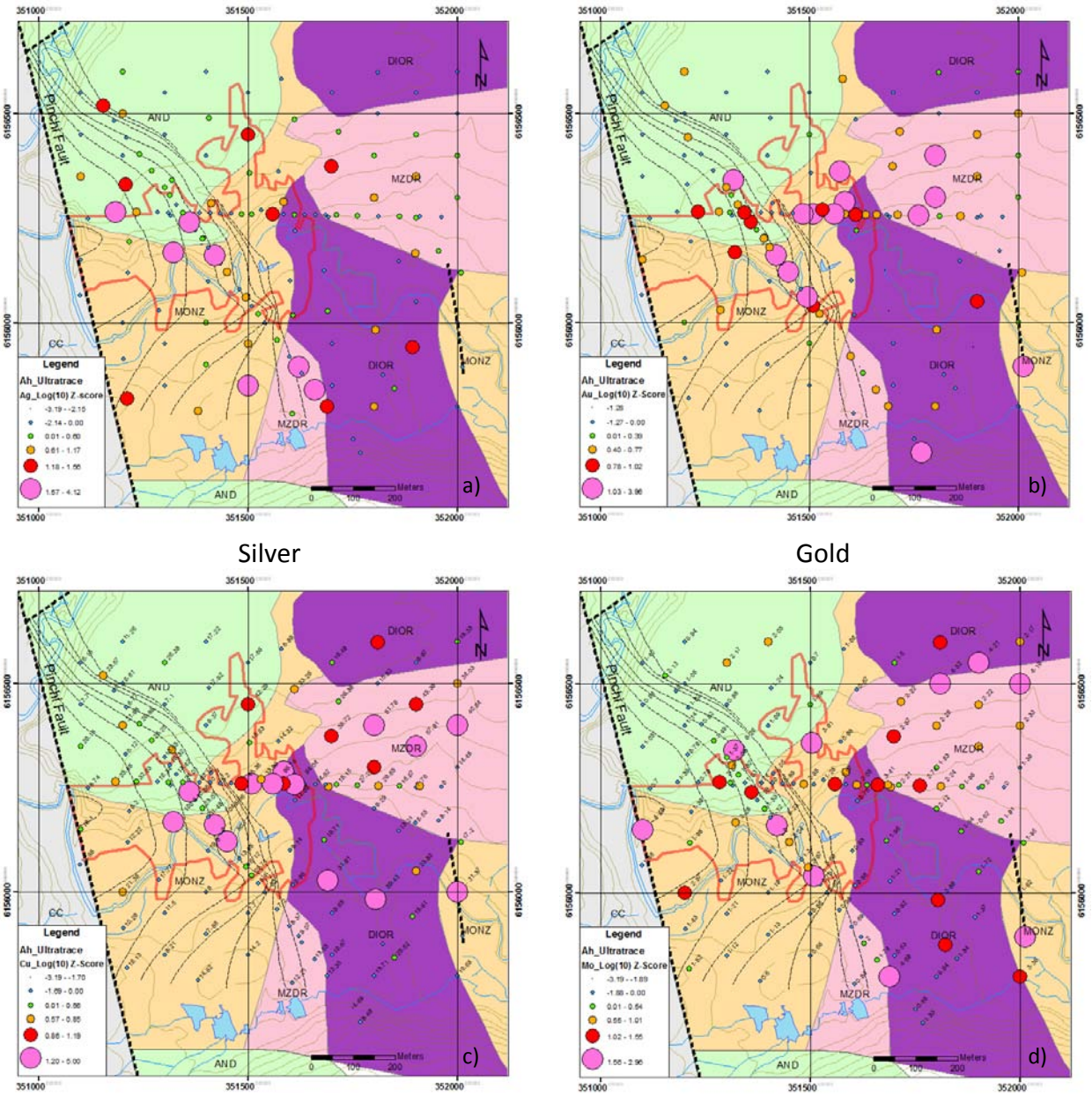

Silver

Gold

Copper

Molybdenum

FIGURE 24 ORE ELEMENT RESULTS FOR THE ULTRATRACE AQUA REGIA DIGESTION FROM AH HORIZON SOILS: AG, AU, CU AND MO

Gold results are illustrated in Figure 24b. Anomalous and highly anomalous values group within the projected limits of the mineralization clearly defining the zone. A second group of three highly anomalous values is present in the monzodiorite immediately to the east. Elsewhere in the study area, with the exception of two isolated samples in the southeast part of the survey area, values are at background levels. Patterns for Cu (Fig. 24c) are similar to those for Au. Copper forms a well defined anomaly over the central and eastern (shallower) parts of the mineralized zone defined by eight highly anomalous and three anomalous samples. As seen in the Au results, the monzodiorite body to the east is also highly anomalous, with a grouping of three highly anomalous and three anomalous samples. Three highly anomalous samples present to the southeast of the mineralized zone follow the Kwanika Creek drainage. These are possibly hydromorphic anomalies occurring in seepage zones along the break in slope on the valley floor.

Patterns for Mo (Fig. 24d) are less convincing than those of the other ore elements. There is a loose grouping of anomalous and highly anomalous values overtop of the mineralization, however similar groupings are also present outside the mineralized zone to the northeast and southeast. The net effect of these anomalous sample clusters is to reduce the significance of the anomaly over the mineralization. If there were no prior knowledge of the mineralization at depth, it would be difficult to identify which cluster represents the most important target.

PATHFINDER ELEMENTS

Results for several pathfinder elements are shown in Figures 25 and 26.

Arsenic (Fig. 25a) has a robust response over the mineralized zone. Eight highly anomalous and nine anomalous samples clearly define the position of the underlying mineralization. Unlike many other elements discussed previously, As seems to be detecting the deeper parts of the mineralization adjacent to the Pinch Fault as well as expressions of shallower mineralization in the central and eastern parts of the zone. The diorite and monzodiorite unit east of the mineralization also have a highly anomalous response. The rest of the grid, particularly over the monzonite and Takla andesite units, has only background values.

Bismuth patterns (Fig. 25b) are quite similar to As. It displays a well focused anomaly consisting of six highly anomalous and four anomalous samples over the mineralization. Unlike As it has no positive response over the deeper parts of the mineralization near the Pinchi Fault. The monzodiorite and diorite intrusions east of the mineralized zone are strongly anomalous for this element. Anomalous and highly anomalous values extend almost over the entire surface area of the intrusions. Samples over the Takla andesite and mineralized monzonite have very low values consistent with background.

Anomalous Pb values are shown in Figure 25c. This element, as illustrated by the sodium pyrophosphate extraction, appears to form a halo around the mineralized zone. Anomalous and highly anomalous values are present at a more or less even distance outside the limits of the mineralization on the north, east and south sides. Samples over the mineralization are erratically anomalous but do not constitute a meaningful response.

Antimony (Fig. 25d) appears to mimic the northeast trend observed in the sodium pyrophosphate Ca. Anomalous and highly anomalous samples occur over the central and eastern (shallower) parts of the mineralized zone. Elevated values continue to the northeast into the monzodiorite where a group of six highly anomalous samples is present. Two highly anomalous samples to the south of the monzodiorite lie within the Kwanika Creek drainage. As observed with Cu (Fig. 24c) these possibly represent hydromorphic concentrations in the damp organic rich soils close to the drainage.

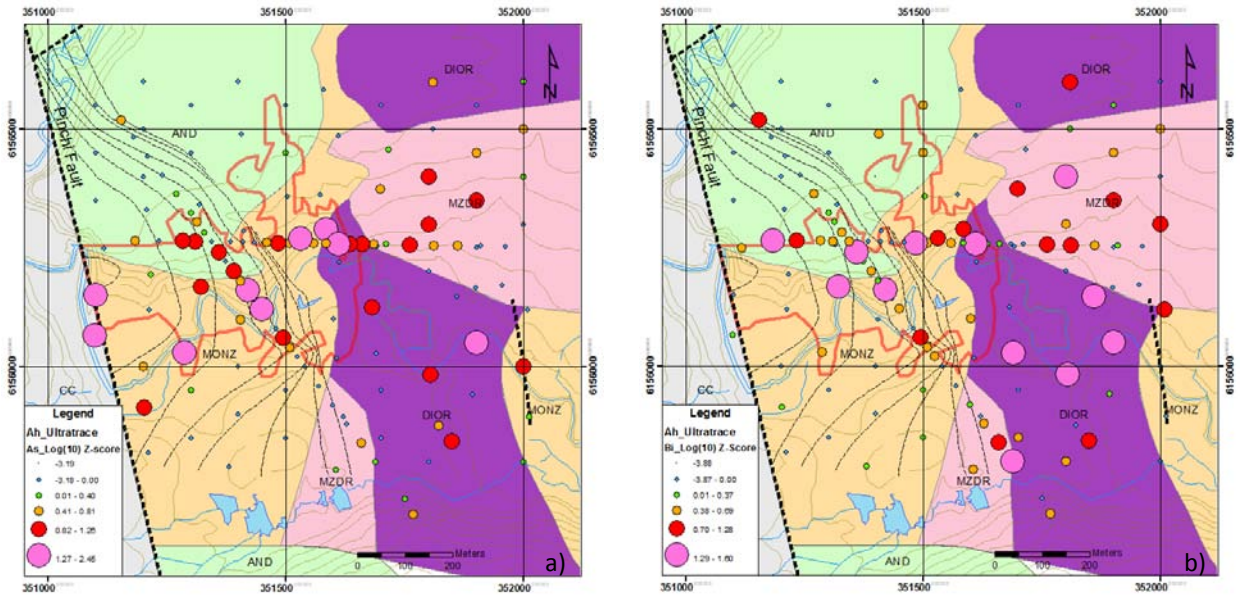

Arsenic

Bismuth

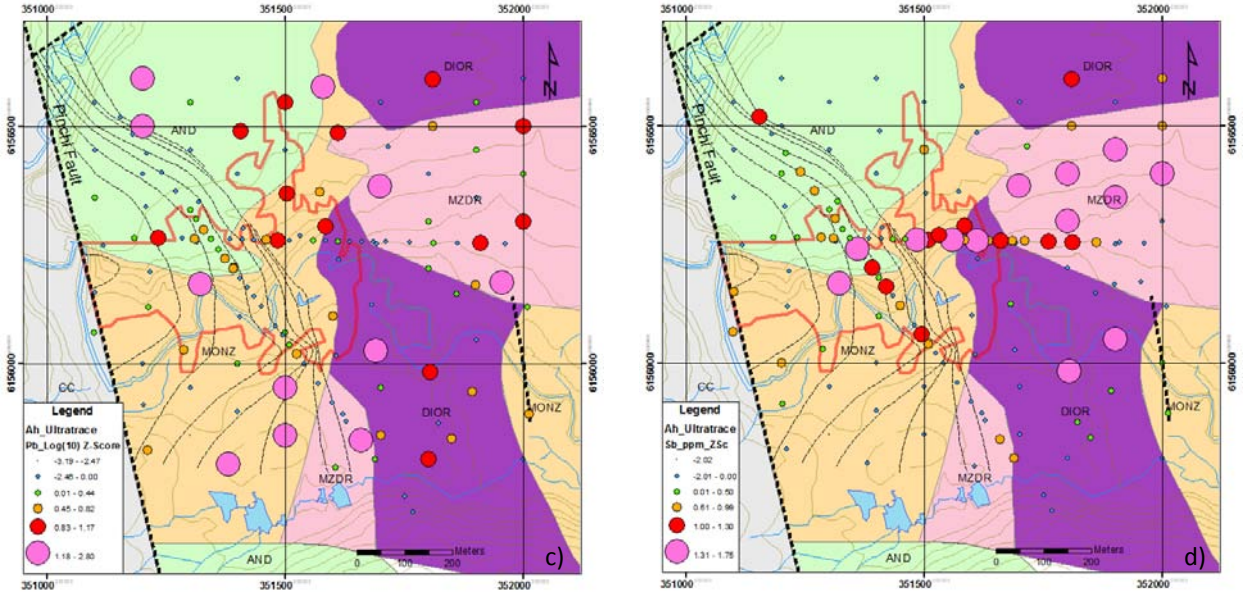

Lead

Antimony

FIGURE 25 ORE ELEMENT RESULTS FOR THE ULTRATRACE AQUA REGIA DIGESTION OF AH HORIZON SOILS: AS, BI, PB, SB

Tungsten once again proves to be a reliable indicator of the mineralization. Figure 26a shows how highly anomalous W values cluster over the central and eastern portions of the mineralized zone. Away from the mineralization, W values are low (mostly at detection limit) with only a few scattered anomalous values that do not form coherent patterns.

Zinc (Fig. 26b) is also fairly tightly constrained to the mineralized zone. Rather than defining a tight apical response like W, it seems to occur as a halo around the edges of the mineralization.

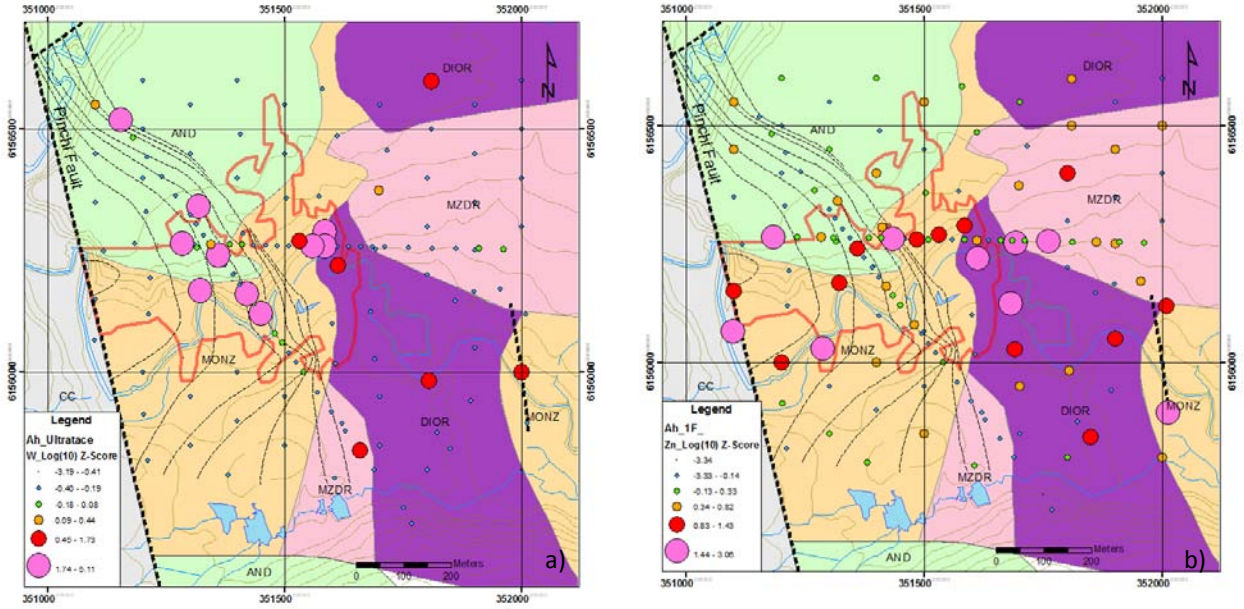

Tungsten Zinc

FIGURE 26 OTHER ELEMENT RESULTS FOR THE ULTRATRACE AQUA REGIA DIGESTION OF AH HORIZON SOILS: W AND ZN

OTHER ELEMENTS

Several other elements show interesting patterns. Results for Ca are shown in Figure 27a. This element highlights the monzodiorite intrusion to the east of the mineralized zone as being highly anomalous. Anomalous values also occur over the eastern part of the mineralization but have lower overall values than the adjacent intrusion. As seen for other elements, the pattern of anomalous samples defines a general northeast trend from the mineralized zone. Cadmium also shows this trend (Fig. 27b) with a line of highly anomalous samples extending northeastwards from the eastern part of the mineralized zone. Highest values occur on the monzodiorite and diorite at the eastern margin of the mineralization.

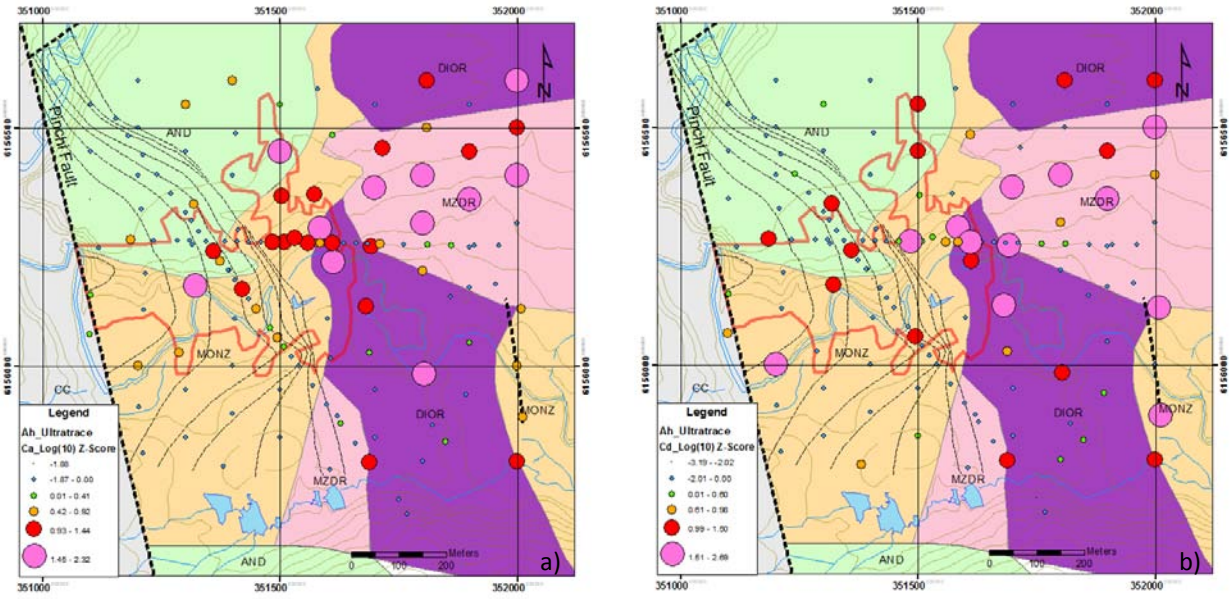

Calcium Cadmium

FIGURE 27 RESULTS FOR THE ULTRATRACE AQUA REGIA DIGESTION OF AH HORIZON SOILS: CA AND CD

CHARCOAL – ULTRATRACE AQUA REGIA EXTRACTION.

The effectiveness of charcoal as a sampling medium is unknown. The widespread occurrence of charcoal in Central BC boreal forest soils and its extremely high adsorption and absorption capacity suggests that it should pick up mobile ions derived from blind mineralization and produce credible multi-element anomalies.

ORE ELEMENTS

Results for the ore elements are presented in Figure 28. Silver (Fig. 28a) has a flat background over most of the grid. Highly anomalous samples occur at two locations: a cluster of five samples located over the western (deeper) part of the mineralized zone; and a pair of highly anomalous samples over monzonite near the south grid boundary. Three of the samples in the first group lie within the outline of the mineralization and the other two occur over Takla andesite slightly north of the zone. Gold (Fig. 28b) has a similar distribution. This element has three distinct groups of anomalous samples. Four anomalous samples occur within the outline of the mineralization. Two more occur in the monzonite near the southern grid limit. These are coincident with the anomalous Ag values in that area. Another pair of highly anomalous samples occurs over diorite to the southeast of the mineralized zone.

Copper (Fig. 28c) results show two distinct groups of anomalous samples. The largest group, consist of three highly anomalous and two anomalous samples straddling the northern margin of the mineralized zone. Three of the samples occur directly over the central-west part of the mineralization. The other two lie just to the north of the zone over the Takla andesites and close to the Pinchi Fault. A second group of four anomalous values occurs at the northeast corner of the survey area over the contact between monzodiorite and diorite. This anomaly is unexplained.

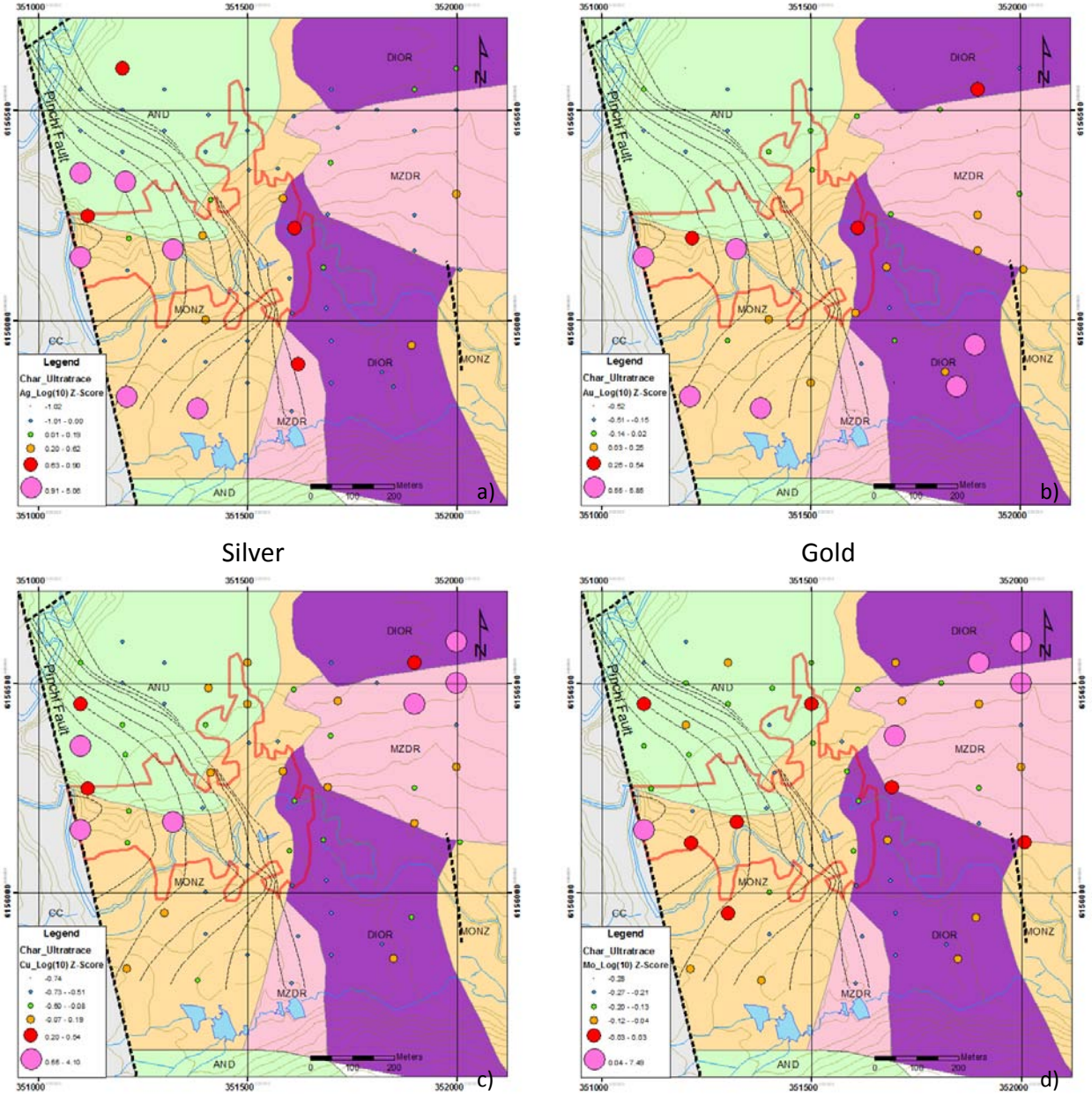

Silver

Gold

Copper

Molybdenum

FIGURE 28 ORE ELEMENT RESULTS FOR THE ULTRATRACE AQUA REGIA DIGESTION OF CHARCOAL: AG, AU, CU AND MO

Results for Mo are shown in Figure 28d. Molybdenum does not have a convincing response over the mineralized zone. Three anomalous samples and one highly anomalous sample are scattered across the surface projection of the mineralization but do not form a coherent anomaly. The most interesting cluster of anomalous samples occurs northeast of the zone at the corner of the grid. Here, three highly anomalous samples cluster over the monzodiorite-diorite contact. There is no known mineralization in this area to explain this feature.

PATHFINDER ELEMENTS

Pathfinder element patterns are presented in Figures 29 and 30. Arsenic (Fig. 29a) displays background values over most of the study area; however two areas of anomalous values stand out. One consists of two highly anomalous samples located over the western, deeper parts of the mineralized zone. One of these samples adjacent to the Pinchi Fault has a Z-Score value of over 7 indicating an extremely anomalous sample. The second anomalous area lies in the northeast corner of the grid and is coincident with the Cu and Mo anomalies mentioned above. This feature is relatively weak in comparison to the response over the mineralization, consisting of one highly anomalous and one anomalous sample.

Bismuth (Fig. 29b) shows a similar pattern to As but with a more noisy background. Two highly anomalous samples (the same two) highlight the deeper parts of the mineralized zone. Values around the mineralization, with the exception of one highly anomalous sample near the Pinchi Fault to the north, tend to be at background levels. Elevated values are present over the intrusions to the east of the mineralized zone. Once again, the northeast corner of the grid shows up as being highly anomalous. Two anomalous values are also noted over the diorite to the southeast of the zone.

The same patterns are shown by Sb (Fig. 29c). The responses over the mineralization and over the northeast corner of the grid are almost identical to those of As and Bi. Tungsten however, shows a quite different pattern (Fig. 29d). This element highlights the mineralization with a group of five highly anomalous samples; three occurring within the projected outline of the zone and two present over the Takla andesites immediately adjacent to the northern edge of the mineralization. Interestingly this element does not have an anomaly in the northeast corner of the grid. Scattered anomalous values also occur in the southern part of the study area but do not present a coherent pattern.

Results for Pb and Zn are shown in Figure 30. Lead (Fig. 30a) appears to form a partial halo around the northern limits of the projected mineralized zone. This feature is defined by an arcuate trend of seven anomalous and highly anomalous samples located just outside of the northern edge of the mineralization. Scattered anomalous values also occur to the south. Two of these occur over the limit of the mineralization but they are too sparse to be able to call them a halo.

Zinc (Fig. 30b) does not have an easily recognizable pattern over the mineralization. Highly anomalous samples are scattered over the mineralized zone with four samples occurring over the edges and one in the centre. Anomalous samples are also loosely clustered in the northeast part of the study area in the same area noted to be anomalous for Cu and Mo.

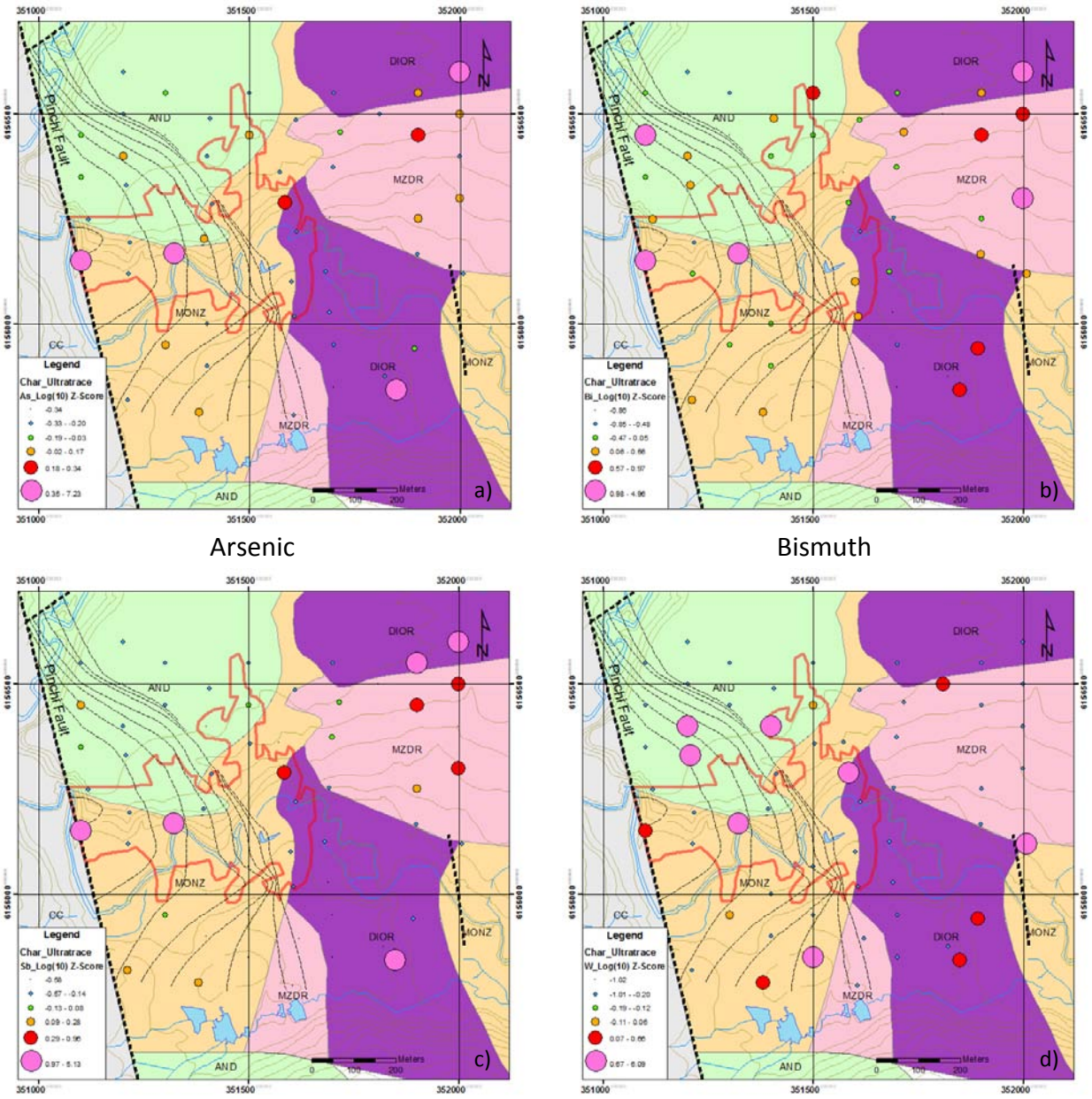

Arsenic

Bismuth

Antimony

Tungsten

FIGURE 29 PATHFINDER ELEMENT RESULTS FOR THE ULTRATRACE AQUA REGIA DIGESTION OF CHARCOAL: AS, BI, SB AND W

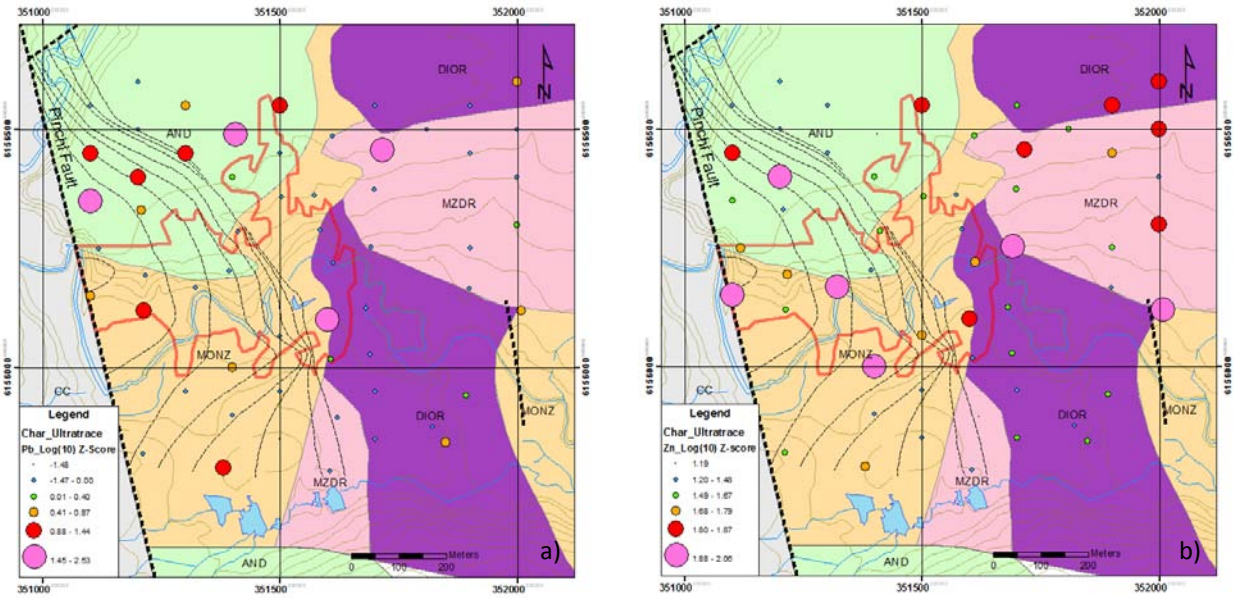

FIGURE 30 PATHFINDER ELEMENT RESULTS FOR THE ULTRATRACE AQUA REGIA DIGESTION OF CHARCOAL: PB AND ZN

VEGETATION RESULTS

FIR NEEDLES – AQUA REGIA

The nitric acid then aqua regia digestion of the dry vegetation tissues is nearly a total digestion for all elements. The precision of the analytical method is good to excellent for most elements except for Au and some of the high field strength elements (e.g. Hf, Nb, Ti, Zr), which generally have inferior precision.

ORE ELEMENTS

Each plant species and type of tissue (i.e. bark, twigs, needles etc.) has a different capability to absorb and store elements. In the case of the subalpine fir needles, they have a low sensitivity to Au in this environment and all samples returned concentrations below the detection level of 0.2 ppb Au. Silver (Fig. 31a) is detectable and, although concentrations are in the low ppb level and barely above detection, 7 of the 17 highest values are in samples from directly over the mineralization, with most of the others loosely clustered over the monzodiorite immediately to the east. Copper (Fig. 31b) is an element that is required for a plant's metabolism and so concentrations of a few ppm Cu are typical and only excesses to those levels are likely to be attributable to any concealed mineralization. In situations where a geochemical signature is subtle, it is commonly difficult to distinguish a 'mineralization' from a 'metabolic' signature. This is the case at Kwanika where the higher Cu concentrations are located near the Pinchi Fault and over the monzodiorite and diorite to the east. Of note is a line of relatively anomalous values following the trend of the small fault in the east. This trend is also seen in Fig. 31c for Mo (also a plant requirement, but only in very small traces). Molybdenum, however, occurs mostly around the periphery of the mineralization and over the monzodiorite to the east.

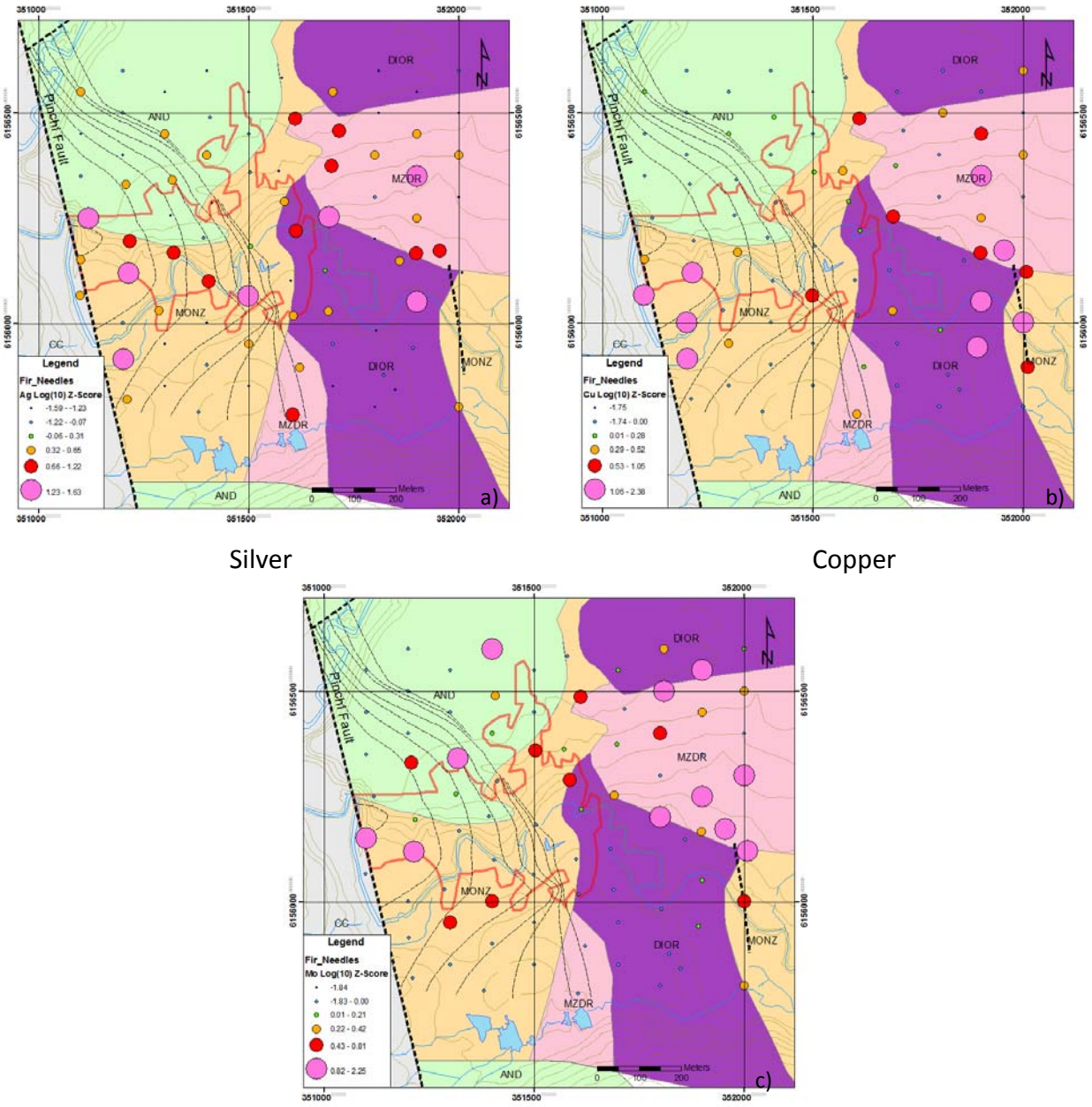

Silver

Copper

Molybdenum

FIGURE 31 ORE ELEMENT RESULTS FOR THE AQUA REGIA DIGESTION OF DRY FIR NEEDLES: AG, CU AND MO

PATHFINDER ELEMENTS

Results for several pathfinder elements are presented in Figure 32.

Arsenic is present at very low levels (Fig. 32a), with few samples above the detection limit of 0.1 ppm, and the highest value only 0.3 ppm at which level precision is rather poor. It is therefore quite surprising that there appears to be a reasonably well-defined halo of slightly elevated concentrations around the deposit. Lead levels are low with only one sample yielding over 0.2 ppm. However, the plot of Pb (Fig. 32b) also shows that slightly elevated levels are marginal to the deposit. Bismuth was below detection in all samples and Sb is mostly at or just above detection.

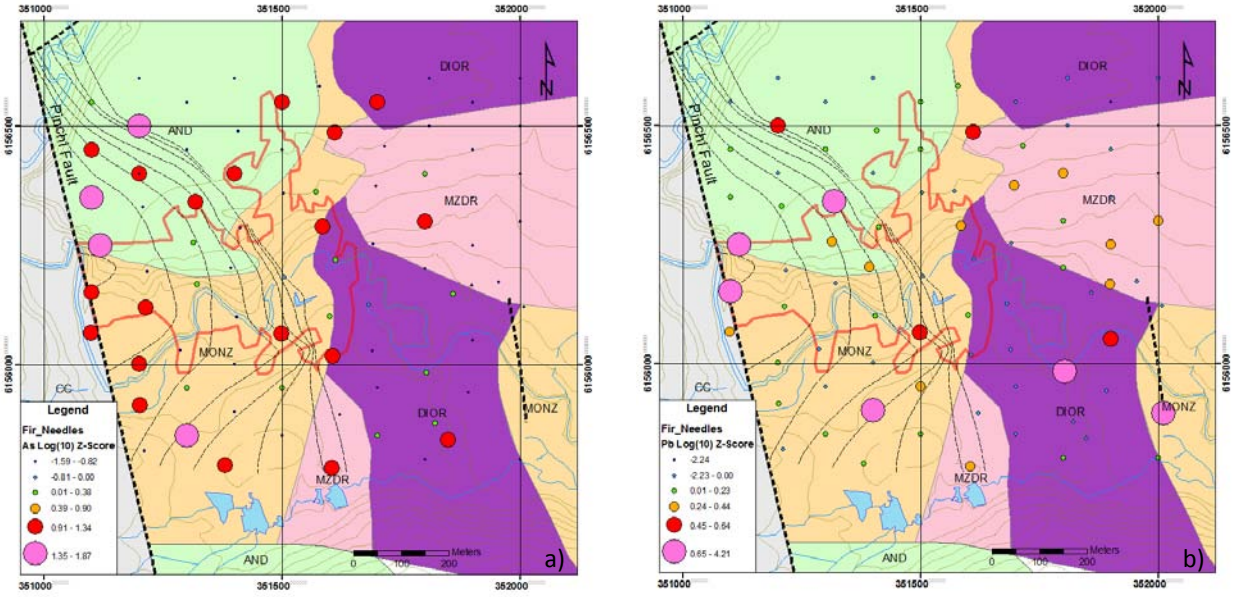

Arsenic Lead

FIGURE 32 ORE ELEMENT RESULTS FOR THE AQUA REGIA DIGESTION OF DRY FIR NEEDLES: AS AND PB

OTHER ELEMENTS

Figure 33 shows plots of several elements that exhibit a spatial relationship to the zone of mineralization.

Of note is an annulus of samples with elevated levels of Tl, Cd, Zn and Ni (Fig. 33). The depletion of the elements shown in Figure 33 over the zone of mineralization is emphasized in Figure 34 by a 3D plot of the Tl data. Other elements showing this depletion are Ca, Sr, Ba and REE (Fig. 35).

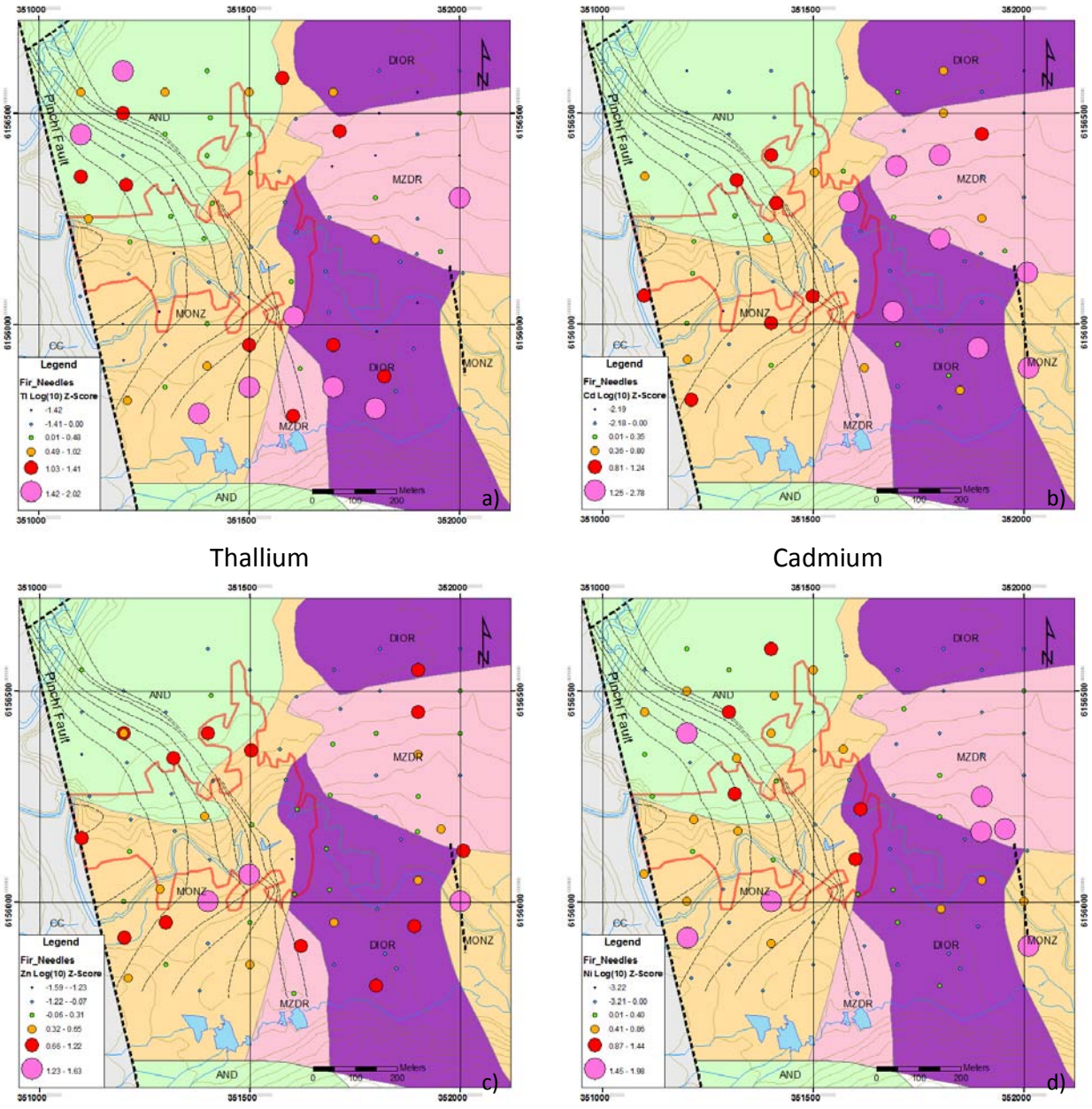

Thallium Cadmium

Zinc Nickel

FIGURE 33 OTHER ELEMENT RESULTS FOR THE AQUA REGIA DIGESTION OF DRY FIR NEEDLES: TL, CD, ZN AND NI

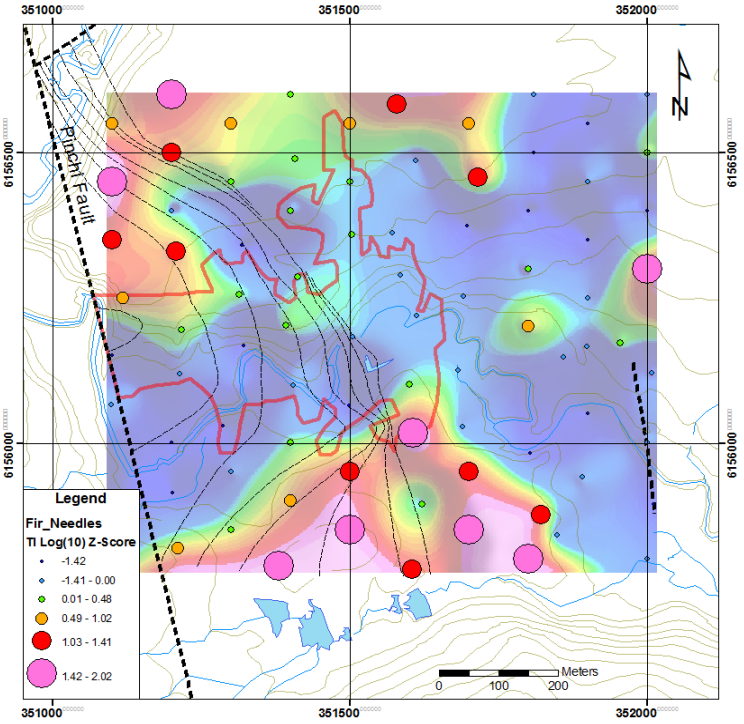

FIGURE 34 A GRIDDED IMAGE OF THALLIUM IN FIR NEEDLES SHOWING DEPLETION OVER MINERALIZATION

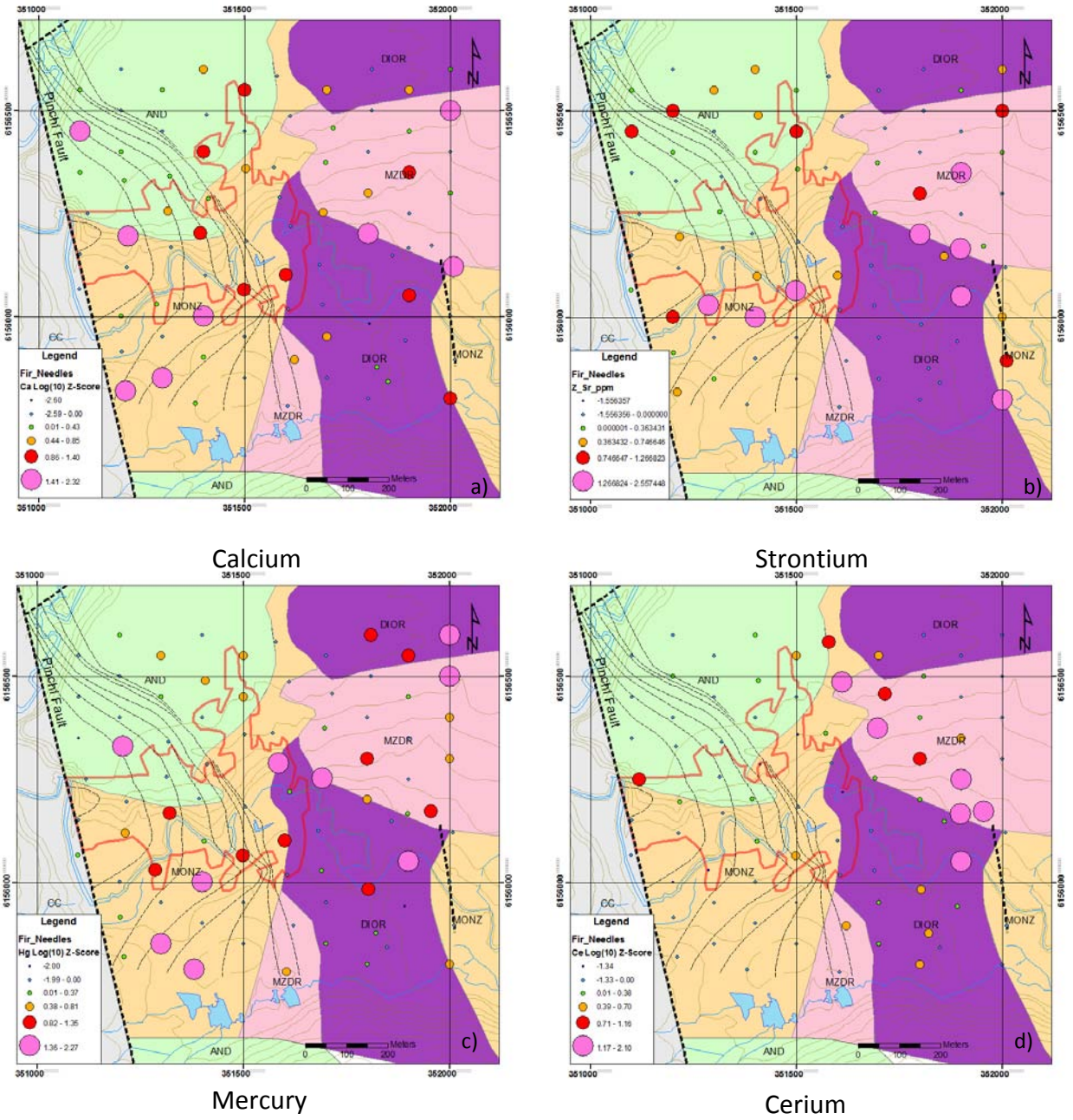

FIGURE 35 OTHER ELEMENT RESULTS FOR THE AQUA REGIA DIGESTION OF DRY FIR NEEDLES: BA, SR, HG AND CE

PINE BARK – AQUA REGIA

The acid digestion and analysis of the dry bark scales was by the same method as for the fir needles. As noted above, because of the different requirements for and tolerances to elements in the substrate, the composition of the bark is different from that of the fir needles. For many elements the concentrations are higher in the bark, because trees tend to move elements that they can tolerate, but are not required for growth, to their extremities.

ORE ELEMENTS

Results for the ore elements Ag, Au, Cu and Mo are presented in Figure 36.

Unlike the fir needles, nearly all the bark samples had detectable Au, and Ag concentrations were more than an order of magnitude higher than in the fir. Copper concentrations were similar to those of the fir needles, and Mo generally lower. Highest concentrations were not over the mineralization but, once again, marginal to that area and concentrated mostly at sites over the monzodiorite and diorite. Some of the highest Cu and Mo concentrations occur in proximity to the fault in the eastern part of the survey area.

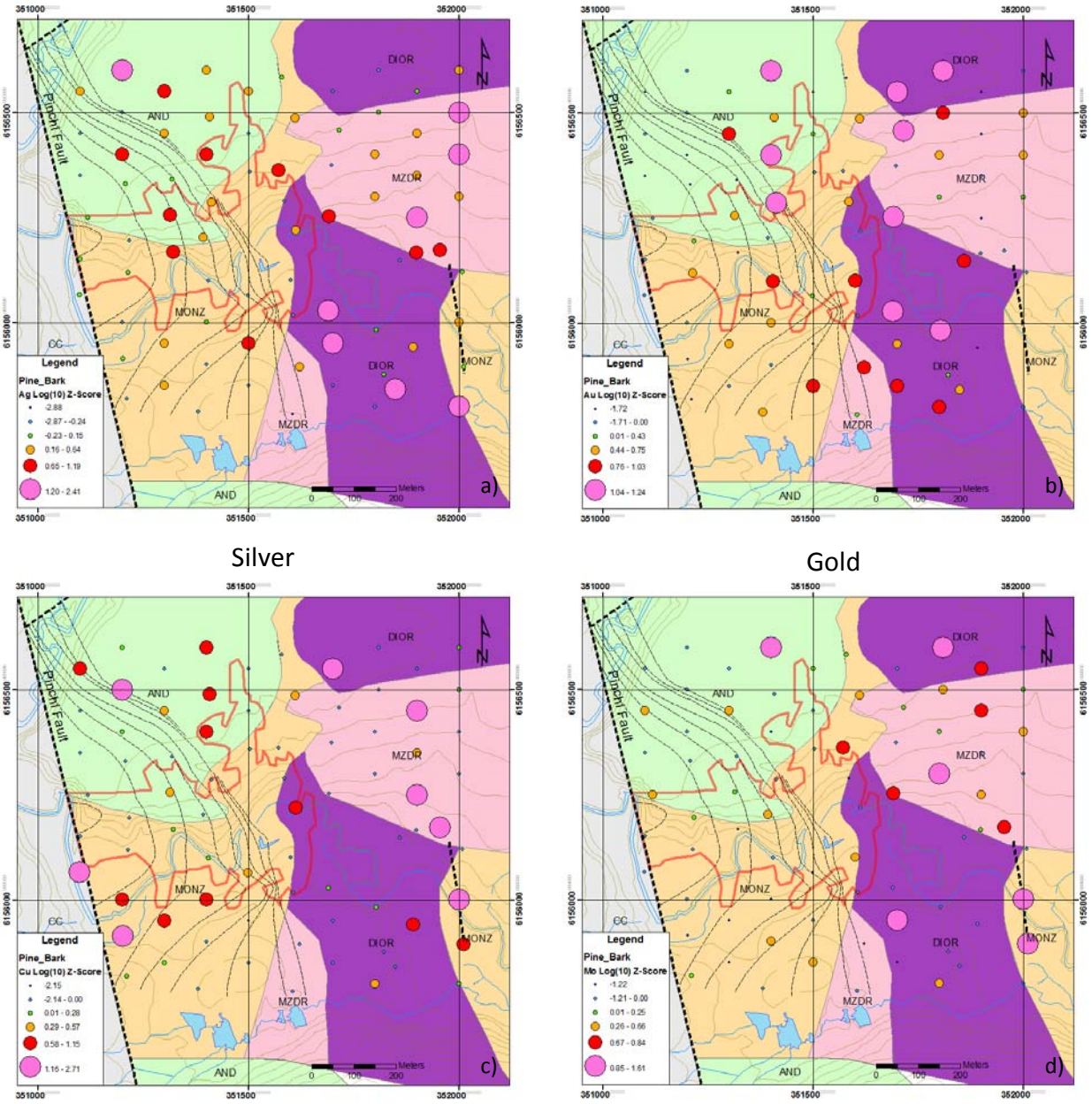

Silver

Gold

Copper

Molybdenum

FIGURE 36 ORE ELEMENT RESULTS FOR THE AQUA REGIA DIGESTION OF DRY PINE BARK: AU, AG, CU AND MO

PATHFINDER ELEMENTS

Almost all the As and Bi concentrations were below detection. Antimony and Pb, however, were detectable in almost all samples and exhibit the familiar pattern of relative enrichments around the periphery of the zone of mineralization (Fig. 37).

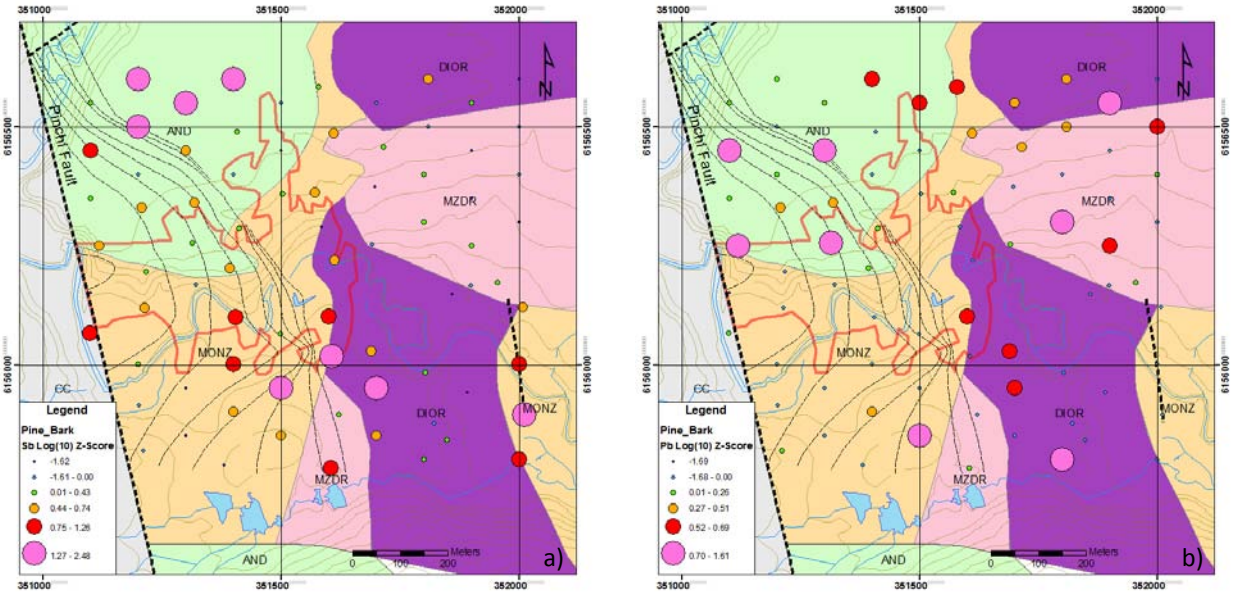

Antimony Lead

FIGURE 37 PATHFINDER ELEMENT RESULTS FOR THE AQUA REGIA DIGESTION OF DRY PINE BARK: SB AND PB

OTHER ELEMENTS

Several other elements are relatively enriched in the areas surrounding the zone of mineralization, and notably to the east where the bedrock is monzodiorite and diorite. Figure 38 shows plots of Zn, Ni, Ce and Ca.

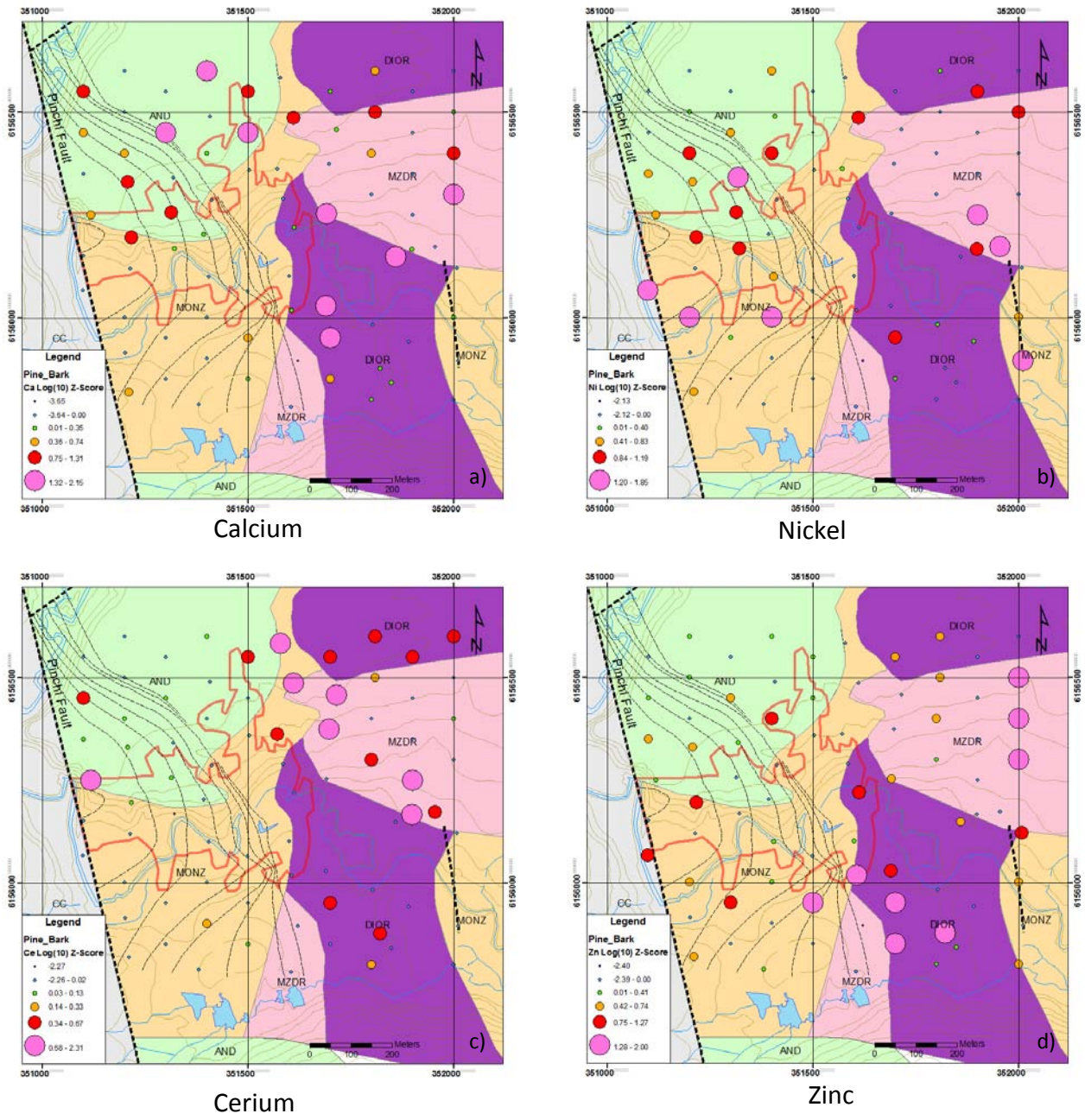

Calcium

Nickel

Cerium

Zinc

FIGURE 38 OTHER ELEMENT RESULTS FOR THE AQUA REGIA DIGESTION OF DRY PINE BARK: CA, NI, CE AND ZN

DISCUSSION

AH HORIZON SOIL

The results presented in this report demonstrate the effectiveness of Ah horizon soils as a viable sample medium in areas of thick glacio-fluvial sediment and post mineral sedimentary basin cover. Two of the three chemical extractions tested at the Kwanika Central Zone performed relatively well at defining the position of the deeply buried mineralization. Results of all three extractions are summarized in Table 5.

TABLE 5 SUMMARY OF AH HORIZON RESULTS

Extraction	Apical Anomaly	Halo Anomaly	Northeast Anomaly
Distilled Water	Ag, Mo, Pb, W		Ag, **Cu**, (Mo), Pb, As, Sb, (Tl), (Zn), **Ca**, Cd, Ce, Sr
Sodium Pyrophosphate	**Ag**, Au, **Cu**, Mo, **As**, **Hg, W,** (Ba), (Ca), Cd, **Cs,** Ce, (La)	Pb, Tl, Zn	**Au**, Cu, (Mo), Ca, Cs, (Ce), La
Ultratrace	(Ag), **Au, Cu,** (Mo), **As,** Bi, Sb, **W,** (Ca), (Cd)	Pb, Zn	**Au, Cu,** Mo, Bi, **Sb, Ca, Cd**

***Bold** = Strong Response; Normal Text = Moderate Response, (Bracket) = Weak Response*

The poorest results were produced by the distilled water extraction. For the ore elements this method defined only vague responses over the zone for Ag, Mo, Pb and W. The strongest ore element response was for Cu, which is located over the monzodiorite intrusion to the east of the Central Zone. For the purposes of the following discussion, this area will be referred to as the Northeast anomaly (Fig. 39). Several other elements have coincident responses with Cu in this area, including: Ag, As, Sb and Ca. There is no known mineralization in that area to explain these responses; however there is a lack of drilling, which means that presence of hitherto unknown mineralization cannot be ruled out.

The sodium pyrophosphate and Ultratrace methods produced quite similar results but only after correction and transformation of the raw values. Robust apical anomalies for Ag, Cu, As, Hg, W and Cs are produced by the sodium pyrophosphate extraction. These elements appear to detect the central and eastern or shallower parts of the underlying mineralization, down to a depth of about 250 metres beneath the post mineral Tertiary sedimentary basin succession. Silver seems to detect the western, deepest parts of the zone as well. A recurring theme in this study is the presence of a W anomaly over the mineralization. This is clearly seen in the sodium pyrophosphate results (Fig. 21a), where all but one of the 13 highly anomalous samples sit within the projected outline of the mineralization. Sodium pyrophosphate also produces clear anomalies in the Northeast anomaly area where the most notable responses are for Au, Cu and Cs, which are consistent with a mineralized source perhaps hosted by the underlying monzodiorite.

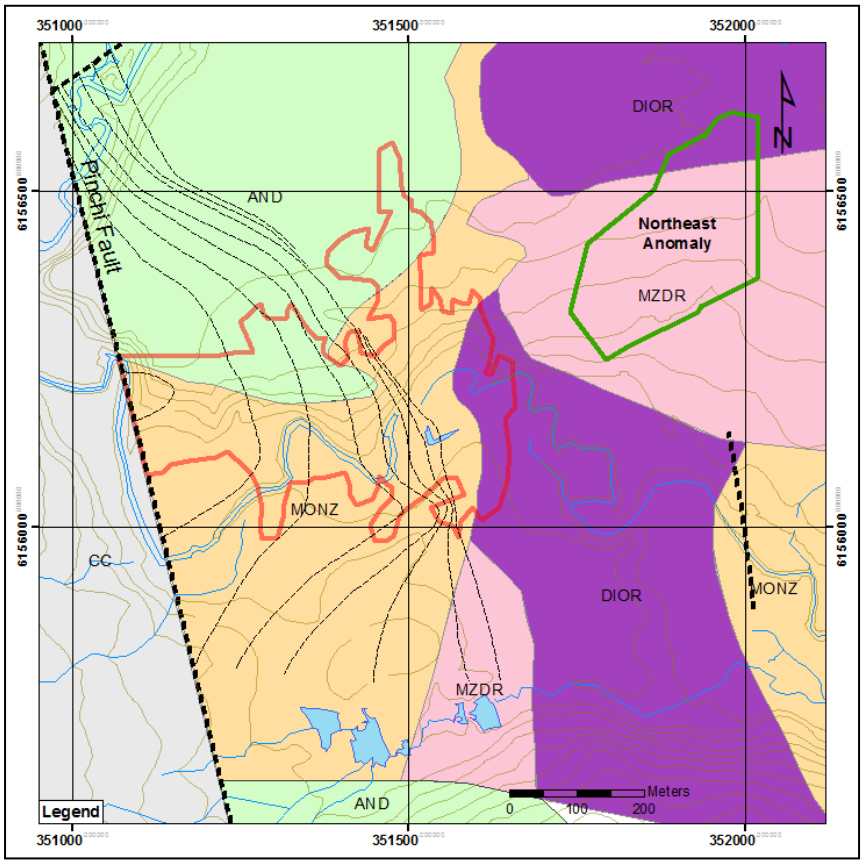

FIGURE 39 LOCATION OF THE NORTHEAST ANOMALY

Halo type anomalies for Pb, Zn and Tl are also defined by the sodium pyrophosphate extraction. While these are not tightly constrained anomalies, they are defined by scattered anomalous and highly anomalous values around the margins of the Central Zone with a conspicuous lack of anomalous values over the mineralization.

Ultratrace aqua regia detects strong apical anomalies for Cu, Au, As and W and credible responses for Sb and Bi. There is no doubt that this method is identifying the position of the blind mineralization. Copper and Au anomalies occur over the shallower parts of the Central Zone with no apparent response to mineralization located more than 300 metres from the surface. Arsenic appears to reflect deeper levels of the mineralized body, however highly anomalous values located on the trace of the Pinchi Fault, which intersects mineralization almost 400 metres below, suggests that the fault may be playing a role in dispersion of some elements to the surface. A similar feature is seen for Zn and possible Mo.

Ultratrace produces robust responses for Au, Cu, Sb, Ca and Cd over the Northeast anomaly. These are similar in size and contrast to the sodium pyrophosphate anomalies described above. The presence of ore and pathfinder element anomalies in this undrilled area are intriguing and could be pointing to the presence of undiscovered mineralization.

CHARCOAL

To the author's knowledge, charcoal has not been used as a sample medium for exploration in British Columbia. Charcoal is a common component of forest soils. It is formed by the thermochemical decomposition of wood by fire (DeLuca and Aplet, 2008). This highly porous material is known to have a strong metal sorption capacity (Johns et al., 1993; McMahon, 2006) and therefore should behave as an effective trap for mobile metal ions in the near-surface environment. It is potentially a useful sampling medium in areas of recent forest fires and logged areas where the vegetation and the Ah horizon may have been damaged or completely destroyed.

Results of the charcoal sampling (Table 6) show encouraging patterns that suggest that this material is indeed acting as a repository for mobile metal ions. Coincident anomalies for Ag, Au, Cu, As, Sb and W directly over the Central Zone, suggest that ions migrating from the mineralization to the surface (by whatever mechanism) or ions being redistributed in the soils in response to changes in parameters such as pH and redox conditions, are being trapped in the charcoal to form detectable anomalies. Several elements (e.g. Ag, Au, Cu, Mo, As, Bi, Sb and W) have elevated values on or close to the surface trace of the Pinchi fault, which intersects the mineralization at depth. A likely scenario is that some of the metals concentrated in the charcoal may have migrated to the surface along the permeable fault zone. There is also evidence that the charcoal may be concentrating hydromorphically dispersed metals, such as Zn. The presence of Zn anomalies along the base of slope on the north side of the Kwanika Creek drainage (Fig. 30b) could be related to seepage zones where groundwater carrying dissolved Zn is emerging at surface. Another possibility is that the charcoal contains metals that were in the original plant tissues. However results from the vegetation sampling do not appear to support this idea (see below) because the charcoal is primarily trunkwood. Trunkwood accumulates only very low levels of trace elements (mostly below the detection level of the ICP-MS instrumentation used) compared to the twigs, foliage or bark that are the usual biogeochemical sampling media because of their abilities to concentrate many elements to much greater levels.

TABLE 6 SUMMARY OF CHARCOAL RESULTS

Medium	Apical Anomaly	Halo Anomaly	NE Anomaly
Fir Twigs		Pb	**Cu, Mo,** (Bi), Sb,

***Bold** = Strong Response; Normal Text = Moderate Response, (Bracket) = Weak Response*

The spotty nature of the element responses over the mineralized zone is curious. This may be a function of the relatively erratic distribution of sample sites (Fig. 11b) and the quantity, quality and source of the charcoal (e.g. different tree species) available at each location, which was found to be highly variable. At most sites only the coarsest charcoal fragments could be collected by hand-picking. This sampling method may not be providing a truly representative or consistent sample. There was a wide range of sample weights (5 to 15g) and relatively high RSD% values for the field duplicate results (Table 3). Better results may be obtained by using a more sophisticated sampling technique that would concentrate charcoal particles from the finer fractions of the soil. McMahon (2006) advocates floating the charcoal particles (specific gravity <1.0g/cm^2) in distilled water and concentrating them by filtering. More experimentation is needed in order to perfect the sampling technique. Nevertheless the results of this study suggest that with more rigorous sampling techniques, charcoal could be a viable sampling medium.

VEGETATION

The vegetation results show different patterns to those observed in the Ah horizon soils. These patterns are summarized in Table 7. Unlike the soils, most elements in the vegetation show elevated values around the periphery of the mineralized zone. Some elements, notably Cu, and to a lesser extent Mo, Ni and Zn are elevated in the vicinity of faults. Only Ag in the fir needles has a response approaching an apical anomaly over the mineralization.

TABLE 7 SUMMARY OF AQUA REGIA RESULTS FOR VEGETATION SAMPLES

Medium	Apical Anomaly	Faults	Halo/Depletion	NE Anomaly
Fir needles	Ag	Cd, Cu, (Mo), Ag	Ag, **As**, Ce, (Hg), Mo, Ni, (Pb), **Tl**, (Sr), Zn	(Ag), Ba, (Cu), Cd, (Mo)
Pine bark		**Cu,** Mo, Ni, Zn	(Ag), Ca, Ce, Cu, Ni, **Sb,** (Pb), Zn	(Ag), (Au), (Cu), Mo

***Bold** = Strong Response; Normal Text = Moderate Response, (Bracket) = Weak Response*

It is to be expected that the geochemical signatures of the pine bark would be somewhat different from those of the fir needles because of their differing requirements for trace elements and abilities to tolerate various elements. For example, pine bark is significantly enriched in Ag compared to the fir needles, whereas the needles are more enriched in Tl. The plants obtain their elemental compositions from the soils and groundwater, and are therefore performing a type of selective leach of the substrate. Measurements of pH taken in the field do not indicate that this is a significant control of the element uptake by the plants. Some considerations to the differences from the Ah signatures are:

- Bedrock alteration is having a control on the relative element uptake by the trees across the survey area. The zone of mineralization is reported to be related to albitization, whereas the surrounding rocks are potassic. Conceivably, the albitization has flushed trace elements outward to the surrounding rocks and thereby giving rise to the halo of multi-element enrichments;

- A more important factor, however, is that the tree roots penetrate *all* soil horizons and each tree integrates the geochemical signature of several cubic metres of the substrate. Studies of this area (Heberlein, 2010) and other areas have demonstrated that each soil horizon has a different composition. Although tree roots first obtain their nutritional requirements from the easily accessible components of the substrate (e.g. elements dissolved in groundwater and adsorbed on to soil particle surfaces) they also attack other more resistant parts of the soil profile, and in fact commonly show their strongest relationship to the C-horizon (Dunn, 2007). Therefore, the tree chemistry will not be directly comparable to that of the Ah horizon because only part of their composition is derived from the Ah.

It appears that, given the depth to the mineralization and the factors described in this study, the vegetation provides a less robust signature than the Ah at this property-scale of study. Perhaps from a more regional perspective the annular anomalies noted here would provide focus for more detailed exploration.

QUANTIFICATION OF THE AH HORIZON SOIL RESULTS

The human eye has an amazing ability to discern patterns. This coupled with the exploration geologist's optimism and perpetual desire to see anomalies in any type of geochemical data often leads to over-statement of the importance of geochemical results. Visual interpretation of the results can be highly subjective and influenced by personal bias of the interpreter or end user of the geochemical data resulting in over optimistic conclusions about the results.

What is needed is a way of quantifying the exploration effectiveness or relative performance of the techniques tested. Such a method, known as the minimum hypergeometric probability method was proposed by Stanley (2003). The hypergeometric probability method evaluates exploration performance by estimating the hypergeometric probability of obtaining a result by chance. The lower the estimated probability of a result, the more likely it is to successfully detect the presence of mineralization. In other words the probability is an objective and quantitative measure of performance of a method. For a full description of the hypergeometric probability method and the statistical background on the calculations required the reader is referred to papers by Stanley (2003) and Stanley and Noble (2007).

In order to apply the hypergeometric probability test to a dataset, some basic knowledge of the geology of the bedrock mineralization, the thickness and nature of the cover, and the physiographic and surficial environment is necessary. Ideally some knowledge of the surface Eh and pH conditions, mobility of key elements under those conditions and possibly geochemical dispersion mechanisms can greatly enhance understanding of a set of results.

In high contrast datasets, the analytical results can be considered as Boolean (i.e. they are either anomalous or they are background with respect to a given threshold). Threshold values can be estimated using a number of different approaches such as probability plots (Sinclair, 1976; Stanley, 1986), percentiles (e.g. 90^{th}, 95^{th} etc.), mean plus two standard deviations or median plus two median absolute deviations (Sanei et al., 2007). With prior knowledge of the location of the mineralization one can determine which sample sites occur in anomalous locations (determined from the position of the mineralization and knowledge of local dispersion processes) and which sites fall in background areas. Using a threshold value one can determine the extent to which anomalous results occur over anomalous sample sites (i.e. successes) and background samples occur over background sites. The occurrence of anomalous samples over background site and background samples over anomalous sites (i.e. failures) can also be assessed.

Using probabilities determined from the hypergeometric distribution (Spiegel, 1975; Neter et al., 1978) the chance of obtaining an outcome with the same number of successes and failures at random can be determined. To determine the probability of obtaining a given result by chance the following values must be known:

(t) – the total number of sample sites

(a) – the number of anomalous sample sites (determined from the known position of the mineralization and knowledge of dispersion mechanisms).

(k) – the number of anomalous samples (analytical values above a threshold); and

(x) – the number of correct anomalies (anomalous values coinciding with anomalous sites).

The probability that a given result would be produced by random chance is determined from the following equation:

$$P(x) = \binom{a}{x}\binom{t-a}{k-x} \Big/ \binom{t}{k} \; x\; 100$$

With these parameters, the number of background samples over anomalous sites (m), 'false anomalies' or anomalous samples over background sites, and truly background samples can be determined.

An example of a synthetic result is illustrated in Figure 40. An orientation line consisting of 31 sample sites crosses a mineralized zone represented by 10 anomalous sites (leaving 21 background sites). The results show four anomalous samples: three coinciding with anomalous sites and one with a background site. In addition, six background samples occur at anomalous sites. Visually this result appears to represent an exploration success. Using the hypergeometric distribution equation, the probability of obtaining this result by random chance is 8.68% or about one in 12. Consequently this result is positive but cannot be considered to be conclusively successful. A result with a probability of less than 10% is judged to be an exploration success.

This approach is applied to the three Ah horizon extractions in order to assess which method has the best exploration performance. Anomalous sample sites from the study area are determined based on the surface projection of the mineralization as defined by the 0.2% Cu equivalent grade contour as shown in Figure 41. The total number sites (t) varies with each method with both sodium pyrophosphate and Ultratrace aqua regia having results from the 2009 and 2010 campaigns, and distilled water, only, from the 2010 sampling program. For the purpose of this study, a uniform threshold equivalent to the 90th percentile is used. At this value a constant 10% of the sample population has anomalous results. Optimization of the threshold values using the method described by Stanley and Noble (2007) has not been done on these results. Optimization of individual elements may improve the probability results from those reported below. Hypergeometric probabilities are calculated using a spreadsheet published by Dr. Cliff Stanley of Acadia University. This is available free of charge from http://www.acadiau.ca/~cstanley/Software.html.

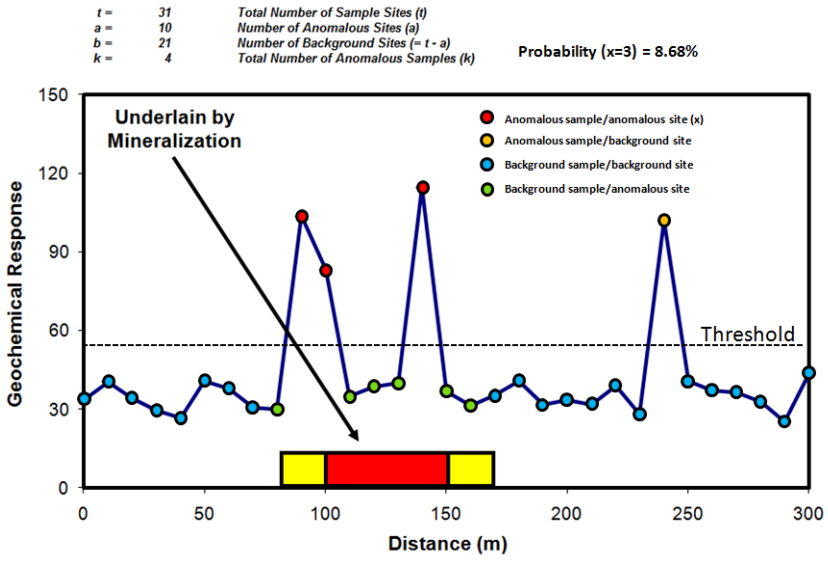

FIGURE 40 AN EXAMPLE OF A SYNTHETIC RESULT SHOWING AN APPARENT EXPLORATION SUCCESS

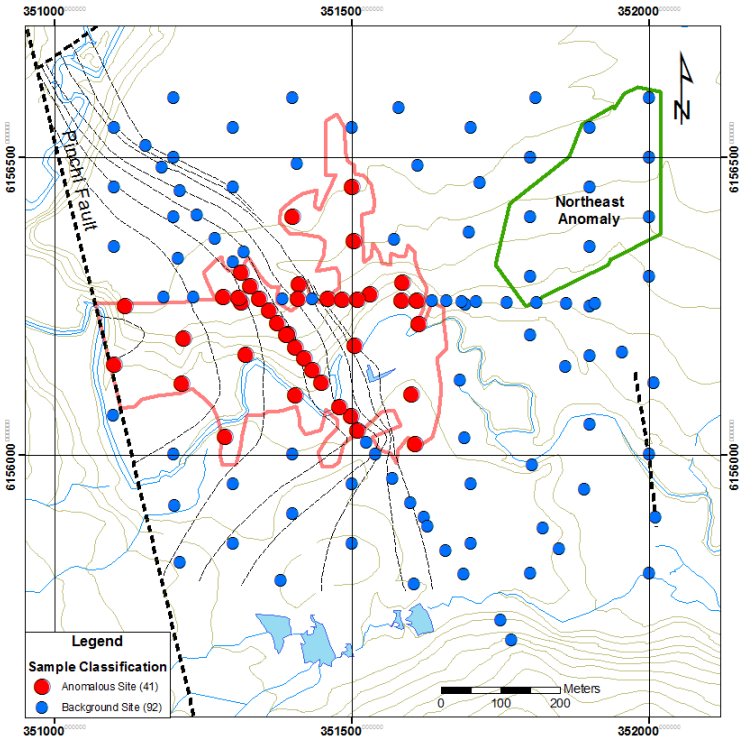

FIGURE 41 CLASSIFICATION OF SAMPLE SITES INTO ANOMALOUS AND BACKGROUND POPULATIONS AT THE KWANIKA CENTRAL ZONE: ANOMALOUS SITES – RED; BACKGROUND SITES - BLUE

Figure 42 presents the results for Ultratrace As in Ah horizon soils. In this example there is a total of 133 sample sites (t), 92 background sites (b), 41 anomalous sites (a) and 16 anomalous samples (k). Ten of the anomalous samples (red) coincide with anomalous sites and six with background sites (orange). Fifteen background samples occupy anomalous sites (green). A hypergeometric probability of 0.55% or a one in 181 chance of obtaining this result from random chance is produced using these parameters. This means that this result is a conclusive exploration success.

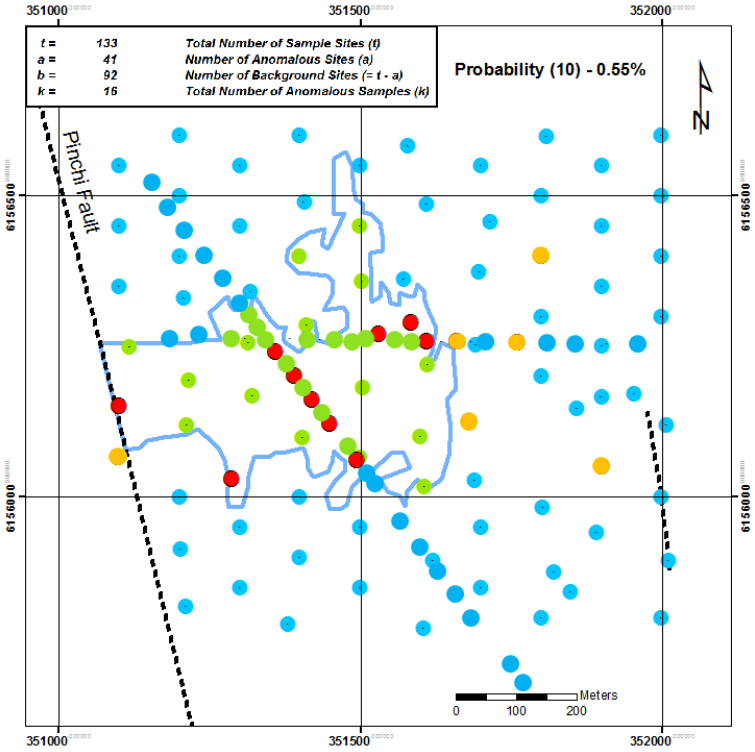

FIGURE 42 HYPERGEOMETRIC PROBABILITY ESTIMATE FOR ARSENIC IN AH HORIZON ULTRATRACE EXTRACTION: RED = ANOMALOUS SAMPLE/ANOMALOUS SITE; ORANGE = ANOMALOUS SAMPLE/BACKGROUND SITE; GREEN = BACKGROUND SAMPLE/ANOMALOUS SITE; BLUE = BACKGROUND SAMPLE/BACKGROUND SITE.

This procedure was carried out for a suite of ore and pathfinder elements for all three extractions. Results are summarized in Tables 8, 9 and 10. These tables show the parameters used in the hypergeometric probability equation (t, a, b, k and x, see above) and include the probability that a result is produced by random chance. Probabilities of less than 10% are considered to be successes.

Despite visually compelling patterns for a number of elements, only four: As, Au, Cu and W demonstrate unequivocal successes in the Ultratrace extraction results (Table 8). For these elements it is highly unlikely that the observed results are the product of random chance. Sodium pyrophosphate results (Table 9) show much the same thing. In this extraction, As Cu, Sb and W are successes. All the results for the distilled water extraction (Table 10) are failures suggesting that this method is not an effective exploration technique in this environment.

TABLE 8 HYPERGEOMETRIC PROBABILITY STATISTIS FOR AH HORIZON ULTRATRACE EXTRACTION

Element	t	a	b	k	x	Probability	Chance	Result
Ag	133	41	92	14	5	44.29%	1 in 2	Failure
As	133	41	92	16	10	0.55%	1 in 181	Success
Au	133	41	92	14	4	9.34%	1 in 11	Success
Bi	133	41	92	14	6	23.02%	1 in 4	Failure
Cd	133	41	92	13	3	82.86%	1 in 1.2	Failure
Co	133	41	92	13	6	17.15%	1 in 6	Failure
Cu	133	41	92	13	7	6.12%	1 in 16	Success
Hg	133	41	92	13	5	17.15%	1 in 6	Failure
Mo	133	41	92	14	4	68.16%	1 in 1.5	Failure
Pb	133	41	92	13	2	95.20%	1 in 1	Failure
Sb	133	41	92	14	6	23.02	1 in 4	Failure
W	133	41	92	14	10	0.12%	1 in 833	Success
Zn	133	41	92	14	5	44.29%	1 in 2	Failure

TABLE 9 HYPERGEOMETRIC PROBABILITY STATISTICS FOR AH HORIZON SODIUM PYROPHOSPHATE EXTRACTION

Element	t	a	b	k	x	Probability	Chance	Result
Ag	132	41	92	14	5	23.02	1 in 4	Failure
As	132	41	92	14	8	3.04%	1 in 33	Success
Au	132	41	92	14	4	68.87%	1 in 1.5	Failure
Bi	132	41	92	14	5	45.10%	1 in 2	Failure
Cd	132	41	92	14	4	68.87%	1 in 1.5	Failure
Co	132	41	92	13	3	83.34%	1 in 1.2	Failure
Cu	132	41	92	13	7	9.69%	1 in 10	Success
Hg	132	41	92	12	6	29.83%	1 in 3	Failure
Mo	132	41	92	14	4	23.65%	1 in 4	Failure
Pb	132	41	92	14	3	87.29%	1 in 1.3	Failure
Sb	132	41	92	13	7	6.36%	1 in 16	Success
W	132	41	92	14	10	0.12%	1 in 833	Success
Zn	132	41	92	15	5	97.71%	1 in 1	Failure

TABLE 10 HYPERGEOMETRIC PROBABILITY STATISTICS FOR AH HORIZON DISTILLED WATER EXTRACTION. BLANKS DENOTE INSUFFICIENT DATA (ELEMENTS MOSTLY BELOW DETECTION LIMIT)

Element	t	a	b	k	x	Probability	Chance	Result
Ag	79	19	60	8	2	62.05%	1 in 1.6	Failure
As	79	19	60	9	3	37.12%	1 in 3	Failure
Au	79	19	60	8	3	29.25%	1 in 3	Failure
Bi								
Cd	79	19	60	9	1	92.81%	1 in 1	Failure
Co	79	19	60	8	1	90.19%	1 in 1	Failure
Cu	79	19	60	8	1	90.19%	1 in 1	Failure
Hg								
Mo	79	19	60	9	3	37.10%	1 in 3	Failure
Pb	79	19	60	8	3	29.25%	1 in 3	Failure
Sb	79	19	60	9	1	92.82%	1 in 1	Failure
W	79	19	60	8	3	29.25%	1 in 4	Failure
Zn	79	19	60	9	1	92.82%	1 in 1	Failure

These results are estimated for an apical response in very flat terrain directly over the footprint of the mineralization. This model does not adequately describe results for elements with halo-like (or rabbit-ear) patterns around the periphery of the zone (e.g. in vegetation), like Pb and Zn or elements with lateral dispersion caused by mechanical or hydromorphic dispersion. Such patterns can be assessed by modifying the anomalous sites to reflect these dispersion processes and recalculating the probabilities. Consequently the probabilities for these elements are likely to be overly pessimistic.

SUMMARY

This study tested the effectiveness of several types of organic sample media at detecting the blind Central Zone Cu-Au mineralization at Kwanika. The aim of this work is to provide the mineral exploration community with guidance on the most appropriate sampling medium and chemical extraction to use in a boreal forest environment where thick glacial (or post-mineral) sedimentary cover is present. It also provides suggestions for alternative sampling media in areas where the surface has been disturbed by logging or forest fires.

The 2010 study (Heberlein and Samson, 2010) showed that best results are obtained by sampling the organic-rich Ah horizon. The present study examined the effectiveness of a three extractions on this sampling medium. The weakest extraction, distilled water, was found to be ineffective at detecting the mineralization. It did produce visually interesting patterns over the zone, however hypergeometric probability analysis demonstrates that there is a reasonable chance of similar results being produced by random chance. Sodium pyrophosphate and Ultratrace aqua regia both performed well in defining statistically meaningful apical anomalies for As, Cu and W. Gold and Sb anomalies were also detected by the Ultratrace and sodium pyrophosphate methods respectively. Tungsten has by far the strongest response of all elements tested and appears to be the most effective pathfinder for the blind mineralization. Interestingly, these anomalies do not necessarily reflect the composition of the primary mineralization at depth as shown in Table 11. Copper is highly elevated in drill core samples and in the Ah soils but As and W display only modest concentrations in the primary mineralization yet strong enrichment in the soil.

There is little to choose between the Ultratrace and sodium pyrophosphate extractions in terms of performance. Both methods detect the mineralization with similar contrast and element associations. From a practical standpoint however, Ultratrace is a more attractive method to use. It is less expensive than sodium pyrophosphate and does not require a second analysis such as LOI in order to correct for a controlling variable.

Charcoal results, while not definitive, do show that this material has promise as a sampling medium. Patterns produced by Ultratrace aqua regia digestion of this medium are comparable with those seen in the Ah soils. Unfortunately the relatively small number of samples over the mineralized zone and the highly variable nature of charcoal distribution across the study area resulted in relatively poor precisions for most elements that translate into noisy patterns. Nevertheless, this study has demonstrated that recognizable anomalies for ore elements can be obtained over the mineralization in this medium and with improved sampling techniques more reliable results could be achieved. More work is needed to refine charcoal as a sample medium.

The vegetation results show different patterns from the Ah soils and charcoal suggesting that the metals in the soil have not been derived exclusively through recycling of plant tissues. Furthermore, the occurrence of halo-like patterns with lows directly over the mineralization imply that different geochemical dispersion processes are responsible for the formation of soil and vegetation anomalies and this is probably because the roots of an individual large tree integrate the geochemical signature of several cubic metres of the substrate, including all soil horizons. As a sampling medium to detect deeply buried mineralization, fir needles show promise particularly for pathfinder elements like Tl and As that form compelling halo patterns around the edges of the mineralized zone. Dispersion patterns for these elements significantly enlarge the size of the target making it easier to find. A combination of fir needles and Ultratrace analysis of Ah horizon soils would be an effective exploration approach in boreal forest environment. Pine bark had less clear results but did produce base metal anomalies in close

proximity to known faults of which one, the Pinchi Fault, is known to intersect mineralization at depth. This observation could be useful in interpretation of pine bark survey results.

TABLE 11 SUMMARY STATISTICS FOR SELECTED ELEMENTS FROM AQUA REGIA DIGESTION OF DRILL CORE SAMPLES.

	N	Mean	Std. Dev.	Min	Percentiles									Max
					25	*50*	*60*	*70*	*80*	*90*	*95*	*98*	*99*	
Ag_ppm	3412	1.2	1.6	0.1	0.2	0.7	1	1.3	1.8	2.8	3.5	5	6.3	56
Al_%	3412	0.94	0.51	0.02	0.54	0.81	0.98	1.17	1.38	1.66	1.91	2.17	2.347	3.2
As_ppm	3412	32	94	1	8	14	18	23	29	48	97	209	426	1882
Ba_ppm	3412	179	225	5	47	87	117	170	259	465	677	923	1082	2777
Bi_ppm	3412	3.0	1.95	2.5	2.5	2.5	2.5	2.5	2.5	2.5	6	9	12	46
Ca_ppm	3412	2.82	1.52	0.1	1.922	2.76	3.028	3.36	3.75	4.34	5.003	5.995	6.943	21.6
Cd_ppm	3412	0.76	1.34	0.5	0.5	0.5	0.5	0.5	0.5	1	2	4	6	52
Co_ppm	3412	11	7.1	0.5	6	9	10	12	14	19	24	31	37	104
Cr_ppm	3412	35	25	2	19	30	34	39	46	60	75	102	133	490
Cu_ppm	3412	3534	3972	1	795	2443	3149	4088	5804	8230	11207	14470	18034	51160
Fe_%	3412	4.47	1.70	0.15	3.26	4.23	4.65	5.17	5.76	6.77	7.62	8.725	9.536	13.1
K_%	3412	0.29	0.18	0.005	0.19	0.26	0.29	0.32	0.37	0.48	0.59	0.86	1.08	1.73
La_ppm	3412	5.3	4.3	1	2	4	6	7	8	11	13	17	20	29
Mg_%	3412	1.02	0.65	0.08	0.72	0.925	1.02	1.13	1.29	1.517	1.77	2.067	2.299	13.36
Mn_ppm	3412	761	417	130	499	677	753	840	966	1226	1507	1993	2366	4423
Mo_ppm	3412	8.0	31	1	1	1	2	3	5	11	24	63	228	341
Na_%	3412	0.098	0.036	0.02	0.07	0.09	0.1	0.11	0.12	0.14	0.16	0.19	0.23	0.5
Ni_ppm	3412	5.1	8.6	0.5	3	4	4	5	6	9	13	18	23	184
P_ppm	3412	1057	438	5	780	1030	1139	1273	1399	1580	1764	2026	2247	4501
Pb_ppm	3412	6.0	9.7	2	2	4	5	6	7	10	17	39	50	191
S_%	404	1.62	1.2	0.025	0.74	1.425	1.74	2.13	2.56	3.205	3.633	4.449	5.755	7.05
Sb_ppm	3412	2.8	4.0	2.5	2.5	2.5	2.5	2.5	2.5	2.5	2.5	8	14	177
Se_ppm	404	5.3	5.5	2.5	2.5	2.5	2.5	6	8	11	14	19	24.9	74
Sn_ppm	3412	1.4	0.92	1	1	1	1	1	1	2	3	4	5	21
Sr_ppm	3412	134	116	5	48	102	141	174	215	276	341	428	513	1967
Ti_ppm	3412	0.028	0.05	0.005	0.005	0.005	0.005	0.01	0.03	0.09	0.14	0.217	0.24	0.4
V_ppm	3412	92	49	1	57	83	94	107	125	160	189	225	245	324
W_ppm	3412	1.54	6.5	1	1	1	1	1	2	3	3	5	6	372
Y_ppm	3412	7.0	2.8	1	5	7	8	8	9	11	12	13	14	24
Zn_ppm	3412	62	159	12	36	46	52	59	73	97	128	239	316	8844

An interesting outcome of this project is the identification of the Northeast anomaly. This feature was detected in all media and extractions by several elements. The anomaly appears to be centred on a body of monzodiorite located about 300 metres east-northeast of known mineralization, in an area with no historical drilling. Further investigation of the area is warranted in order to explain the anomaly.

CONCLUSIONS

Main conclusions from this study are:

1) Of the media and methods tested Ultratrace aqua regia on Ah horizon soils appears to be the most effective at detecting the deeply buried porphyry style Cu-Au mineralization.
2) Charcoal shows great promise as a sample medium. It produces recognizable anomalies over the mineralized zone. More work is needed to optimize sampling procedures to obtain higher levels of precision.
3) Fir needles outperform pine bark as a biogeochemical sample medium. Robust halo anomalies with central depletions over the mineralization for As and Tl potentially greatly enhance the size of the detectable footprint of the mineralization thus making it easier to detect.
4) A recommended sampling strategy for undisturbed boreal forest is to collect Ah horizon soils and analyze them using an Ultratrace (low detection limit) aqua regia method. In addition, fir needles could be collected at the same time as the Ah soils and analyzed by aqua regia-ICP-MS. This method is used to define haloes in metals such as Tl that would increase the probability of detecting a target.

5) In areas where the forest is disturbed by logging, Ah horizon is a viable sample medium if pristine sites can be found. If significant ground disturbance is present, charcoal may be a practical alternative medium.

6) Charcoal should be an effective medium in recently burned forest and in older burns where this material resides in the upper parts of the soil profile.

ACKNOWLEDGEMENTS

Funding for this study was provided by Geoscience BC. The authors would like to thank Serengeti Resources Inc. for allowing access to the property and for generous support with field accommodation and logistical expenses. Thanks also to Katie and Graeme Heberlein for their valuable assistance with the sampling. This project would not have been possible without their hard work. To Kirstie Simpson and Kim Heberlein for their editorial help and excellent suggestions for improvements to the report; and finally to Mark Rebagliati for asking the hard questions and planting the seeds that led to the development of this project.

REFERENCES

DeLuca, T.H. and Aplet, D.H. (2008): Charcoal and carbon storage in forest soils of the Rocky Mountain West; *in* Frontiers of Ecology and the Environment, The Ecological Society of America, v. 6, p. 1–8.

Dunn, C.E. (2007): Biogeochemistry in Mineral Exploration. (Handbook of Exploration and Environmental Geochemistry 9, Series editor, M. Hale), Elsevier, Amsterdam, 462 pp.

Garnett, J. A., (1978): Geology and Mineral Occurrences of the Southern Hogem Batholith. Province of British Columbia, Ministry of Energy, Mines and Petroleum Resources, Bulletin 70, 75 pp.

Heberlein, D. R. (2010): Comparative Study of Partial and Selective Extractions of Soils over Blind Porphyry Copper-Gold Mineralization at Kwanika and Mount Milligan, British Columbia (NTS 093N/01, /19); *in* Geoscience BC Summary of Activities2009, Report 2010-1, p. 11-24

Heberlein, D.R. And Samson, H. (2010): An assessment of soil geochemical methods for detecting copper-gold porphyry mineralization through Quaternary glaciofluvial sediments at the Kwanika Central Zone, north-central British Columbia; Geoscience BC, Report 2010-3, 89 pp.

Johns, M.M., Skogley, E.O. and Inskeep, W.P. (1993): Characterization of carbonaceous adsorbents by soil fulvic and humic acid adsorption; Soil Science Society of America Journal, v. 57, p. 1485–1490.

McMahon, C. (2006): Characteristics and sorption properties of charcoal in soil with a specific study of the charcoal in an arid region soil of Western Australia; M.Sc. thesis, University of Western Australia.

Mills, K. (2008): Technical report – feasibility, Mt. Milligan Property - northern BC; unpublished report to Terrane Metals Corp.

Neter, J., Wasserman, W. and Whitmore, G.A. (1978): Applied Statistics. Allyn and Bacon, Inc., Boston, 743 pp.

Nelson, J., and Bellefontaine, K. (1996): The Geology and Mineral Deposits of North-Central Quesnellia; Tezzeron Lake to Discovery Creek, Central British Columbia; British Columbia Geological Survey, Bulletin 99, p. 1-43.

Osatenko, M. (2005): Geophysical and Geochemical Report on the Kwanika Property; British Columbia Ministry of Energy and Mines Assessment Report #28180.

Rennie, D.W. and Scott, K.C. (2009): Technical report on the Kwanika project, Fort St. James, British Columbia, Canada; unpublished report to Serengeti Resources Inc., Scott Wilson Mining.

Sanei, H., Goodarzi, F and Hilts, S. (2007): Site-specific natural background concentrations of metals in topsoil from the Trail region, British Columbia, CanadA: Geochemistry: Exploration, Environment, Analysis 2007; v. 7; p. 41-47.

Sinclair, A.J. (1976): Applications of Probability Graphs in Mineral Exploration. Special Volume, 4. Association of Exploration Geochemists, Rexdale, Ontario, Canada.

Speigel, M.R. (1975): Theory and Problems of Probability and Statistics. Schaum's Outline Series. McGraw-Hill Book Co., New York, 372 pp.

Stanley, C.R. (1986): PROBPLOT – An interactive computer program to fit mixtures of normal (or log-normal) distributions using maximum likelihood optimization procedures. Special Volume, 14. Association of Exploration Geochemists, Rexdale, Ontario, Canada.

Stanley, C.R. (2003): A statistical evaluation of anomaly recognition performance. Geochemistry: Exploration, Environment, Analysis, 3, p. 3–12.

Stanley, C.R. and Noble, R.R.P. (2007): Optimizing geochemical threshold selection while evaluating exploration techniques using a minimum hypergeometric probability method. Geochemistry: Exploration, Environment, Analysis, 7; p. 341-351.